FIVE-HOLE PITOT PROBE TIME-MEAN VELOCITY MEASUREMENTS IN CONFINED SWIRLING FLOWS

By

HYUNG KEE YOON

Bachelor of Engineering

Korea University

Seoul, Korea

1980

Submitted to the Faculty of the Graduate College
of the Oklahoma State University
in partial fulfillment of the requirements
for the Degree of
MASTER OF SCIENCE
July, 1982

FIVE-HOLE PITOT PROBE TIME-MEAN VELOCITY

MEASUREMENTS IN CONFINED SWIRLING FLOWS

Thesis Approved:

David G. Lilley
Thesis Adviser

Robert M. Worth

A. J. Ghajar

Norman N. Durham
Dean of the Graduate College

ACKNOWLEDGMENTS

The author wishes to express his sincere gratitude to his major adviser, Dr. David G. Lilley for his guidance and encouragement. Appreciation is also extended to other committee members, Dr. Peter M. Moretti and Dr. Afshin J. Ghajar.

The author would like to extend a special thank you to Dr. Sherry Southard for reading the manuscripts, Miss Moonsook Choi for typing the rough draft, and Mrs. Barbara Vick for typing the final copy.

The author also wishes to gratefully acknowledge NASA Lewis Research Center for financial support under NASA Grant No. NAG 3-74.

This study is dedicated to the author's parents, Mr. In Shik and Mrs. Chil Sung Yoon, for their encouragement, prayer and love.

TABLE OF CONTENTS

LIST OF TABLES

LIST OF FIGURES

NOMENCLATURE

C	velocity coefficient = $\rho V^2/[2(P_C - P_W)]$
CRZ	corner recirculation zone
CRTZ	central recirculation zone
D	test section diameter
d	inlet nozzle diameter
G	axial flux of momentum
L	contraction block station
P	time-mean pressure
Re	Reynolds number
Q	volume flow rate
S	swirl number
$\underline{v} = (u,v,w)$	time-mean velocity (in x-, r-, θ-directions)
V, $\bar{V}$	time-mean vector velocity magnitude
x, r, θ	axial, radial, azimuthal cylindrical polar coordinates
α	side-wall expansion angle
β	yaw angle of probe = $\tan^{-1}$ (w/u)
δ	pitch angle of probe = $\tan^{-1}$ $[v/(u^2 + w^2)^{1/2}]$
ρ	density
ϕ	swirl vane angle = $\tan^{-1}$ (w_{in}/u_{in}), assuming perfect vanes; general dependent variable

Subscripts

C	central pitot pressure port

d	relating to inlet nozzle diameter
in	inlet conditions
N,S,E,W	north, south, east, west pitot pressure ports
o	value at inlet to flowfield
h	swirl vane hub; expansion step height
p	relating to probe sensing tip diameter
rms	root-mean-squared quantity

Superscripts

$\overline{\quad}$	time mean average
'	fluctuating quantity

CHAPTER I

INTRODUCTION

1.1 The Investigation of the Flowfield in a Confined Jet

A need for more thorough understanding of the fluid dynamics of the flow in a gas turbine combustor chamber has been recognized by designers in recent years. The flowfield is presently being investigated using various methods of approach, such as computer simulation (1-5), flow visualization (5-6) and time-mean velocity measurements (7-14) for both swirling and nonswirling flows.

Until recently, extensive and reliable experimental data for swirling flow have been unavailable, and more experimental data are needed. Such data together with combustion characteristics would be very useful to designers as well as to theoretical investigators who could compare the experimental data with the data obtained from the simulated mathematical methods.

Current research focuses on measuring time-mean velocity and investigating the extent of the recirculation zone (known to have great effects on flame stability and length) and the effects of geometric parameters on the flowfield in a confined can-type gas turbine combustor.

In order to study the flow phenomena in the combustor, it is necessary not only to know the static pressure and flow velocity, but also the flow direction. In addition, the sensing probe must be sufficiently

small to be capable of point measurement without appreciably affecting the flow in the passages by its presence. In these experiments, the five-hole pitot probe was used because it is acutely sensitive to flow, convenient to manipulate and relatively compact. Measurements were taken for nonsirling and swirling flow with and without a contraction block in an axisymmetrical confined jet facility simulating typical geometry. All flowfields were nonreacting.

1.2 Review of Previous Flowfield Measurement Studies

Lee and Ash (7) developed and calibrated a three-dimensional spherical pitot probe which would measure the static pressure and the magnitude and direction of the velocity vector for any arbitrary flow angle without needing to be adjusted. It was designed mainly for measuring the relative flow through rotating three-dimensional blade cascades.

An investigation of flow patterns in the gas turbine combustion chamber with a three-dimensional probe was done by Hiett and Powell (8) in the early nineteen sixties. They found that there is a large recirculation zone between the main flow along the centerline and the second flow along the chamber wall, and that there is a high temperature zone in this area.

Janjua (9) measured three velocity components and turbulence levels for nonswirling flows with the six-orientation hot-wire technique. An uncertainty analysis done on this technique reveals that turbulence intensities and shear stresses are extremely sensitive to some input parameters such as yaw factor and mean voltages.

Velocity distribution in a sudden expanding circular duct was

investigated by Moon and Rudinger (10) with a Laser-Doppler velocimeter. These experiments located both the dividing streamline, which separates the main flow from the recirculation region, and the point of the flow reversal in the recirculation region.

Chaturvedi (11) measured the mean velocity and pressure and the characteristics of the turbulence by using a stagnation tube and pitot probe in a can-type axisymmetric expansion combustor for isothermal nonswirling flowfields. His data will be compared with the current research results because of the close geometric similarity and experimental conditions. Furthermore, in his experiment a single and cross-hot wire were used to measure the longitudinal component of turbulence intensity, u'_{rms}, radial intensity, v'_{rms}, and turbulent shear stress, $\overline{u'v'}$.

Systematic research of swirl was done by Mathur and MacCallum (12). The test facilities which they used for the free jet consisted of two concentric tubes with supplies of air to both the central (primary) and annular (secondary) streams. They used a three-dimensional probe to measure the velocity components in the three-dimensional flow. They measured the pressure drop across the vane swirler by both experimental work and theoretical analysis. They also investigated the distribution of the static pressure along the axis of the jets and the variations of the velocity distributions in the tube according to the change of swirl vane angle in the free jet. Mathur and MacCallum (12) followed the same procedure in the experiments for the enclosed jets as for the free jets and observed similar physical characteristics for the flows according to geometric changes. They determined that a large central recirculation exists along the axis in the swirling free and confined jets. A combustion chamber of square cross-section was used.

Pratte and Keffer (14) have investigated a swirling jet having a moderate ratio of swirling to axial momentum. They showed that the flow achieved a self similarity for the mean velocities rather quickly while the normal turbulent intensities reached a self-similar state after a longer period of jet development. Also the entrainment rate and angle of spread for the swirling jet was found to be nearly twice that of the nonswirling free jet.

1.3 Flowfield Independence of Reynolds Number

Although the current experiments are being done under low speed and nonreacting conditions because of the limitations of the experimental facilities, the results can be applied to actual combustor hardware, which usually operate at higher Reynolds numbers than those used in the present test facility.

Moon and Rudinger (10) noticed that the location of the flow reversal is practically independent of the flow velocity over the range from about 40 to 90 m/s in the small tube. They also observed that, as the Reynolds number increases, the uncertainty in determining the reattachment point appears to decrease.

Rhode (5), who performed experiments to investigate the asymptotic invariance of Re_d on the flowfield, showed that there is little change in the flowfield for $Re_d \geq 47{,}000$, where Re_d is based on the nozzle inlet velocity and diameter. His study was done for $x/D = 2.5$, $\alpha = 90$ degrees, and $\phi = 38$ degrees. Because the flow was considered to be most sensitive to Re_d at a location slightly downstream of the recirculation zone and the recirculation zone was observed just before the axial station of 2.5. Also the central rather than corner recirculation zone was selected

since most of the combustion and flame stability occur there (17-19). Measurement traverses were repeated for the same conditions while increasing Re_d for each of the flowfields. In the present study the experiments were repeated using the same procedure as Rhode but for x/D = 0.5, α = 90 degrees, and ϕ = 45 degrees, where the most extensive and strongest turbulent reverse flows had been observed in previous experiments. The results indicate also the excellent consistency of velocity profiles independent of Reynolds numbers for $Re_d \geq 90{,}000$ at the axial location as shown later in Figure 11. The present study uses Reynolds numbers ranging from 53,000 to 220,000 as tabulated in Table I. For strong swirling flow with swirl vane angle ϕ = 70 degrees, the Reynolds number is 53,000. This is not high enough to be sure that the flowfiled is independent of Reynolds number, but 53,000 is the highest value which can be reached for ϕ = 70 degrees in the current experimental facilities. In this study, a flowfield is assumed to be independent of Reynolds number for $Re_d \geq$ 53,000.

1.4 The Scope and Significance of the Present Research

In the present study, a five-hole pitot probe was used to measure the magnitude and direction of the time-mean velocity in the combustor. Measurements have been carried out for sudden expansion and gradual expansion (side-wall expansion angle α = 90 and 45 degrees) for nonswirling and swirling flows [swirl vane angle zero (swirler removed), 38, 45, 60, and 70 degrees]; and then with contraction block inserted at certain axial stations (L/D = 1.0 and 2.0). The raw data measured by a five-hole pitot probe are reduced by a FORTRAN computer program (which is described

in Appendix C) and plotted as axial, radial, and swirl velocity components by a plotting program using a complot plotter.

The current research is significant for the following reasons (23):

1. The magnitude and direction of the flow velocity is measured.

2. The extent of the corner and central recirculation zones is identified.

3. The effects of geometric parameters on the flowfields in the combustor chamber are determined.

4. Miscellaneous results such as the performance of the swirl vanes and the independence of the flowfields from the Reynolds number are provided.

The research is limited by the following factors:

1. The difficulty in investigating the exact reattachment points of the flows.

2. The low sensitivity of the probe to small velocities.

1.5 Outline of the Thesis

In the previous sections, the significance and scope of this study are introduced. Basic concepts are also given with reference to previous studies.

Chapter II describes the facilities and instrumentation employed. This chapter also explains the operation of the five-hole pitot probe, the concept of swirling flow, and the way a swirler performs.

The procedures of data measurements and reduction are described in Chapter III. A separate documentation in Appendix C contains a detailed description of the data reduction computer program and instructions for

its use. Descriptions of the calibrations of the voltmeter and the five-hole pitot probe are also included in this chapter.

Results for sudden expansion flows are discussed with emphasis on the extent of the recirculation zone in Section 4.1. Effects of geometric parameters such as a gradual expansion and a contraction nozzle are described in Sections 4.2 and 4.3.

Chapter V summarizes all of these results and suggests further research.

Appendix A and B include tables and figures, respectively. User's guide to five-hole pitot probe data reduction computer program is in Appendix C.

CHAPTER II

EXPERIMENTAL FACILITIES AND FIVE-HOLE PITOT PROBE INSTRUMENTATION

2.1 An Idealized Flowfield

The test facility used to obtain a uniform flow of relatively low turbulence level is a wind tunnel designed and built at Oklahoma State University. The test section of the swirling confined-jet facility is a simulation of a typical axisymmetric can-type combustion chamber from a gas turbine engine as shown in Figure 1. A schematic of the facility is given in Figure 2. Since the actual gas turbine combustor is too complicated to be simulated in a laboratory, it is simplified, but the typical geometric features such as the presence of a sudden or gradual expandion block, a contraction nozzle, a swirler and a can-type shape of the flowfield domain are kept.

Ambient air enters the low-speed wind tunnel through an air filter consisting of a large box covered with foam rubber. Next a six-blade propeller fan, driven by a 5 h.p. varidrive motor which can be varied continuously from 1600 rpm to 3100 rpm, accelerates the air to the desired velocity.

The intensity of the turbulence caused by the driving fan is partially reduced by gradually expanding the flow into a stilling chamber containing numerous fine mesh screens. The turbulence intensity is further

reduced by passage through a turbulence management section. This section consists of a perforated aluminium plate (2 mm diameter holes) followed by a fine mesh screen, a 12.7 cm length of packed straws, and five more fine mesh screens. Most of the control of the turbulence occurs in this portion. The airflow, which is now relatively uniform and of low turbulence, then enters a contoured nozzle, which was designed to produce a minimum adverse pressure gradient on the boundary layer and thus avoid local separation and flow unsteadiness. The ratio of the area of the maximum cross section of the contour nozzle to that of the nozzle throat is approximately 22.5. The diameter of the nozzle throat is about 15 cm. There is a hole of 1 cm diameter just upstream of the nozzle throat for insertion of a standard pitot-static probe, so that the dynamic pressure can be measured upstream of the swirler. With the measured dynamic pressure, the corresponding nozzle throat velocity and Reynolds number are obtained from the dynamic pressure conversion characteristic shown in Figure 3.

2.2 Test Section

The test section is composed of a swirl vane assembly, an expansion or contraction block, a contraction nozzle, and a simplified can-type gas turbine combustion chamber. Details concerning the swirl vane assembly are given in Section 2.4.

The expansion or contraction block can be used optionally to give the simulated geometric characteristics desired for a certain expansion condition. The expansion blocks are interchangeable and those currently in use have expansion angles of 90 and 45 degrees. The expansion blocks have an inside diameter the same as that of the nozzle throat, and an

outside diameter approximately twice that of the nozzle throat, to match the test section inside diameter. The experimental results of Rhode (5) show that varying the expansion angle of the side wall does not affect the flowfield much except that the corner recirculation region decreases sharply as the expansion angle is decreased. The current study was conducted with side-wall expansion angles of α = 90 and 45 degrees, to investigate the effects of both sudden and gradual expansions. A contraction block is used to simulate the confining wall of a real gas turbine combustor at the downstream end. The block was designed with a rounded profile that is one-quarter of a circle and a downstream cross-sectional area half that of the test section. The rounded upstream face is smoothly finished to reduce the surface shear stress. Details of the contraction block employed are given in Figure 4.

The test section used in this study is a straight, long circular plexiglass tube having a 30 cm inside diameter. Holes with 2.54 cm diameter are located along the length of the tube at distances which are multiples of x/D = 0.5, so that the pitot probe can be inserted into the flow and traverses made in the radial direction. It does not have film cooling holes or dilution air holes. The test section is carefully aligned with a low-power laser beam so that the centerlines of the test section and the wind tunnel coincide.

2.3 Five-Hole Pitot Probe Instrumentation

A five-hole pitot probe is one of the few instruments capable of measuring both the magnitude and the direction of fluid velocity simultaneously. The five-hole pitot probe used in this study is a model DC-125-12-CD manufactured by United Sensor and Control Corp. The

sensing head is hook-shaped to allow for probe shaft rotation without altering the probe tip location. Little information is available concerning the effects of turbulence on a pressure probe in a swirling flow. However, it is asserted that the five-hole pitot probe is accurate within approximately 5 percent for most of the measurements (5). This value may increase to 10 percent as the velocity magnitude falls below approximately 2.0 m/s because of the insensitivity of the probe to low dynamic pressure and the dependence of probe calibration on the probe Reynolds number.

There are three standard methods of operating the five-hole pitot probe:

1. To adjust the orientation of the probe in both pitch and yaw so that the probe is aligned with the local flow direction.

2. To determine the flow direction from the calibration relationship between probe pressures and flow direction while maintaining a fixed probe orientation.

3. To align the probe yaw angle with the flow yaw angle while deducing the pitch angle and total velocity coefficient calibration characteristics.

The third method was employed in this study because it used readily available orientation equipment and relatively simple data reduction procedures.

The instrumentation assembly, in addition to the five-hole pitot probe, is composed of a manual traverse mechanism, two five-way ball valves, a differential pressure transducer, a power supply, and an integrating digital voltmeter. The differential pressure transducer is model 590D from Datametrics, Inc. It has a differential pressure range of from

0 to 1.3 x 10^3 N/m^2. The integrating voltmeter is the TSI model 1076. As auxillary equipment, a model 631-B strobotac from General Radio, Inc. was used to check the fan speed and a micro-manometer along with a pitot-static probe was used to measure the dynamic pressure in the nozzle throat just upstream of the swirler. Also, a barometer/thermometer unit from Cenco Corporation was used for local pressure and temperature readings. Measurement apparatus are shown in Figure 5.

2.4 Swirler

Swirling jets are used as a means of controlling the length and stability of the flame in many combustor designs. The effects of the degree of swirl on the flowfields and combustion have been extensively investigated (5, 12, 19-21). A swirl number characterizes the degree of swirl. It is usually defined as the ratio of axial flux of tangential momentum to the axial flux of axial momentum (including a pressure contribution), nondimensionalized by use of the inlet nozzle radius. Thus:

$$S = \frac{G_\theta}{G_x d/2} \tag{2.1}$$

where:

G_θ = the axial flux of tangential momentum flux; and

G_x = the axial flux of axial momentum, including pressure contribution.

Often the pressure term is neglected, and the expression reduces to (20)

$$S = \frac{2}{3}\left(\frac{1 - Z^3}{1 - Z^2}\right) \tan \phi \tag{2.2}$$

where $Z = d_h/d$ for the case of an annular vane swirler idealized with

flat axial and flat swirl velocity profiles at the inlet. This is the case in the present study.

The swirler used currently was constructed at Oklahoma State University according to preliminary design plans from NASA. The schematic of the swirler is shown in Figure 6. It has ten adjustable vanes and a hub with a streamlined nose and a flat downstream face. The nose has a hyperbolic shape with a very smooth surface to reduce the pressure drop. The flat face and location of the hub is a simulation of an actual fuel injector. The flat blades are wedge-shaped to give a constant pitch-to-chord ratio of approximately one which should give good turning efficiency (21).

Mathur and MacCallum (12) thought that an overlap between the adjacent vanes is a determinant parameter to give a complete deflection of air. They found that a positive overlap is essential for effective directing of the air and a 30 degrees overlap is adequate for complete deflection. An approximately variable 20 degrees overlap is provided by the swirler used in this study. The positive axial velocity which was observed near to the hub might be the result of an insufficient overlap. An extensive study concerning the swirler performance is being conducted by Sander (24).

CHAPTER III

MEASUREMENT AND REDUCTION OF DATA

A schematic of the five-hole pitot probe is shown in Figure 7. To obtain all the components of the velocities in the axial, radial and azimuthal directions at a given location in the model combustor, one must know the yaw angle β, the pitch angle δ, and the magnitude of the total velocity V at that point. The yaw angle β can be measured directly from the reading of the rotary vernier. The pitch angle δ and the total velocity V can be found from the corresponding calibration in a free jet.

With the above information, Rhode (5) wrote a data reduction computer program. This program reduces the raw pressure data from direct measurement into u, v, and w velocity component data.

3.1 Measurement Procedures

When using the five-hole pitot probe, one aligns the probe tip with the direction of the air flow in the horizontal plane and then reads the yaw angle β and the two differential pressures $(P_N - P_S)$ and $(P_C - P_W)$. These pressures are used to obtain the pitch angle δ in the vertical plane and the magnitude of total velocity vector from the calibration characteristics.

The first step in preparing to take measurements with the five-hole pitot probe is to measure the dynamic pressure of flow with a pitot-static probe at the nozzle throat just before the swirler. Then the

pressure transducer must be nulled for zero differential pressure. This is done by turning an adjustment screw on the transducer until the voltmeter reading for zero differential pressure (both ports open to atmosphere) is zero.

The next step in preparing for measurements is to adjust the position of the test section until the wind tunnel and test section axes coincide, and also to adjust the traverse mount until the probe zero point lies on the test section axis. Then the varidrive motor is set at the proper rpm to give the desired air velocity at the nozzle throat. The fan speed is checked regularly with a strobotac to keep the air velocity constant.

Before the production measurements are taken, the five-hole pitot probe rotary vernier must be set for zero yaw angle so that the x and θ axes of the measurement coordinate frame coincide with those of the test section. This is achieved by adjusting the yaw angle to be zero at the center of the test section inlet for nonswirling flow. Each radial traverse measurement begins at the centerline, which is identified with a low-power laser beam. The pressure and yaw angle data are read at 0.3 inch increments up to 5.7 inches from the centerline. In this study, 10 seconds time-mean data readings are used. To measure 10 seconds time-mean values, 30 to 40 seconds settling time is needed to allow transients to subside in the measuring apparatus.

The first measurement for each location is the yaw angle for a zero reading of $(P_W - P_E)$. This means that the probe tip is aligned with the flow direction in a horizontal plane. Then the five-way switching valves are set so that $(P_N - P_S)$ is sensed by the pressure transducer. Finally, the reading of $(P_C - P_W)$ is similarly measured.

3.2 Calibrations

Two kinds of calibration are employed to reduce the raw data from the direct measurements. One is the calibration of the voltmeter, which determines a relationship between the voltmeter output and the magnitude of velocity. The other is the calibration of the five-hole pitot probe, which consists of two calibration characteristics: pitch angle δ versus differential pressure ratio $(P_N - P_S)/(P_C - P_W)$, and velocity coefficient

$$C = \rho V^2/[2(P_C - P_W)] \tag{3.1}$$

versus pitch angle δ.

Proper calibration is extremely critical to the accuracy of the experimental work. The calibration of the five-hole pitot probe is based on the investigation, which concluded that the calibration coefficients are independent of Re_p, which is based on probe tip diameter (5). The investigation determined that this conclusion is true for $Re_p \geq 1090$, or a local velocity of 5.4 m/s. Low velocity might cause some calibration error. However, the investigation also shows that this calibration error affects the velocity measurements typically by less than 6 percent for $Re_p \geq 400$, corresponding to a local velocity greater than 2.0 m/s. In this study, all calibrations are conducted at air velocity of 4.6 m/s.

A schematic of the calibration facilities is given in Figure 8. The jet employed for calibrations is a free jet with a contoured nozzle which has a 3.5 cm diameter throat. Compressed air is used for the calibrating jet and its mass flow rate is controlled by a small pressure regulartor and a Fisher and Porter model 10A1735A rotameter. The five-hole pitot probe is rotated by the rotary table model BH-9 from Troyke Manufacturing Co., whose rotary vernier is readable to $\pm$ 0.5 minutes of arc.

The calibration procedure of the voltmeter consists of reading the micro-manometer with a pitot static probe for a known air flow rate. The volume flow rate is incremented by 0.5 ft^3/min [1 ft^3/min = 0.000472 m^3/s] over the range $0.5 \leq Q \leq 9.0$. As shown in Figure 9, there exists a linear relationship between the velocity magnitude and the pressure reading.

The first step to calibrate the five-hole pitot probe is to set the probe tip in the horizontal plane so that the yaw is aerodynamically nulled. This condition can be maintained by frequently checking the zero reading for $(P_W - P_E)$ during the whole calibration proceeding. The next step consists of reading the voltage output from the pressure transducer for differential pressures $(P_N - P_S)$ and $(P_C - P_W)$. These data are measured at 5 degrees increments in δ over the range $-55 \leq \delta \leq 55$.

Figure 10 shows the calibration characteristics from which the pitch angle δ and the velocity coefficient C are obtained, respectively. The calibration is conducted two times to be sure that the measurements are exact and that they remain the same. Even if the measurements are taken by different observers and at different times, the consistency is splendid. Most of the discrepancies lie within 2-3 percent, and the maximum is within 10 percent.

3.3 Data Reduction

It is difficult to define in a word what turbulence is. According to Hinze's (22) defninition, "Turbulent fluid motion is an irregular condition of flow in which the various quantities show a random variation with time and space coordinates, so that statistically distinct values can be disconcerned." The vector velocity of turbulent flow consists of

a time-mean velocity and a fluctuating velocity component. As mentioned in the previous section, the differential pressure readings from the five-hole pitot probe are utilized directly to obtain the square of the vector velocity in the velocity coefficient. With the information from the five-hole pitot probe measurements alone, it is impossible to express the square of the vector velocity $\overline{V^2}$ as the sum of the square of the magnitude of the time-mean velocity $\overline{V}^2$ and the time-mean fluctuation term $\overline{V'^2}$, as given by

$$\overline{V^2} = \overline{V}^2 + \overline{V'^2} \tag{3.2}$$

Obtaining the fluctuation term $\overline{V'^2}$ depends on other methods of measurement. But the available data for the term $\overline{V'^2}$ is not thought to be reliable. Furthermore, an established theory for the effect of turbulence in swirl flows on pressure probes is unavailable. So even though some discrepancy is to be expected, the reduced velocity is taken to be the time-mean velocity magnitude $\overline{V}$ which is written without the overbar onward. In this study, all properties of the acting fluid are assumed to be those of ambient air.

With the measurement data of the differential pressure ratio $(P_N - P_S)/(P_C - P_W)$, the corresponding pitch angle δ is obtained with a cubic spline interpolation technique from the calibration characteristics shown in Figure 10(a). The velocity coefficient C is determined from this value by using the corresponding calibration characteristic in Figure 10(b). The magnitude of the velocity vector is calculated by

$$V = [\frac{2}{\rho} (P_C - P_W) \cdot C]^{1/2} \tag{3.3}$$

The velocity components are easily calculated by elementary geometry using the measured yaw angle β, the derived pitch angle δ, and the total velocity V.

All data used in this investigation were reduced with the FORTRAN data reduction computer program written by Rhode (5). Full details of the data reduction procedure are given in Appendix C, including a program listing, sample input and output, and a user's guide.

CHAPTER IV

RESULTS

Nonswirling and swirling nonreacting flows are investigated in an axisymmetric test section with expansion ratio D/d = 2, which may be equipped with a contraction nozzle of area ratio 2 and 4. Velocity measurements are made with the five-hole pitot probe as described in Chapter III. An analysis is made of the effects of various geometric parameters on the extent of the recirculation zones in the flowfield. These parameters include side-wall expansion angle α = 90 and 45 degrees, swirl vane angle ϕ = 0, 38, 45, 60, and 70 degrees, and contraction nozzle location L/D = 1 and 2 (if present). The nozzle inlet velocities and Reynolds numbers employed in this study are high enough to ensure that the flowfields are investigated under conditions independent of Reynolds number variation. All nozzle inlet velocities and Reynolds numbers employed are listed in Table I. Flow characteristics are tabulated in terms of normalized u, v, and w velocity components, yaw angle β and pitch angle δ in Tables II through XII. Axial and swirl velocity profiles for all flows studied are shown in Figures 12 through 16 and 18 through 20.

4.1 Effects of Swirl on Sudden Expansion Flows

Swirling flows result from the application of a spiraling motion, with a swirl velocity component being imparted to the flow via the use

of swirl vanes. A swirl number S characterizes the degree of swirl. The swirl vane angles employed in this study are 0 (swirler removed), 38, 45, 60, and 70 degrees. These correspond to swirl numbers s of 0, 0.52, 0.67, 1.15, and 1.83, under the definition of swirl number introduced in Section 2.4. Figure 12 parts a through e show the axial and swirl velocity profiles for ϕ = 0, 38, 45, 60, and 70 degrees, respectively, with side-wall expansion angle α = 90 degrees.

The nonswirling flow investiaged is obtained with the swirler removed. Figure 12(a) shows an uniform axial velocity entering the test section. The corner recirculation zone extends to just beyond x/D = 2.0. The measurements for a corresponding flow taken with a stagnation tube and pitot tube by Chaturvedi (11). He found the reattachement point to be at x/D = 2.3 which is in good agreement with the present study. Moon and Rudinger (10) measured the reattahcment point with both theoretical and experimental methods in a similar circular test section with an expansion ratio D/d = 1.43, which is different from the present study [with D/d = 2]. The result yielded a value of x/D = 1.25 as a reattachment point, which corresponds to an attachment point approximately eight step-heights downstream. This is in good agreement with the present study.

The velocity profiles for swirling flows shown in Figure 12 parts b through e reveal that the flow entering through the swirl vanes is not uniform and has steep velocity gradients in the radial direction especially at high swirl numbers. Furthermore, a considerable back flow around the hub is observed for ϕ = 70 degrees, as shown in Figure 12(e). For all values of swirl vane angle used in this study, the corner recirculation zone is not seen at x/D = 0.5 the closest axial location to the expansion block; instead, the maximum axial velocity is observed close

to the top wall at x/D = 0.5. The effects result from the strong centrifugal forces present in the incoming swirling flow.

The central recirculation zone and precessing vortex core are now discussed. The precessing vortex core is defined as the region of high swirl, low axial velocity flow along the axis, which has a relatively constant small diameter. In flow visualization studied, it is seen to precess along the axis of the test section. The central recirculation zone is defined as the wide reverse flow region encountered near the inlet. Artistic impressions are given later in Figure 21 in which lines have been drawn connecting the radial positions of zero axial velocity. In case of the vortex core, that region is drawn along the zero axial velocity boundary in the downstream direction after the central recirculation region. The size of the central recirculation zone increases with the increasing swirl vane angle until a certain value of swirl vane angle is reached (around 40 degrees). Then its length begins to decrease under stronger swirl conditions. The results are tabulated in Table XIII. The core vortex was present at all values of swirl vane angle used in this investigation. In contrast to the central recirculation zone, the vortex core gets larger and larger continuously as the swirl vane angle increases.

The swirl velocity peaks sharply around the edge of the expansion block before becoming more uniform farther downstream as shown in Figure 12 parts b through e. A considerably nonuniform swirl velocity profile is observed at x/D = 0.5. Thereafter, relatively steady and uniform velocity profiles are seen, except for the region around the axis. The radial location where the maximum swirl velocity occurs goes up as the swirl vane angle increases. This trend is caused by the increase of

centrifugal effects. The swirl velocity along the axis is found to be zero as expected because of symmetry.

4.2 Effects of Gradual Expansion on Flows

Gradual expansion flows with α = 45 degrees were measured at two axial stations of x/D = 0.5 and 1.0 for swirl vane angles of 0, 38, 45, 60, and 70 degrees. Only the upstream flowfield needed to be thoroughly investigated in these cases, since inlet expansion effects affect this region the most, and their influence rapidly diminishes in the downstream direction (5, 13). Measurements were not taken at the inlet in this geometry because the presence of the expansion block interferes with probe positioning.

The corresponding sequence of axial and swirl velocity profiles to a sudden expansion is given in Figure 13 parts a through e for α = 45 degrees. Velocity profiles for a gradual expansion follow a similar trend to those for a sudden expansion. The major effect of a gradual inlet expansion is to encourage the air to flow along the side sloping wall, shorten the corner recirculation zone and accelerate axial velocities close to the top wall. Influence on the central recirculation zone for the swirl flow cases is minimal.

4.3 Effects of Contraction Nozzle on Flows

It is best to interpret the data obtained when the contraction block is inserted at different axial stations on the flowfields by comparing them to the data obtained without the contraction block. The measurements were taken at axial locations ranging from the inlet plane to the axial station just upstream of the station where the contraction block

was located. The effect of a contraction nozzle was investigated with the contraction block at L/D = 1 and 2 for a range of swirl strengths ϕ = 0, 45, and 70 degrees with sudden expansion α = 90 degrees only. Figures 14, 15, and 16 present these velocity profiles with L/D = 1 and 2 in parts a and b, respectively.

Figure 14 shows that the contraction block generally affects the flowfield very little under nonswirling conditions. Furthermore, as the block is moved farther in the downstream direction, its effect on the flowfield decreases. The only effect that can be noticed from the velocity profiles is decreased in length of the corner recirculation region due to the nozzle effect.

Figure 15(a) shows the axial and swirl velocity profiles for the intermediate swirling flow of ϕ = 45 degrees with a contraction block at L/D = 1. Significant positive axial velocities are observed along the center line. This situation is in striking contrast to that of the intermediate swirling flow without the contraction block, in which case the central recirculation zone spreads extensively along the centerline to x/D = 1.5 with vortex core following it in the test section. Slightly larger swirl velocities are seen in Figure 15(a) with contraction block at L/D = 1 than in Figure 12(c) without contraction block. Velocity Profiels shown in Figure 15(b), for ϕ = 45 degrees with contraction block at L/D = 2, follow a trend similar to the corresponding flow without the contraction block at the first two axial stations of x/D = 0 and 0.5. But the axial velocities have quite different profiles at two axial stations of x/D = 1.0 and 1.5 being affected by the proximity of the contraction nozzle. At the axial station of x/D = 1.0, reverse flow is not observed at all, and considerable positive axial velocities are measured

near the axis. A rather uniform velocity profile is obtained at x/D = 1.5. The effect of the contraction block on the swirl velocity profiles is negligible. The presence of a contraction block, in the intermediate swirling flowfield, results in the existence of positive axial velocities near the axis.

For strong swirling flows of ϕ = 70 degrees, the axial and swirl velocity profiles are shown in Figure 16. A contraction block does not affect the flowfield much except at the axial station immediately upstream of the block.

In comparison with corresponding cases without downstream blockages, Figure 16(a) shows a wider central recirculation zone when L/D = 1 and Figure 16(b) shows a narrower precessing vortex core when L/D = 2. The swirl velocity profiles do not change significantly with or without presence of downstream blockages.

In summary, a nozzle has most effect on the intermediate swirl case ϕ = 45 degrees. Its contraction effect in this case is strong enough to overwhelm the swirling recirculation region.

However, a contraction has little effect on weakly swirling and strongly swirling flows, which are dominated by forward flow and centrifugal forces, respectively.

Since the most drastic change in the velocity profile was observed at x/D = 1.0 for intermediate swirling flow of ϕ = 45 degrees with a contraction block at L/D = 2, the measurements were repeated to ensure confidence in them. The new results, obtained at a slightly higher Reynolds number, confirm the previous results. Both sets of results are shown in

Figure 17, and seem to be very consistent.

The effect of a stronger contraction nozzle was investigated for a range of swirl lengths ϕ = 0, 45 and 70 degrees with side-wall expansion angle α = 90 degrees. The contraction nozzle, of area ratio 4 with 45 degree sloping upstream face, is located at L/D = 1 and 2. Figures 18, 19, and 20 show these velocity profiles with L/D = 1 and 2 in parts a and b, respectively.

Figure 18 shows that the flowfield with a strong contraction nozzle changes very little as compared to the corresponding flowfield with a weak contraction nozzle shown in Figure 14.

Figure 19 shows the axial and swirl velocity profiles for a swirl vane angle ϕ = 45 degrees. The presence of a strong contraction nozzle generates the high positive axial velocity near the axis. However, it deccelerates the axial velocity close to the top wall. The central recirculation zone is smaller and located in an annular region, which excludes the axis. The swirl velocity profiles show narrower and stronger core swirl velocity gradients than previously.

For swirl vane angle ϕ = 70 degrees, the axial and swirl velocity profiles are given in Figure 20. It shows that the axial velocity near the axis is highly positive and the central recirculation region extends only to less than x/D = 1.0, much less than its corresponding case with the weak contraction block. At the axial station x/D = 1.0, forward flow occurs across the whole test section. This situation is in sharp contrast to that of a weak contraction nozzle, in which case the contraction block affects the flowfiled very little under strong swirling conditions. Swirl velocity profiles given in Figure 20 show the narrower strong core swirl velocity gradient, as also observed in the

swirl vane angle ϕ = 45 degree case.

The above observances are summerized as follows. The effect of a weak contraction nozzle of area ratio 2 is confined to intermediate swirling flow case, while a strong contraction nozzle of area ratio 4 affects both intermediate and strong swirling flow cases. Artistic impressions for a weak contraction nozzle and a strong contraction nozzle with emphasis on the recirculation zones are given in Figures 20 and 23, for a range of swirl strengths with blockage located at L/D = 2.

CHAPTER V

CLOSURE

5.1 Summary

This study is five-hole pitot probe time-mean velocity measurements in confined swirling flows under low speed and nonreacting conditions. Three velocity components normalized with the inlet axial velocity are tabulated along with yaw and pitch angles. This provides an extensive data base for later verification of a theoretical simulation of the complex turbulent flowfield.

The extent of the recirculation zone for sudden expansion flows with α = 90 degrees is characterized for swirl vane angles ϕ = 0, 38, 45, 60, and 70 degrees. For a nonswirling flow, the corner recirculation zone extends to just beyond 2 with no central recirculation zone. The presence of a swirler shortens the corner recirculation zone and generates a central recirculation zone followed by a precessing vortex core. The largest central recirculation zone was shown to be in the intermediate swirling flow case of ϕ = 38 degrees; the strongest precessing core vortex was found to be in the strongest swirling flow considered with ϕ = 70 degrees.

Effects of a gradual inlet expansion of α = 45 degrees are investigated for the same swirl vane angles as employed for a sudden inlet expansion. Velocity profiels for a gradual expansion follow a similar

trend to those for a sudden expansion. The only major effect of a gradual inlet expansion is to encourage the flow to remain close to the sloping side wall and shorten the extent of the corner recirculation zone in all cases investigated.

Effects of the presence of a contraction nozzle at L/D = 1 and 2 are investigated for ϕ = 0, 45, and 70 degrees. A contraction nozzle has little effect on weakly swirling and strongly swirling flows, which are dominated by forward flow and centrifugal forces, respectively. For the intermediate swirl case of ϕ = 45 degrees, it encourages forward movement of otherwise slow-moving air and thereby shortens the central recirculation zone. A strong contraction nozzle of area ratio 4 has a more dramatic effect on the flowfields.

5.2 Recommendations for Further Work

The five-hole pitot probe technique is a useful cost-effective tool to investigate turbulent swirling recirculating confined flow. It enables time-mean axial, radial and swirl velocities to be deduced at any location in the flowfield. It is strongly recommended for use to obtain further flowfield measurements in the test facility at Oklahoma State University. It has, however, some inherent problems:

1. Weak sensitivity to small velocities, which might permit large relative errors.

2. Turbulence effects on the measurement of time-mean data cannot be easily accounted for.

3. The measurement of normal and shear turbulent stresses is not possible.

It is recommended that further work be done on the repeatability,

reliability, and accuracy of this technique. Results may be compared with hot-wire and laser doppler anemometers measurements in corresponding flow situations.

REFERENCES

(1) Rhode, D. L., D. G. Lilley, and D. K. McLaughlin. "On the Prediction of Swirling Flowfields Found in Axisymmetric Combustor Geometries." Proceedings, ASME Symposium on Fluid Mechanics of Combustion Systems. Boulder, Colo., June 22-24, 1981, pp. 257-266. See Also: ASME Journal of Fluids Engineering, 1982 (in press).

(2) Lilley, D. G. "Prospects for Computer Modeling in Ramjet Combustors." AIAA Paper No. 80-1189. Harford, Conn., June 30-July 2, 1980.

(3) Serag-Eldin, M. A. and D. B. Spalding. "Computations of Three Dimensional Gas Turbine Combustion Chamber Flow." Transaction ASME, Journal of Engineering for Power, Vol. 101 (July, 1979), pp. 326-336.

(4) Novick, A. S., G. A. Miles, and D. G. Lilley. "Numerical Simulation of Combustor Flow Fields." Journal of Energy, Vol. 3, No. 2 (March-April, 1979), pp. 95-105.

(5) Rhode, D. L. "Predictions and Measurements of Isothermal Flowfields in Axisymmetric Combustor Geometries." Ph.D. Thesis (December, 1981), Oklahoma State University.

(6) Bird, J. D. "Visualization of Flowfields by Use of a Tuft Grid Technique." Journal of Aeronautical Science, Vol. 19 (1952), pp. 481-485.

(7) Lee, J. C. and J. E. Ash. "A Three-Dimensional Spherical Pitot Probe." Transactions, ASME (April, 1956), pp. 603-608.

(8) Hiett, G. F. and G. E. Powell. "Three-Dimensional Probe for Investigation of Flow Patterns." The Engineer (January, 1962), pp. 165-170.

(9) Janjua, S. I. "Turbulence Measurements in a Complex Flowfield Using a Six-Orientation Hot-Wire Probe Technique." M.S. Thesis (December, 1981), Oklahoma State University.

(10) Moon, L. F. and G. Rudinger. "Velocity Distribution in an Abruptly Expanding Circular Duct," Journal of Fluids Engineering (March, 1977), pp. 226-230.

(11) Chaturvedi, M. C. "Flow Characteristics of Axisymmetric Expansions." Proceedings, Journal of the Hydraulics Division, ASCE, Vol. 89, No. HY3 (1963), pp. 61-92.

(12) Mathur, M. L. and N. R. L. MacCallum. "Swirling Air Jets Issuing from Vane Swirlers. Part 1: Free Jets; Part 2: Enclosed Jets." Journal of the Inst. of Fuel, Vol. 40 (May, 1967), pp. 238-245.

(13) Rhode, D. L., D. G. Lilley, and D. K. McLaughlin. :Mean Flowfields in Axisymmetric Combustor Geometrics with Swirl." AIAA Paper No. 82-0177, Orlando, Florida, January 11-14, 1982.

(14) Pratte, B. D. and J. F. Keffer. "The Swirling Turbulent Jet." Journal of Basic Engineering, Vol. 94 (December, 1972), pp. 739-748.

(15) Back, L. H. and E. J. Roschke. "Shear Layer Flow Regimes and Wave Instabilities and Reattachment Lengths Downstream of an Abrupt Circular Channel Expansion." Journal of Applied Mechanics Vol. 94 (September, 1972), pp. 677-681.

(16) McMahon, H. M., D. D. Hester, and J. G. Palfery. "Vortex Shedding from a Turbulent Jet in a Cross-Wind." Journal of Fluid Mechanics, Vol. 48 (1971), pp. 73-80.

(17) Lilley, D. G. "Flowfield Modeling in Practical Combustors: A Review." Journal of Energy, Vol. 3 (July-August, 1979), pp. 193-210.

(18) Krall, K. M. and E. M. Sparrow. "Turbulent Heat Transfer in the Separated, Reattached, and Redevelopment Regions of a Circular Tube." Journal of Heat Transfer (February, 1966), pp. 131-136.

(19) Kerr, N. M. and D. Fraser. "Swirl. Part 1: Effect on Axisymmetrical Turbulent Jets." Journal of Institute of Fuel, Vol. 38 (December, 1965), pp. 527-538.

(20) Beer, J. M. and N. A. Chigier. Combustion Aerodynamics. London: Applied Science; and New York: Halsted-Wiley, 1972.

(21) Supta, A. K., D. G. Lilley, and N. Syred. Swirl Flows. Abacus Press, Tunbridge Wells, England, 1982 (in press).

(22) Hinze, J. O. Turbulence: An Introduction to Its Mechanism and Theory. McGraw-Hill Book Company, Inc., 1959.

(23) Yoon, H. K. "Five-Hole Pitot Probe Time-Mean Velocity Measurements In Combustor Flowfield." Thirteenth Southwestern Graduate Research Conference in Applied Mechanics, Norman, Oklahoma, April 16-17, 1982, pp. 131-137.

(24) Sander, G. F. "Annular Vane Swirler Performance." Thirteenth Southwestern Graduate Research Conference in Applied Mechanics, Norman, Oklahoma, April 16-17, 1982, pp. 274-280.

(25) Gurtis, F. G. Applied Numerical Anaysis 2nd Edition . Addison-Wesley Publishing Company, Massachusetts, May, 1980.

APPENDIX A

TABLES

TABLE I

NOZZLE INLET VELOCITIES AND REYNOLDS NUMBERS

ϕ	$\alpha = 90°$		$\alpha = 45°$		$\alpha = 90°$, L/D = 1, 2	
	U_{in} (m/s)	Re_d	U_{in} (m/s)	Re_d	U_{in} (m/s)	Re_d
0°	15.7	150,000	15.5	154,000	22.3	220,000
38°	10.5	100,000	10.6	105,000		
45°	12.6	120,000	14.9	148,000	13.5	134,000
60°	8.84	84,000	9.58	95,000		
70°	5.57	53,000	6.25	62,000	6.8	67,500

TABLE II

VELOCITY DATA FOR NONSWIRLING FLOW $\phi = 0°$

	I =	1	2	3	4	5	6
	X =	0.0	0.14935	0.29845	0.44780	0.59695	0.74625
J	Y						
20	0.14478	0.0	1.80E+02	1.80E+02	0.0	0.0	3.57E+02
19	0.13716	0.0	1.80E+02	1.80E+02	0.0	0.0	3.57E+02
18	0.12954	0.0	1.80E+02	1.80E+02	3.58E+02	0.0	3.57E+02
17	0.12192	0.0	1.80E+02	1.80E+02	3.58E+02	3.60E+02	3.58E+02
16	0.11430	0.0	1.80E+02	1.80E+02	3.58E+02	3.60E+02	3.58E+02
15	0.10668	0.0	1.80E+02	3.60E+02	3.58E+02	3.60E+02	3.58E+02
14	0.09906	0.0	1.80E+02	3.60E+02	3.58E+02	3.60E+02	3.58E+02
13	0.09144	0.0	3.60E+02	3.60E+02	3.58E+02	3.60E+02	3.58E+02
12	0.08382	0.0	3.60E+02	3.60E+02	3.59E+02	3.60E+02	3.58E+02
11	0.07620	0.0	3.60E+02	3.60E+02	3.59E+02	3.60E+02	3.58E+02
10	0.06858	3.60E+02	3.60E+02	3.60E+02	3.60E+02	3.60E+02	3.58E+02
9	0.06096	3.60E+02	3.60E+02	3.60E+02	3.60E+02	3.60E+02	3.58E+02
8	0.05334	3.60E+02	3.60E+02	3.60E+02	3.60E+02	3.60E+02	3.59E+02
7	0.04572	3.60E+02	3.60E+02	3.60E+02	3.60E+02	3.60E+02	3.59E+02
6	0.03810	3.60E+02	3.60E+02	3.60E+02	3.60E+02	3.60E+02	3.59E+02
5	0.03048	3.60E+02	3.60E+02	3.60E+02	3.60E+02	3.60E+02	3.59E+02
4	0.02286	3.60E+02	3.60E+02	3.60E+02	3.60E+02	3.60E+02	3.60E+02
3	0.01524	3.60E+02	3.60E+02	3.60E+02	3.60E+02	3.60E+02	3.60E+02
2	0.00762	3.60E+02	3.60E+02	3.60E+02	3.60E+02	3.60E+02	3.60E+02
1	0.0	3.60E+02	3.60E+02	3.60E+02	3.60E+02	3.60E+02	3.60E+02

(a) Yaw Angle

TABLE II (Continued)

	I =	1	2	3	4	5	6
	X =	0.0	0.14935	0.29845	0.44760	0.59690	0.74625
J	Y						
20	0.14478	0.0	-3.00E+01	-2.52E+01	0.0	0.0	2.97E+00
19	0.13716	0.0	-4.79E+01	-3.71E+01	0.0	0.0	3.50E+01
18	0.12954	0.0	0.0	-3.65E+01	0.0	0.0	2.47E+01
17	0.12192	0.0	-5.79E+01	-2.72E+01	5.50E+01	4.08E+01	2.04E+01
16	0.11430	0.0	-4.92E+01	-3.00E+01	4.42E+01	3.59E+01	2.29E+01
15	0.10668	0.0	4.39E+01	4.25E+01	3.24E+01	2.13E+01	2.13E+01
14	0.09906	0.0	0.0	2.09E+01	2.49E+01	1.35E+01	1.58E+01
13	0.09144	0.0	2.24E+01	1.45E+01	1.80E+01	1.10E+01	1.49E+01
12	0.08382	0.0	8.83E+00	8.21E+00	1.22E+01	8.79E+00	1.44E+01
11	0.07620	0.0	5.09E+00	6.05E+00	9.87E+00	9.37E+00	1.10E+01
10	0.05858	4.96E+00	3.18E+00	4.29E+00	7.74E+00	7.40E+00	1.07E+01
9	0.06096	3.15E+00	1.33E+00	3.07E+00	6.20E+00	5.56E+00	8.12E+00
8	0.05334	1.57E+00	3.68E-01	1.75E+00	4.89E+00	4.43E+00	7.05E+00
7	0.04572	8.47E-01	-1.49E-01	7.98E-01	3.91E+00	3.53E+00	6.03E+00
6	0.03810	5.08E-01	-5.05E-01	1.39E-01	3.00E+00	2.32E+00	5.12E+00
5	0.03048	3.84E-01	-6.36E-01	-2.50E-01	2.52E+00	1.93E+00	4.60E+00
4	0.02286	3.50E-01	-9.34E-01	-5.98E-01	2.17E+00	1.09E+00	3.88E+00
3	0.01524	4.76E-01	-9.06E-01	-8.47E-01	1.63E+00	7.31E-01	2.91E+00
2	0.00762	5.64E-01	-1.07E+00	-7.13E-01	1.36E+00	6.74E-02	2.40E+00
1	0.0	8.79E-01	-1.06E+00	-9.35E-01	1.47E+00	-3.58E-01	1.70E+00

(b) Pitch Angle

Table II (Continued)

	I =	1	2	3	4	5	6
	X =	0.0	0.50042	1.00000	1.50042	2.00000	2.50042
J	Y						
20	0.48511	0.0	-7.45E-02	-1.30E-01	0.0	0.0	2.91E-02
19	0.45957	0.0	-9.90E-02	-1.59E-01	0.0	0.0	4.63E-02
18	0.43404	0.0	-7.74E-02	-1.23E-01	2.93E-02	0.0	9.49E-02
17	0.40851	0.0	-6.64E-02	-1.17E-01	5.57E-02	8.57E-02	1.33E-01
16	0.38298	0.0	-5.82E-02	-8.33E-02	1.05E-01	1.19E-01	1.41E-01
15	0.35745	0.0	-6.94E-02	9.60E-02	1.60E-01	1.92E-01	1.92E-01
14	0.33191	0.0	0.0	2.09E-01	2.37E-01	3.10E-01	2.39E-01
13	0.30638	0.0	1.20E-01	3.16E-01	3.18E-01	3.71E-01	2.64E-01
12	0.28085	0.0	3.38E-01	4.69E-01	4.11E-01	4.39E-01	2.98E-01
11	0.25532	0.0	6.19E-01	6.29E-01	5.00E-01	4.42E-01	3.64E-01
10	0.22979	1.01E+00	8.70E-01	7.85E-01	6.05E-01	5.11E-01	3.93E-01
9	0.20425	1.01E+00	1.02E+00	8.74E-01	6.97E-01	5.88E-01	4.62E-01
8	0.17872	9.96E-01	1.04E+00	9.66E-01	7.70E-01	6.39E-01	5.08E-01
7	0.15319	9.94E-01	1.04E+00	1.01E+00	8.49E-01	7.29E-01	5.64E-01
6	0.12766	9.96E-01	1.04E+00	1.03E+00	9.04E-01	7.74E-01	6.04E-01
5	0.10213	9.95E-01	1.04E+00	1.04E+00	9.25E-01	8.14E-01	6.45E-01
4	0.07660	9.94E-01	1.04E+00	1.04E+00	9.47E-01	8.53E-01	6.92E-01
3	0.05106	9.96E-01	1.04E+00	1.04E+00	9.53E-01	8.80E-01	7.12E-01
2	0.02553	9.95E-01	1.04E+00	1.04E+00	9.58E-01	8.88E-01	7.28E-01
1	0.0	9.95E-01	1.04E+00	1.04E+00	9.61E-01	8.96E-01	7.38E-01

(c) u/u_o

TABLE II (Continued)

	I =	1	2	3	4	5	6
	X =	0.0	0.50042	1.00000	1.50042	2.00000	2.50042
J	Y						
20	0.48511	0.0	-4.30E-02	-6.11E-02	0.0	0.0	1.51E-03
19	0.45957	0.0	-1.09E-01	-1.20E-01	0.0	0.0	3.25E-02
18	0.43404	0.0	0.0	-9.10E-02	0.0	0.0	4.38E-02
17	0.40851	0.0	-1.06E-01	-5.98E-02	7.95E-02	7.38E-02	4.94E-02
16	0.38298	0.0	-6.73E-02	-4.81E-02	1.02E-01	8.61E-02	5.95E-02
15	0.35745	0.0	-6.69E-02	8.80E-02	1.01E-01	7.49E-02	7.49E-02
14	0.33191	0.0	0.0	8.01E-02	1.10E-01	7.42E-02	6.75E-02
13	0.30638	0.0	4.97E-02	8.16E-02	1.03E-01	7.24E-02	7.03E-02
12	0.28085	0.0	5.25E-02	6.77E-02	8.90E-02	6.79E-02	7.64E-02
11	0.25532	0.0	5.51E-02	6.66E-02	8.71E-02	7.30E-02	7.05E-02
10	0.22979	8.77E-02	4.84E-02	5.89E-02	8.23E-02	6.64E-02	7.41E-02
9	0.20425	5.55E-02	2.37E-02	4.69E-02	7.57E-02	5.72E-02	6.59E-02
8	0.17872	2.73E-02	6.69E-03	2.96E-02	6.59E-02	4.55E-02	6.28E-02
7	0.15319	1.47E-02	-2.70E-03	1.41E-02	5.80E-02	4.50E-02	5.96E-02
6	0.12766	8.83E-03	-9.18E-03	2.49E-03	4.74E-02	3.14E-02	5.42E-02
5	0.10213	6.66E-03	-1.16E-02	-4.52E-03	4.07E-02	2.74E-02	5.19E-02
4	0.07660	6.06E-03	-1.70E-02	-1.08E-02	3.58E-02	1.63E-02	4.69E-02
3	0.05106	8.28E-03	-1.65E-02	-1.54E-02	2.70E-02	1.12E-02	3.62E-02
2	0.02553	9.80E-03	-1.95E-02	-1.29E-02	2.28E-02	1.04E-03	3.05E-02
1	0.0	1.53E-02	-1.93E-02	-1.70E-02	2.46E-02	-5.60E-03	2.18E-02

(d) v/u_o

TABLE II (Continued)

	I =	1	2	3	4	5	6
	X =	0.0	0.50042	1.CCCCC	1.50042	2.00000	2.50042
J	Y						
20	0.48511	0.0	2.60E-07	4.53E-07	0.0	0.0	-1.53E-03
19	0.45957	0.0	3.45E-07	5.56E-07	0.0	0.0	-2.43E-03
18	0.43404	0.0	2.70E-07	4.29E-07	-1.02E-03	0.0	-4.64E-03
17	0.40851	0.0	2.32E-07	4.07E-07	-1.95E-03	-5.16E-07	-5.12E-03
16	0.38298	0.0	2.03E-07	2.90E-07	-3.68E-03	-7.18E-07	-5.40E-03
15	0.35745	0.0	2.42E-07	-5.78E-07	-5.58E-03	-1.16E-06	-7.37E-03
14	0.33191	0.0	0.0	-1.26E-06	-8.29E-03	-1.87E-06	-9.17E-03
13	0.30638	0.0	-7.25E-07	-1.91E-06	-1.11E-02	-2.24E-06	-7.37E-03
12	0.28085	0.0	-2.03E-06	-2.83E-06	-7.17E-03	-2.65E-06	-8.34E-03
11	0.25532	0.0	-3.73E-06	-3.79E-06	-8.73E-03	-2.66E-06	-1.02E-02
10	0.22979	-6.09E-06	-5.24E-06	-4.73E-06	-3.65E-06	-3.08E-06	-1.10E-02
9	0.20425	-6.06E-06	-6.13E-06	-5.26E-06	-4.20E-06	-3.54E-06	-1.29E-02
8	0.17872	-6.00E-06	-6.26E-06	-5.82E-06	-4.64E-06	-3.85E-06	-1.06E-02
7	0.15319	-5.99E-06	-6.26E-06	-6.11E-06	-5.11E-06	-4.39E-06	-9.85E-03
6	0.12766	-6.00E-06	-6.27E-06	-6.19E-06	-5.45E-06	-4.66E-06	-1.06E-02
5	0.10213	-5.99E-06	-6.27E-06	-6.25E-06	-5.57E-06	-4.90E-06	-9.01E-03
4	0.07660	-5.99E-06	-6.28E-06	-6.26E-06	-5.70E-06	-5.14E-06	-6.04E-03
3	0.05106	-6.00E-06	-6.28E-06	-6.26E-06	-5.74E-06	-5.30E-06	-4.98E-03
2	0.02553	-6.00E-06	-6.28E-06	-6.26E-06	-5.77E-06	-5.35E-06	-5.09E-03
1	0.0	-5.99E-06	-6.29E-06	-6.26E-06	-5.79E-06	-5.40E-06	-5.16E-03

(e) w/u_o

TABLE III

VELOCITY DATA FOR SWIRL VANE ANGLE ϕ = 38° [SIDE-WALL EXPANSION ANGLE α = 90° WITHOUT CONTRACTION BLOCK]

	I =	1	2	3	4	5	6
	X =	0.0	0.14935	C.29845	C.45237	0.60325	0.75413
J	Y						
20	0.14478	0.0	1.90E+01	2.93E+01	6.23E+01	5.78E+01	5.25E+01
19	0.13716	0.0	1.94E+01	3.50E+01	5.80E+01	6.20E+01	6.02E+01
18	0.12954	0.0	1.94E+01	4.02E+01	5.80E+01	6.20E+01	6.08E+01
17	0.12192	0.0	1.96E+01	4.94E+01	5.80E+01	6.14E+01	6.12E+01
16	0.11430	0.0	2.12E+01	5.72E+01	5.80E+01	6.14E+01	6.16E+01
15	0.10668	0.0	2.60E+01	6.54E+01	5.90E+01	6.14E+01	6.22E+01
14	0.09906	0.0	3.92E+01	7.36E+01	6.20E+01	6.14E+01	6.30E+01
13	0.09144	0.0	7.92E+01	7.98E+01	6.10E+01	6.20E+01	6.44E+01
12	0.08382	0.0	1.16E+02	8.54E+01	6.30E+01	6.32E+01	6.62E+01
11	0.07620	0.0	1.28E+02	8.98E+01	6.50E+01	6.50E+01	6.80E+01
10	0.06858	2.64E+01	1.34E+02	9.18E+01	6.70E+01	6.70E+01	7.04E+01
9	0.05096	3.01E+01	1.36E+02	9.46E+01	6.90E+01	7.04E+01	7.32E+01
8	0.05334	3.00E+01	1.38E+02	9.58E+01	7.20E+01	7.36E+01	7.58E+01
7	0.04572	2.43E+01	1.40E+02	9.72E+01	7.50E+01	7.64E+01	7.90E+01
6	0.03810	3.56E+02	1.42E+02	9.96E+01	7.80E+01	8.00E+01	8.18E+01
5	0.03048	0.0	1.46E+02	1.02E+02	8.30E+01	8.34E+01	8.54E+01
4	0.02286	0.0	1.50E+02	1.05E+02	8.90E+01	8.58E+01	8.92E+01
3	0.01524	0.0	1.59E+02	1.12E+02	9.10E+01	8.90E+01	9.20E+01
2	0.00762	0.0	1.68E+02	1.20E+02	9.80E+01	8.90E+01	9.36E+01
1	0.0	0.0	1.78E+02	1.45E+02	1.06E+02	7.54E+01	8.30E+01

(a) Yaw Angle

TABLE III (Continued)

	I =	1	2	3	4	5	6
	X =	0.0	0.14935	0.29845	0.45237	0.60325	0.75413
J	Y						
20	0.14478	0.0	2.32E+01	7.23E-01	1.22E+01	1.10E+01	2.18E+00
19	0.13716	0.0	2.04E+01	-7.21E+00	-1.20E+00	2.76E+00	4.30E-01
18	0.12954	0.0	2.06E+01	-1.14E+01	-3.99E+00	-1.81E+00	-1.61E+00
17	0.12192	0.0	1.91E+01	-1.70E+01	-4.73E+00	-2.47E+00	-2.51E+00
16	0.11430	0.0	1.77E+01	-1.95E+01	-6.13E+00	-2.81E+00	-2.97E+00
15	0.10668	0.0	1.53E+01	-2.30E+01	-6.01E+00	-3.15E+00	-3.27E+00
14	0.09906	0.0	1.77E+01	-2.26E+01	-7.35E+00	-3.98E+00	3.90E+00
13	0.09144	0.0	-3.79E+01	-2.15E+01	-6.67E+00	-4.80E+00	-4.51E+00
12	0.08382	0.0	2.00E+01	-1.86E+01	-7.31E+00	-5.28E+00	-6.05E+00
11	0.07620	0.0	7.69E+00	-1.65E+01	-6.74E+00	-6.71E+00	-6.56E+00
10	0.06858	1.14E+01	5.78E+00	-1.46E+01	-7.17E+00	-7.90E+00	-7.68E+00
9	0.06096	1.18E+01	4.41E+00	-1.43E+01	-7.49E+00	-9.67E+00	-1.00E+01
8	0.05334	9.70E+00	4.76E+00	-1.35E+01	-7.75E+00	-1.16E+01	-1.14E+01
7	0.04572	1.00E+01	3.36E+00	-1.33E+01	-8.83E+00	-1.40E+01	-1.37E+01
6	0.03810	0.0	2.97E+00	-1.44E+01	-1.05E+01	-1.69E+01	-1.64E+01
5	0.03048	0.0	2.97E+00	-1.77E+01	-1.35E+01	-2.09E+01	-2.06E+01
4	0.02286	0.0	2.97E+00	-2.15E+01	-1.79E+01	-2.68E+01	-2.82E+01
3	0.01524	0.0	2.97E+00	-3.08E+01	-2.41E+01	-3.71E+01	-4.50E+01
2	0.00762	0.0	7.42E-01	-4.60E+01	-4.42E+01	0.0	0.0
1	0.0	0.0	1.26E+00	0.0	0.0	5.11E+01	0.0

(b) Pitch Angle

TABLE III (Continued)

	I =	1	2	3	4	5	6
	X =	0.0	0.50042	1.00000	1.50042	2.00000	2.50042
J	Y						
20	0.48511	0.0	6.83E-01	5.12E-01	2.15E-01	2.70E-01	2.94E-01
19	0.45957	0.0	9.06E-01	5.85E-01	2.73E-01	2.57E-01	2.70E-01
18	0.43404	0.0	9.79E-01	4.94E-01	2.79E-01	2.56E-01	2.65E-01
17	0.40851	0.0	9.32E-01	3.60E-01	2.87E-01	2.62E-01	2.62E-01
16	0.38298	0.0	7.71E-01	2.68E-01	2.86E-01	2.64E-01	2.59E-01
15	0.35745	0.0	5.12E-01	1.85E-01	2.83E-01	2.66E-01	2.57E-01
14	0.33191	0.0	2.38E-01	1.20E-01	2.59E-01	2.67E-01	2.51E-01
13	0.30638	0.0	2.13E-02	7.41E-02	2.69E-01	2.62E-01	2.39E-01
12	0.28085	0.0	-1.12E-01	3.49E-02	2.54E-01	2.54E-01	2.22E-01
11	0.25532	0.0	-2.32E-01	1.59E-03	2.39E-01	2.35E-01	2.07E-01
10	0.22979	1.46E+00	-2.84E-01	-1.49E-02	2.18E-01	2.14E-01	1.82E-01
9	0.20425	1.57E+00	-3.13E-01	-3.85E-02	1.98E-01	1.79E-01	1.52E-01
8	0.17872	1.64E+00	-3.25E-01	-4.94E-02	1.69E-01	1.46E-01	1.26E-01
7	0.15319	9.25E-01	-3.19E-01	-5.99E-02	1.34E-01	1.15E-01	9.22E-02
6	0.12766	1.15E-01	-3.17E-01	-7.61E-02	9.81E-02	7.92E-02	6.35E-02
5	0.10213	0.0	-3.06E-01	-8.72E-02	5.05E-02	4.63E-02	3.08E-02
4	0.07660	0.0	-3.04E-01	-8.83E-02	6.12E-03	2.41E-02	4.25E-03
3	0.05106	0.0	-2.93E-01	-8.98E-02	-4.40E-03	4.15E-03	-6.23E-03
2	0.02553	0.0	-3.02E-01	-6.43E-02	-1.85E-02	2.02E-03	-6.13E-03
1	0.0	0.0	-2.86E-01	-5.38E-02	-1.21E-02	3.12E-02	1.19E-02

(c) u/u_o

TABLE III (Continued)

	I =	1	2	3	4	5	6
	X =	0.0	0.50042	1.00000	1.50042	2.00000	2.50042
J	Y						
20	0.48511	0.0	3.10E-01	7.41E-03	9.98E-02	9.83E-02	1.84E-02
19	0.45957	0.0	3.58E-01	-9.03E-02	-1.08E-02	2.64E-02	4.08E-03
18	0.43404	0.0	3.91E-01	-1.31E-01	-3.67E-02	-1.72E-02	-1.53E-02
17	0.40851	0.0	3.43E-01	-1.69E-01	-4.48E-02	-2.36E-02	-2.38E-02
16	0.38298	0.0	2.63E-01	-1.76E-01	-5.79E-02	-2.71E-02	-2.82E-02
15	0.35745	0.0	1.56E-01	-1.89E-01	-5.78E-02	-3.06E-02	-3.15E-02
14	0.33191	0.0	9.80E-02	-1.77E-01	-7.12E-02	-3.88E-02	-3.76E-02
13	0.30638	0.0	8.85E-02	-1.65E-01	-6.49E-02	-4.69E-02	-4.37E-02
12	0.28085	0.0	9.38E-02	-1.46E-01	-7.17E-02	-5.21E-02	-5.84E-02
11	0.25532	0.0	5.11E-02	-1.35E-01	-6.67E-02	-6.53E-02	-6.37E-02
10	0.22979	3.28E-01	4.17E-02	-1.24E-01	-7.01E-02	-7.61E-02	-7.33E-02
9	0.20425	3.79E-01	3.35E-02	-1.22E-01	-7.28E-02	-9.09E-02	-9.28E-02
8	0.17872	3.23E-01	3.64E-02	-1.17E-01	-7.43E-02	-1.06E-01	-1.03E-01
7	0.15319	1.79E-01	2.45E-02	-1.13E-01	-8.05E-02	-1.22E-01	-1.18E-01
6	0.12766	0.0	2.08E-02	-1.18E-01	-8.75E-02	-1.38E-01	-1.31E-01
5	0.10213	0.0	1.92E-02	-1.30E-01	-9.95E-02	-1.54E-01	-1.44E-01
4	0.07660	0.0	1.81E-02	-1.31E-01	-1.13E-01	-1.67E-01	-1.63E-01
3	0.05106	0.0	1.63E-02	-1.40E-01	-1.13E-01	-1.79E-01	-1.79E-01
2	0.02553	0.0	3.99E-03	-1.33E-01	-1.29E-01	0.0	0.0
1	0.0	0.0	6.29E-03	0.0	0.0	1.53E-01	0.0

(d) v/u_o

TABLE III (Continued)

	I =	1	2	3	4	5	6
	X =	0.0	0.50042	1.00000	1.50042	2.00000	2.50042
J	Y						
20	0.48511	0.0	2.35E-01	2.67E-01	4.10E-01	4.29E-01	3.83E-01
19	0.45957	0.0	3.19E-01	4.09E-01	4.36E-01	4.83E-01	4.71E-01
18	0.43404	0.0	3.45E-01	4.18E-01	4.46E-01	4.81E-01	4.74E-01
17	0.40851	0.0	3.32E-01	4.20E-01	4.60E-01	4.80E-01	4.77E-01
16	0.38298	0.0	2.99E-01	4.16E-01	4.57E-01	4.84E-01	4.79E-01
15	0.35745	0.0	2.50E-01	4.05E-01	4.71E-01	4.88E-01	4.88E-01
14	0.33191	0.0	1.94E-01	4.09E-01	4.87E-01	4.90E-01	4.92E-01
13	0.30638	0.0	1.12E-01	4.12E-01	4.85E-01	4.93E-01	4.99E-01
12	0.28085	0.0	2.32E-01	4.33E-01	4.98E-01	5.03E-01	5.04E-01
11	0.25532	0.0	2.99E-01	4.56E-01	5.12E-01	5.03E-01	5.13E-01
10	0.22979	7.24E-01	2.99E-01	4.75E-01	5.13E-01	5.05E-01	5.12E-01
9	0.20425	9.11E-01	3.02E-01	4.79E-01	5.17E-01	5.03E-01	5.04E-01
8	0.17872	9.46E-01	2.92E-01	4.86E-01	5.19E-01	4.96E-01	4.96E-01
7	0.15319	4.18E-01	2.68E-01	4.74E-01	5.00E-01	4.76E-01	4.74E-01
6	0.12766	-7.65E-03	2.46E-01	4.50E-01	4.61E-01	4.49E-01	4.41E-01
5	0.10213	0.0	2.09E-01	3.97E-01	4.11E-01	4.00E-01	3.83E-01
4	0.07660	0.0	1.73E-01	3.20E-01	3.51E-01	3.29E-01	3.04E-01
3	0.05106	0.0	1.13E-01	2.18E-01	2.52E-01	2.38E-01	1.78E-01
2	0.02553	0.0	6.19E-02	1.11E-01	1.32E-01	1.15E-01	9.74E-02
1	0.0	0.0	9.99E-03	3.77E-02	4.23E-02	1.20E-01	9.69E-02

(e) w/u_o

TABLE IV

VELOCITY DATA FOR SWIRL VANE ANGLE ϕ = 45° [SIDE-WALL EXPANSION ANGLE α = 90° WITHOUT CONTRACTION BLOCK]

	I =	1	2	3	4	5	6
	X =	0.0	0.14935	0.29845	0.44780	0.59690	0.74625
J	Y						
20	0.14478	0.0	2.00E+01	3.28E+01	6.20E+01	6.30E+01	5.65E+01
19	0.13716	0.0	2.40E+01	3.86E+01	6.38E+01	6.20E+01	5.75E+01
18	0.12954	0.0	2.72E+01	4.56E+01	6.14E+01	6.20E+01	5.88E+01
17	0.12192	0.0	3.16E+01	5.32E+01	6.04E+01	6.14E+01	5.98E+01
16	0.11430	0.0	4.20E+01	6.04E+01	6.00E+01	6.10E+01	5.98E+01
15	0.10668	0.0	6.60E+01	6.80E+01	6.00E+01	6.10E+01	6.08E+01
14	0.09906	0.0	9.92E+01	7.48E+01	6.08E+01	6.16E+01	6.18E+01
13	0.09144	0.0	1.18E+02	8.12E+01	6.20E+01	6.24E+01	6.32E+01
12	0.08382	0.0	1.26E+02	8.64E+01	6.32E+01	6.40E+01	6.46E+01
11	0.07620	0.0	1.29E+02	9.00E+01	6.54E+01	6.56E+01	6.64E+01
10	0.06858	2.58E+01	1.30E+02	9.36E+01	6.70E+01	6.80E+01	6.86E+01
9	0.06096	2.72E+01	1.30E+02	9.56E+01	6.94E+01	7.12E+01	7.14E+01
8	0.05334	2.66E+01	1.30E+02	9.82E+01	7.22E+01	7.50E+01	7.48E+01
7	0.04572	2.82E+01	1.30E+02	1.00E+02	7.60E+01	7.84E+01	7.74E+01
6	0.03810	2.56E+01	1.32E+02	1.03E+02	7.96E+01	8.28E+01	8.12E+01
5	0.03048	3.60E+01	1.33E+02	1.06E+02	8.44E+01	8.92E+01	8.50E+01
4	0.02286	1.01E+02	1.38E+02	1.10E+02	9.00E+01	9.16E+01	8.96E+01
3	0.01524	1.53E+02	1.44E+02	1.17E+02	9.70E+01	9.66E+01	9.52E+01
2	0.00762	1.75E+02	1.56E+02	1.31E+02	1.06E+02	1.04E+02	1.02E+02
1	0.0	1.97E+02	1.76E+02	1.67E+02	1.49E+02	1.77E+02	1.30E+02

(a) Yaw Angle

TABLE IV (Continued)

	I =	1	2	3	4	5	6
	X =	0.0	0.14935	C.29845	C.44780	C.59690	0.74625
J	Y						
20	0.14478	C.0	1.89E+00	2.13E+00	1.12E+01	5.73E+00	4.90E+00
19	0.13716	0.0	-2.33E+00	-3.71E+00	2.85E+00	2.84E+00	2.36E+00
18	0.12954	0.0	-8.42E+00	-8.33E+00	3.66E-01	-1.99E-01	3.23E-01
17	0.12192	0.0	-1.24E+01	-1.20E+01	-2.20E-01	-8.47E-01	-1.52E-01
16	0.11430	0.0	-1.89E+01	-1.52E+01	-9.37E-01	-1.16E+00	-6.15E-01
15	0.10668	0.0	-2.75E+01	-1.61E+01	-1.41E+00	-1.52E+00	-9.13E-01
14	0.09906	0.0	-4.15E+00	-1.60E+01	-1.63E+00	-1.81E+00	-1.35E+00
13	0.09144	0.0	3.55E+00	-1.65E+01	-2.08E+00	-2.82E+00	-2.05E+00
12	0.08382	0.0	4.93E+00	-1.64E+01	-2.98E+00	-3.48E+00	-2.12E+00
11	0.07620	0.0	5.12E+00	-1.54E+01	-3.54E+00	-4.24E+00	-2.94E+00
10	0.06858	1.18E+01	4.65E+00	-1.41E+01	-4.26E+00	-5.77E+00	-3.79E+00
9	0.06096	1.18E+01	3.47E+00	-1.42E+01	-5.09E+00	-6.99E+00	-4.49E+00
8	0.05334	1.06E+01	2.61E+00	-1.38E+01	-6.65E+00	-7.75E+00	-5.37E+00
7	0.04572	8.11E+00	9.32E-01	-1.43E+01	-8.00E+00	-9.81E+00	-7.07E+00
6	0.03810	1.49E+01	-7.38E-01	-1.60E+01	-1.11E+01	-1.09E+01	-7.90E+00
5	0.03048	-8.50E-01	-3.94E+00	-1.82E+01	-1.43E+01	-1.52E+01	-8.50E+00
4	0.02286	-5.10E+01	-6.18E+00	-2.12E+01	-2.17E+01	-1.84E+01	-1.20E+01
3	0.01524	-3.10E+01	-1.08E+01	-3.00E+01	-3.06E+01	-2.96E+01	-1.85E+01
2	0.00762	-3.57E+01	-1.72E+01	-3.82E+01	-4.33E+01	-4.50E+01	-2.75E+01
1	0.0	-2.86E+01	-1.17E+01	0.0	0.0	5.04E+01	-4.13E+01

(b) Pitch Angle

TABLE IV (Continued)

	I =	1	2	3	4	5	6
	X =	0.0	0.50042	1.00000	1.50042	2.00000	2.50042
J	Y						
20	0.48511	0.0	9.12E-01	6.92E-01	2.60E-01	2.44E-01	3.07E-01
19	0.45957	0.0	8.54E-01	6.03E-01	2.61E-01	2.67E-01	3.10E-01
18	0.43404	0.0	7.44E-01	4.76E-01	2.89E-01	2.80E-01	3.04E-01
17	0.40851	0.0	5.64E-01	3.65E-01	3.04E-01	2.89E-01	3.02E-01
16	0.38298	0.0	3.36E-01	2.72E-01	3.16E-01	2.94E-01	3.03E-01
15	0.35745	0.0	1.05E-01	1.94E-01	3.23E-01	2.98E-01	2.96E-01
14	0.33191	0.0	-4.67E-02	1.34E-01	3.18E-01	2.95E-01	2.88E-01
13	0.30638	0.0	-1.73E-01	7.67E-02	3.11E-01	2.88E-01	2.76E-01
12	0.28085	0.0	-2.51E-01	3.16E-02	3.00E-01	2.76E-01	2.64E-01
11	0.25532	0.0	-2.97E-01	1.66E-06	2.80E-01	2.56E-01	2.44E-01
10	0.22979	1.68E+00	-3.11E-01	-3.40E-02	2.60E-01	2.28E-01	2.20E-01
9	0.20425	1.82E+00	-3.11E-01	-5.32E-02	2.31E-01	1.92E-01	1.90E-01
8	0.17872	1.93E+00	-3.07E-01	-7.97E-02	1.96E-01	1.49E-01	1.52E-01
7	0.15319	1.34E+00	-2.91E-01	-9.70E-02	1.46E-01	1.10E-01	1.21E-01
6	0.12766	4.05E-01	-2.67E-01	-1.15E-01	9.98E-02	6.46E-02	7.99E-02
5	0.10213	1.70E-01	-2.37E-01	-1.29E-01	4.79E-02	6.33E-03	4.16E-02
4	0.07660	-1.62E-02	-2.16E-01	-1.42E-01	1.23E-06	-1.08E-02	2.82E-03
3	0.05106	-1.39E-01	-1.94E-01	-1.42E-01	-3.45E-02	-3.12E-02	-2.84E-02
2	0.02553	-1.36E-01	-1.73E-01	-1.42E-01	-5.06E-02	-3.97E-02	-4.41E-02
1	0.0	-1.30E-01	-1.83E-01	-1.04E-01	-4.32E-02	-1.01E-01	-7.28E-02

(c) u/u_o

TABLE IV (Continued)

	I =	1	2	3	4	5	6
	X =	0.0	0.50042	1.00000	1.50042	2.00000	2.50042
J	Y						
20	0.48511	0.0	3.20E-02	3.06E-02	1.10E-01	5.39E-02	4.77E-02
19	0.45957	0.0	-3.80E-02	-5.01E-02	2.94E-02	2.83E-02	2.38E-02
18	0.43404	0.0	-1.24E-01	-9.97E-02	3.86E-03	-2.07E-03	3.30E-03
17	0.40851	0.0	-1.46E-01	-1.30E-01	-2.36E-03	-8.92E-03	-1.60E-03
16	0.38298	0.0	-1.55E-01	-1.50E-01	-1.03E-02	-1.23E-02	-6.47E-03
15	0.35745	0.0	-1.35E-01	-1.50E-01	-1.59E-02	-1.63E-02	-9.68E-03
14	0.33191	0.0	-2.12E-02	-1.46E-01	-1.86E-02	-1.95E-02	-1.44E-02
13	0.30638	0.0	2.29E-02	-1.49E-01	-2.41E-02	-3.06E-02	-2.19E-02
12	0.28085	0.0	3.69E-02	-1.48E-01	-3.46E-02	-3.83E-02	-2.27E-02
11	0.25532	0.0	4.22E-02	-1.44E-01	-4.16E-02	-4.60E-02	-3.13E-02
10	0.22979	3.90E-01	3.96E-02	-1.36E-01	-4.96E-02	-6.15E-02	-4.00E-02
9	0.20425	4.29E-01	2.95E-02	-1.38E-01	-5.84E-02	-7.32E-02	-4.68E-02
8	0.17872	4.05E-01	2.16E-02	-1.37E-01	-7.47E-02	-7.85E-02	-5.46E-02
7	0.15319	2.17E-01	7.30E-03	-1.39E-01	-8.46E-02	-9.43E-02	-6.86E-02
6	0.12766	1.19E-01	-5.13E-03	-1.45E-01	-1.09E-01	-9.94E-02	-7.25E-02
5	0.10213	-3.12E-03	-2.38E-02	-1.57E-01	-1.25E-01	-1.23E-01	-7.14E-02
4	0.07660	-1.05E-01	-3.15E-02	-1.61E-01	-1.54E-01	-1.29E-01	-8.56E-02
3	0.05106	-9.37E-02	-4.57E-02	-1.78E-01	-1.68E-01	-1.54E-01	-1.05E-01
2	0.02553	-5.79E-02	-5.85E-02	-1.72E-01	-1.71E-01	-1.59E-01	-1.11E-01
1	0.0	-7.42E-02	-3.80E-02	0.0	0.0	1.22E-01	-5.88E-02

(d) v/u_o

TABLE IV (Continued)

	I =	1	2	3	4	5	6
	X =	0.0	0.50042	1.00000	1.50042	2.00000	2.50042
J	Y						
20	0.48511	0.0	3.32E-01	4.46E-01	4.90E-01	4.78E-01	4.64E-01
19	0.45957	0.0	3.80E-01	4.81E-01	5.30E-01	5.03E-01	4.86E-01
18	0.43404	0.0	3.82E-01	4.86E-01	5.31E-01	5.26E-01	5.01E-01
17	0.40851	0.0	3.47E-01	4.88E-01	5.35E-01	5.30E-01	5.19E-01
16	0.38298	0.0	3.02E-01	4.79E-01	5.47E-01	5.31E-01	5.20E-01
15	0.35745	0.0	2.36E-01	4.81E-01	5.59E-01	5.38E-01	5.30E-01
14	0.33191	0.0	2.88E-01	4.92E-01	5.69E-01	5.45E-01	5.38E-01
13	0.30638	0.0	3.26E-01	4.95E-01	5.86E-01	5.51E-01	5.46E-01
12	0.28085	0.0	3.46E-01	5.02E-01	5.93E-01	5.65E-01	5.56E-01
11	0.25532	0.0	3.66E-01	5.23E-01	6.11E-01	5.65E-01	5.59E-01
10	0.22979	8.10E-01	3.74E-01	5.41E-01	6.13E-01	5.64E-01	5.62E-01
9	0.20425	9.37E-01	3.73E-01	5.42E-01	6.14E-01	5.65E-01	5.64E-01
8	0.17872	9.68E-01	3.61E-01	5.53E-01	6.10E-01	5.57E-01	5.60E-01
7	0.15319	7.18E-01	3.42E-01	5.39E-01	5.85E-01	5.34E-01	5.40E-01
6	0.12766	1.94E-01	2.96E-01	4.92E-01	5.44E-01	5.12E-01	5.16E-01
5	0.10213	1.23E-01	2.51E-01	4.61E-01	4.89E-01	4.53E-01	4.76E-01
4	0.07660	8.35E-02	1.95E-01	3.91E-01	3.87E-01	3.88E-01	4.03E-01
3	0.05106	7.08E-02	1.39E-01	2.73E-01	2.81E-01	2.69E-01	3.12E-01
2	0.02553	1.28E-02	7.62E-02	1.66E-01	1.74E-01	1.55E-01	2.08E-01
1	0.0	-4.08E-02	1.28E-02	2.39E-02	2.55E-02	4.93E-03	8.55E-02

(e) w/u_o

TABLE V

VELOCITY DATA FOR SWIRL VANE ANGLE ϕ = 60° [SIDE-WALL EXPANSION ANGLE α = 90° WIHTOUT CONTRACTION BLOCK]

	I =	1	2	3	4	5	6
	X =	0.0	0.14935	0.29845	C.44780	C.5965C	0.74625
J	Y						
20	0.14478	0.0	4.10E+01	5.24E+01	6.48E+01	6.26E+01	6.60E+01
19	0.13716	0.0	4.24E+01	5.38E+01	6.46E+01	6.26E+01	6.62E+01
18	0.12954	C.0	4.36E+01	5.72E+01	6.44E+01	6.32E+01	6.72E+01
17	0.12192	0.0	4.64E+01	6.12E+01	6.50E+01	6.38E+01	6.88E+01
16	0.11430	0.0	5.26E+01	6.50E+01	6.50E+01	6.50E+01	7.04E+01
15	0.10668	0.0	6.10E+01	6.84E+01	6.56E+01	6.60E+01	7.22E+01
14	0.09906	0.0	7.24E+01	7.14E+01	6.64E+01	6.78E+01	7.36E+01
13	0.09144	0.0	8.54E+01	7.38E+01	6.78E+01	6.94E+01	7.54E+01
12	0.08382	0.0	9.48E+01	7.58E+01	6.92E+01	7.12E+01	7.76E+01
11	0.07620	0.0	1.02E+02	7.76E+01	7.14E+01	7.38E+01	7.98E+01
10	0.06858	3.56E+01	1.05E+02	7.90E+01	7.44E+01	7.64E+01	8.24E+01
9	0.06096	3.42E+01	1.07E+02	8.14E+01	7.76E+01	7.90E+01	8.52E+01
8	0.05334	3.78E+01	1.08E+02	8.32E+01	8.12E+01	8.16E+01	8.78E+01
7	0.04572	7.94E+01	1.09E+02	8.60E+01	8.50E+01	8.50E+01	9.08E+01
6	0.03810	1.17E+02	1.10E+02	9.02E+01	8.84E+01	8.86E+01	9.56E+01
5	0.03048	1.04E+02	1.11E+02	9.44E+01	9.28E+01	9.34E+01	1.00E+02
4	0.02286	9.22E+01	1.14E+02	1.01E+02	9.72E+01	9.86E+01	1.06E+02
3	0.01524	9.40E+01	1.18E+02	1.04E+02	1.03E+02	1.05E+02	1.13E+02
2	0.00762	9.90E+01	1.31E+02	1.13E+02	1.11E+02	1.13E+02	1.36E+02
1	0.0	1.10E+02	1.68E+02	1.39E+02	1.28E+02	1.35E+02	1.66E+02

(a) Yaw Angle

TABLE V (Continued)

	I =	1	2	3	4	5	6
	X =	0.0	0.14935	0.29845	0.44780	0.59690	0.74625
J	Y						
20	0.14473	0.0	2.17E+01	1.01E+01	9.00E+00	6.38E+00	1.10E+01
19	0.13716	0.0	1.40E+01	3.30E+00	3.07E+00	2.86E+00	5.31E+00
18	0.12954	0.0	1.04E+01	-2.70E+00	1.20E+00	2.65E+00	1.87E+00
17	0.12192	0.0	9.60E+00	-3.78E+00	6.62E-01	2.06E+00	1.42E+00
16	0.11430	0.0	6.55E+00	-4.36E+00	1.53E-01	1.44E+00	9.89E-01
15	0.10668	0.0	1.33E+00	-4.77E+00	3.27E-01	7.92E-01	7.66E-01
14	0.09906	0.0	-3.23E+00	-4.51E+00	1.42E-01	2.37E-01	3.17E-02
13	0.09144	0.0	-6.11E+00	-4.31E+00	-2.08E-01	-1.68E-01	-3.18E-01
12	0.08382	0.0	-5.84E+00	-3.87E+00	-8.00E-01	-1.05E+00	-1.09E+00
11	0.07620	0.0	-5.78E+00	-3.42E+00	-1.27E+00	-1.59E+00	-1.73E+00
10	0.06858	7.13E+00	-4.98E+00	-2.99E+00	-2.09E+00	-2.60E+00	-2.33E+00
9	0.06096	4.84E+00	-4.39E+00	-2.34E+00	-3.12E+00	-3.72E+00	-3.34E+00
8	0.05334	-2.82E-01	-4.12E+00	-2.78E+00	-3.79E+00	-4.81E+00	-4.42E+00
7	0.04572	-5.34E+00	-4.19E+00	-3.70E+00	-4.85E+00	-5.86E+00	-6.09E+00
6	0.03810	4.50E+00	-5.04E+00	-5.31E+00	-6.74E+00	-8.66E+00	-7.53E+00
5	0.03048	-2.29E+01	-6.14E+00	-7.84E+00	-8.70E+00	-1.15E+01	-1.11E+01
4	0.02286	-3.46E+01	-7.81E+00	-1.23E+01	-1.27E+01	-1.58E+01	-1.62E+01
3	0.01524	-3.84E+01	-1.34E+01	-1.79E+01	-1.79E+01	-2.30E+01	-2.47E+01
2	0.00762	-4.44E+01	-2.71E+01	-2.83E+01	-2.68E+01	-3.66E+01	-3.82E+01
1	0.0	-5.74E+01	-4.06E+01	-5.79E+01	-5.13E+01	-5.59E+01	0.0

(b) Pitch Angle

TABLE V (Continued)

	I =	1	2	3	4	5	6
	X =	0.0	0.50042	1.00000	1.50042	2.00000	2.50042
J	Y						
20	0.46511	0.0	8.09E-01	5.92E-01	3.54E-01	3.93E-01	3.32E-01
19	0.45957	0.0	7.85E-01	5.92E-01	3.82E-01	4.07E-01	3.48E-01
18	0.43404	0.0	7.28E-01	5.27E-01	3.91E-01	4.02E-01	3.40E-01
17	0.40851	0.0	6.58E-01	4.69E-01	3.91E-01	4.05E-01	3.29E-01
16	0.38298	0.0	5.14E-01	4.06E-01	3.99E-01	3.99E-01	3.12E-01
15	0.35745	0.0	3.66E-01	3.51E-01	3.95E-01	3.87E-01	2.89E-01
14	0.33191	0.0	2.09E-01	3.06E-01	3.90E-01	3.68E-01	2.70E-01
13	0.30638	0.0	5.75E-02	2.73E-01	3.75E-01	3.46E-01	2.46E-01
12	0.28085	0.0	-6.38E-02	2.44E-01	3.55E-01	3.20E-01	2.12E-01
11	0.25532	0.0	-1.64E-01	2.19E-01	3.22E-01	2.80E-01	1.77E-01
10	0.22979	2.59E+00	-2.29E-01	1.97E-01	2.72E-01	2.37E-01	1.33E-01
9	0.20425	2.70E+00	-2.65E-01	1.58E-01	2.15E-01	1.92E-01	8.36E-02
8	0.17872	1.39E+00	-2.89E-01	1.23E-01	1.51E-01	1.44E-01	3.70E-02
7	0.15319	8.13E-02	-2.96E-01	6.98E-02	8.32E-02	8.30E-02	-1.26E-02
6	0.12766	-1.50E-01	-2.91E-01	-3.27E-03	2.50E-02	2.15E-02	-8.22E-02
5	0.10213	-4.51E-02	-2.82E-01	-6.43E-02	-4.00E-02	-4.72E-02	-1.30E-01
4	0.07660	-7.61E-03	-2.69E-01	-1.28E-01	-8.88E-02	-1.03E-01	-1.72E-01
3	0.05106	-1.38E-02	-2.34E-01	-1.33E-01	-1.28E-01	-1.41E-01	-1.80E-01
2	0.02553	-2.51E-02	-2.11E-01	-1.41E-01	-1.47E-01	-1.39E-01	-2.17E-01
1	0.0	-3.06E-02	-1.95E-01	-1.16E-01	-1.27E-01	-1.37E-01	-1.22E-01

(c) u/u_o

TABLE V (Continued)

	I =	1	2	3	4	5	6
	X =	0.0	0.50042	1.00000	1.50042	2.00000	2.50042
J	Y						
20	0.43511	0.0	4.28E-01	1.72E-01	1.32E-01	9.55E-02	1.59E-01
19	0.45957	0.0	2.65E-01	5.77E-02	4.78E-02	4.41E-02	8.02E-02
18	0.43404	0.0	1.85E-01	-4.60E-02	1.89E-02	4.12E-02	2.86E-02
17	0.40851	0.0	1.61E-01	-6.44E-02	1.07E-02	3.30E-02	2.26E-02
16	0.38298	0.0	9.72E-02	-7.33E-02	2.52E-03	2.38E-02	1.60E-02
15	0.35745	0.0	1.76E-02	-7.96E-02	5.45E-03	1.32E-02	1.26E-02
14	0.33191	0.0	-3.91E-02	-7.55E-02	2.41E-03	4.02E-03	5.29E-04
13	0.30638	0.0	-7.67E-02	-7.37E-02	-3.60E-03	-2.88E-03	-5.42E-03
12	0.28085	0.0	-7.80E-02	-6.72E-02	-1.40E-02	-1.82E-02	-1.88E-02
11	0.25532	0.0	-8.28E-02	-6.10E-02	-2.23E-02	-2.80E-02	-3.02E-02
10	0.22979	3.98E-01	-7.60E-02	-5.40E-02	-3.68E-02	-4.57E-02	-4.09E-02
9	0.20425	2.76E-01	-6.96E-02	-4.30E-02	-5.46E-02	-6.54E-02	-5.83E-02
8	0.17872	-8.68E-03	-6.65E-02	-5.04E-02	-6.53E-02	-8.31E-02	-7.45E-02
7	0.15319	-4.13E-02	-6.77E-02	-6.46E-02	-8.10E-02	-9.76E-02	-9.61E-02
6	0.12766	2.59E-02	-7.66E-02	-8.73E-02	-1.06E-01	-1.34E-01	-1.11E-01
5	0.10213	-8.09E-02	-8.48E-02	-1.15E-01	-1.25E-01	-1.63E-01	-1.44E-01
4	0.07660	-1.37E-01	-9.13E-02	-1.46E-01	-1.60E-01	-1.95E-01	-1.81E-01
3	0.05106	-1.56E-01	-1.19E-01	-1.73E-01	-1.81E-01	-2.32E-01	-2.12E-01
2	0.02553	-1.57E-01	-1.65E-01	-1.97E-01	-2.05E-01	-2.68E-01	-2.36E-01
1	0.0	-1.43E-01	-1.71E-01	-2.45E-01	-2.55E-01	-2.86E-01	0.0

(d) v/u_o

TABLE V (Continued)

	I =	1	2	3	4	5	6
	X =	0.0	0.50042	1.00000	1.50042	2.00000	2.50042
J	Y						
20	0.48511	0.0	7.04E-01	7.68E-01	7.53E-01	7.57E-01	7.46E-01
19	0.45957	0.0	7.17E-01	8.08E-01	8.04E-01	7.84E-01	7.89E-01
18	0.43404	0.0	6.93E-01	8.18E-01	8.16E-01	7.95E-01	8.09E-01
17	0.40851	0.0	6.91E-01	8.53E-01	8.38E-01	8.22E-01	8.47E-01
16	0.38298	0.0	6.72E-01	8.71E-01	8.55E-01	8.56E-01	8.75E-01
15	0.35745	0.0	6.61E-01	8.87E-01	8.70E-01	8.69E-01	9.00E-01
14	0.33191	0.0	6.60E-01	9.08E-01	8.92E-01	9.01E-01	9.17E-01
13	0.30638	0.0	7.14E-01	9.38E-01	9.18E-01	9.21E-01	9.44E-01
12	0.28085	0.0	7.60E-01	9.65E-01	9.35E-01	9.39E-01	9.65E-01
11	0.25532	0.0	8.00E-01	9.98E-01	9.57E-01	9.65E-01	9.85E-01
10	0.22979	1.85E+00	8.42E-01	1.02E+00	9.74E-01	9.79E-01	9.97E-01
9	0.20425	1.84E+00	8.67E-01	1.04E+00	9.79E-01	9.87E-01	9.96E-01
8	0.17872	1.08E+00	8.78E-01	1.03E+00	9.76E-01	9.77E-01	9.63E-01
7	0.15319	4.34E-01	8.78E-01	9.98E-01	9.51E-01	9.48E-01	9.01E-01
6	0.12766	2.94E-01	8.19E-01	9.39E-01	8.94E-01	8.81E-01	8.38E-01
5	0.10213	1.86E-01	7.35E-01	8.36E-01	8.17E-01	7.95E-01	7.24E-01
4	0.07660	1.98E-01	6.09E-01	6.57E-01	7.03E-01	6.83E-01	6.00E-01
3	0.05106	1.97E-01	4.43E-01	5.18E-01	5.46E-01	5.27E-01	4.24E-01
2	0.02553	1.58E-01	2.42E-01	3.38E-01	3.79E-01	3.34E-01	2.07E-01
1	0.0	8.60E-02	4.14E-02	1.00E-01	1.60E-01	1.36E-01	3.04E-02

(e) w/u_o

TABLE VI

VELOCITY DATA FOR SWIRL VANE ANGLE ϕ = 70° [SIDE-WALL EXPANSION ANGLE α = 90° WITHOUT CONTRACTION BLOCK]

	I =	1	2	3	4	5	6
	X =	0.0	0.14935	0.29845	0.44780	0.59690	0.74625
J	Y						
20	0.14478	0.0	2.90E+01	6.58E+01	6.94E+01	6.70E+01	5.58E+01
19	0.13716	0.0	3.98E+01	6.76E+01	7.02E+01	6.86E+01	5.84E+01
18	0.12954	0.0	4.94E+01	6.86E+01	7.08E+01	6.94E+01	6.14E+01
17	0.12192	0.0	5.96E+01	7.00E+01	7.18E+01	7.10E+01	6.36E+01
16	0.11430	0.0	7.12E+01	7.14E+01	7.22E+01	7.28E+01	6.58E+01
15	0.10668	0.0	8.14E+01	7.32E+01	7.44E+01	7.46E+01	6.80E+01
14	0.09906	0.0	8.98E+01	7.48E+01	7.58E+01	7.70E+01	6.98E+01
13	0.09144	0.0	9.60E+01	7.64E+01	7.80E+01	7.94E+01	7.22E+01
12	0.08382	0.0	9.98E+01	7.86E+01	8.04E+01	8.18E+01	7.44E+01
11	0.07620	0.0	1.02E+02	8.06E+01	8.32E+01	8.44E+01	7.70E+01
10	0.06858	4.38E+01	1.03E+02	8.32E+01	8.60E+01	8.70E+01	7.96E+01
9	0.06096	4.28E+01	1.03E+02	8.64E+01	8.92E+01	9.04E+01	8.26E+01
8	0.05334	6.30E+01	1.03E+02	9.00E+01	9.26E+01	9.37E+01	8.54E+01
7	0.04572	1.12E+02	1.05E+02	9.46E+01	9.58E+01	9.70E+01	8.86E+01
6	0.03810	1.24E+02	1.07E+02	9.90E+01	9.98E+01	1.01E+02	9.26E+01
5	0.03048	1.18E+02	1.09E+02	1.03E+02	1.04E+02	1.05E+02	9.64E+01
4	0.02286	1.08E+02	1.11E+02	1.07E+02	1.08E+02	1.10E+02	1.02E+02
3	0.01524	1.04E+02	1.14E+02	1.10E+02	1.13E+02	1.17E+02	1.09E+02
2	0.00762	1.08E+02	1.20E+02	1.17E+02	1.21E+02	1.27E+02	1.22E+02
1	0.0	1.27E+02	1.36E+02	1.34E+02	1.41E+02	1.59E+02	1.64E+02

(a) Yaw Angle

TABLE VI (Continued)

	I =	1	2	3	4	5	6
	X =	0.0	0.14935	0.29845	0.44780	0.59695	0.74625
J	Y						
20	0.14478	0.0	1.56E+01	1.07E+01	8.46E+00	6.45E+00	1.27E+01
19	0.13716	0.0	4.60E+00	3.21E+00	3.91E+00	1.27E+00	6.95E+00
18	0.12954	0.0	-2.13E+00	-2.90E+00	5.53E-01	-2.13E-01	1.16E+00
17	0.12192	0.0	-6.80E+00	-3.61E+00	-6.47E-02	-1.48E+00	6.79E-01
16	0.11430	0.0	-9.49E+00	-4.67E+00	-1.20E+00	-2.04E+00	-5.44E-02
15	0.10668	0.0	-1.05E+01	-5.37E+00	-1.75E+00	-2.74E+00	-6.29E-01
14	0.09906	0.0	-1.12E+01	-6.01E+00	-2.80E+00	-3.77E+00	-9.63E-01
13	0.09144	0.0	-1.03E+01	-6.07E+00	-3.87E+00	-4.44E+00	-1.46E+00
12	0.08382	0.0	-9.67E+00	-6.13E+00	-5.02E+00	-5.05E+00	-2.20E+00
11	0.07620	0.0	-8.78E+00	-6.44E+00	-6.20E+00	-6.09E+00	-2.66E+00
10	0.06858	1.20E+00	-8.13E+00	-7.39E+00	-7.49E+00	-7.03E+00	-3.17E+00
9	0.06096	-3.71E+00	-7.97E+00	-8.35E+00	-8.91E+00	-7.81E+00	-4.04E+00
8	0.05334	-2.38E+01	-8.24E+00	-9.60E+00	-1.07E+01	-9.57E+00	-4.74E+00
7	0.04572	-1.76E+01	-8.85E+00	-1.11E+01	-1.30E+01	-1.14E+01	-5.72E+00
6	0.03810	-9.40E+00	-1.07E+01	-1.37E+01	-1.59E+01	-1.34E+01	-6.52E+00
5	0.03048	-1.22E+01	-1.24E+01	-1.64E+01	-1.96E+01	-1.61E+01	-8.86E+00
4	0.02286	-2.35E+01	-1.69E+01	-2.19E+01	-2.59E+01	-2.21E+01	-1.21E+01
3	0.01524	-3.24E+01	-2.46E+01	-2.89E+01	-3.41E+01	-2.90E+01	-1.75E+01
2	0.00762	-4.36E+01	-3.46E+01	-4.11E+01	-4.72E+01	-3.93E+01	-2.92E+01
1	0.0	-5.48E+01	-5.41E+01	0.0	0.0	0.0	0.0

(b) Pitch Angle

TABLE VI (Continued)

	I =	1	2	3	4	5	6
	X =	0.0	0.50042	1.00000	1.50042	2.00000	2.50042
J	Y						
20	0.48511	0.0	1.62E+00	5.19E-01	4.38E-01	4.78E-01	5.96E-01
19	0.45957	0.0	1.30E+00	4.91E-01	4.48E-01	4.67E-01	5.98E-01
18	0.43404	0.0	9.77E-01	5.01E-01	4.35E-01	4.60E-01	5.94E-01
17	0.40851	0.0	6.75E-01	4.79E-01	4.23E-01	4.36E-01	5.78E-01
16	0.38298	0.0	3.89E-01	4.52E-01	4.19E-01	4.05E-01	5.50E-01
15	0.35745	0.0	1.73E-01	4.17E-01	3.75E-01	3.69E-01	5.15E-01
14	0.33191	0.0	4.11E-03	3.84E-01	3.46E-01	3.17E-01	4.84E-01
13	0.30638	0.0	-1.29E-01	3.51E-01	2.95E-01	2.63E-01	4.38E-01
12	0.28085	0.0	-2.16E-01	2.99E-01	2.39E-01	2.07E-01	3.88E-01
11	0.25532	0.0	-2.70E-01	2.50E-01	1.71E-01	1.43E-01	3.27E-01
10	0.22979	3.47E+00	-3.02E-01	1.80E-01	1.01E-01	7.70E-02	2.61E-01
9	0.20425	2.77E+00	-3.05E-01	9.44E-02	2.02E-02	-1.02E-02	1.81E-01
8	0.17872	6.03E-01	-3.19E-01	4.60E-06	-6.35E-02	-9.02E-02	1.09E-01
7	0.15319	-3.34E-01	-3.36E-01	-1.10E-01	-1.33E-01	-1.59E-01	3.13E-02
6	0.12766	-4.76E-01	-3.55E-01	-1.96E-01	-2.07E-01	-2.19E-01	-5.31E-02
5	0.10213	-2.88E-01	-3.51E-01	-2.48E-01	-2.49E-01	-2.76E-01	-1.13E-01
4	0.07660	-1.39E-01	-3.16E-01	-2.63E-01	-2.64E-01	-2.91E-01	-1.79E-01
3	0.05106	-9.55E-02	-2.62E-01	-2.42E-01	-2.59E-01	-3.02E-01	-2.10E-01
2	0.02553	-8.68E-02	-2.13E-01	-2.05E-01	-2.21E-01	-2.64E-01	-2.25E-01
1	0.0	-1.07E-01	-1.54E-01	-2.08E-01	-2.34E-01	-2.38E-01	-1.35E-01

(c) u/u_o

TABLE VI (Continued)

	I =	1	2	3	4	5	6
	X =	0.0	0.50042	1.00000	1.50042	2.00000	2.50042
J	Y						
20	0.48511	0.0	5.18E-01	2.39E-01	1.85E-01	1.38E-01	2.40E-01
19	0.45957	0.0	1.36E-01	7.23E-02	9.03E-02	2.84E-02	1.39E-01
18	0.43404	0.0	-5.58E-02	-6.96E-02	1.28E-02	-4.87E-03	2.52E-02
17	0.40851	0.0	-1.59E-01	-8.83E-02	-1.53E-03	-3.46E-02	1.54E-02
16	0.38298	0.0	-2.02E-01	-1.16E-01	-2.87E-02	-4.87E-02	-1.27E-03
15	0.35745	0.0	-2.14E-01	-1.36E-01	-4.27E-02	-6.65E-02	-1.51E-02
14	0.33191	0.0	-2.33E-01	-1.54E-01	-6.90E-02	-9.28E-02	-2.35E-02
13	0.30638	0.0	-2.24E-01	-1.59E-01	-9.61E-02	-1.11E-01	-3.66E-02
12	0.28085	0.0	-2.17E-01	-1.62E-01	-1.26E-01	-1.29E-01	-5.54E-02
11	0.25532	0.0	-2.04E-01	-1.73E-01	-1.57E-01	-1.57E-01	-6.76E-02
10	0.22979	1.01E-01	-1.98E-01	-1.98E-01	-1.91E-01	-1.82E-01	-8.02E-02
9	0.20425	-2.45E-01	-1.95E-01	-2.21E-01	-2.27E-01	-2.00E-01	-9.91E-02
8	0.17872	-5.86E-01	-2.02E-01	-2.45E-01	-2.65E-01	-2.36E-01	-1.13E-01
7	0.15319	-2.83E-01	-2.07E-01	-2.70E-01	-3.05E-01	-2.63E-01	-1.28E-01
6	0.12766	-1.40E-01	-2.31E-01	-3.06E-01	-3.46E-01	-2.83E-01	-1.34E-01
5	0.10213	-1.31E-01	-2.38E-01	-3.25E-01	-3.78E-01	-3.01E-01	-1.58E-01
4	0.07660	-1.92E-01	-2.63E-01	-3.70E-01	-4.24E-01	-3.42E-01	-1.80E-01
3	0.05106	-2.44E-01	-2.95E-01	-3.82E-01	-4.49E-01	-3.66E-01	-2.01E-01
2	0.02553	-2.70E-01	-2.96E-01	-3.99E-01	-4.69E-01	-3.59E-01	-2.35E-01
1	0.0	-2.51E-01	-2.95E-01	0.0	0.0	0.0	0.0

(d) v/u_o

TABLE VI (Continued)

	I =	1	2	3	4	5	6
	X =	0.0	0.50042	1.00000	1.50042	2.00000	2.50042
J	Y						
20	0.48511	0.0	8.98E-01	1.16E+00	1.16E+00	1.13E+00	8.77E-01
19	0.45957	0.0	1.08E+00	1.19E+00	1.24E+00	1.19E+00	9.72E-01
18	0.43404	0.0	1.14E+00	1.28E+00	1.25E+00	1.22E+00	1.09E+00
17	0.40851	0.0	1.15E+00	1.32E+00	1.29E+00	1.27E+00	1.16E+00
16	0.38298	0.0	1.14E+00	1.34E+00	1.30E+00	1.31E+00	1.22E+00
15	0.35745	0.0	1.15E+00	1.38E+00	1.34E+00	1.34E+00	1.27E+00
14	0.33191	0.0	1.18E+00	1.41E+00	1.37E+00	1.37E+00	1.31E+00
13	0.30638	0.0	1.23E+00	1.45E+00	1.39E+00	1.41E+00	1.36E+00
12	0.28085	0.0	1.25E+00	1.48E+00	1.42E+00	1.44E+00	1.39E+00
11	0.25532	0.0	1.29E+00	1.51E+00	1.44E+00	1.46E+00	1.42E+00
10	0.22979	3.33E+00	1.35E+00	1.51E+00	1.45E+00	1.47E+00	1.42E+00
9	0.20425	2.57E+00	1.36E+00	1.50E+00	1.45E+00	1.46E+00	1.39E+00
8	0.17872	1.18E+00	1.36E+00	1.45E+00	1.40E+00	1.39E+00	1.36E+00
7	0.15319	8.26E-01	1.29E+00	1.37E+00	1.31E+00	1.29E+00	1.28E+00
6	0.12766	7.01E-01	1.16E+00	1.24E+00	1.20E+00	1.17E+00	1.17E+00
5	0.10213	5.36E-01	1.02E+00	1.07E+00	1.03E+00	1.00E+00	1.00E+00
4	0.07660	4.18E-01	8.06E-01	8.83E-01	8.33E-01	7.92E-01	8.16E-01
3	0.05106	3.72E-01	5.87E-01	6.50E-01	6.11E-01	5.87E-01	6.03E-01
2	0.02553	2.70E-01	3.72E-01	4.09E-01	3.74E-01	3.51E-01	3.55E-01
1	0.0	1.41E-01	1.48E-01	2.17E-01	1.89E-01	9.61E-02	3.97E-02

(e) w/u_o

TABLE VII

VELOCITY DATA FOR NONSWIRLING FLOW $\phi = 0°$
[SIDE-WALL EXPANSION ANGLE $\alpha = 90°$
WITH CONTRACTION BLOCK AT L/D = 1]

	I =	1	2
	X =	0.0	0.14935
J	Y		
20	0.14478	0.0	1.80E+02
19	0.13716	0.0	1.80E+02
18	0.12954	0.0	1.84E+02
17	0.12192	0.0	1.85E+02
16	0.11430	0.0	1.87E+02
15	0.10668	0.0	1.87E+02
14	0.09906	0.0	3.60E+02
13	0.09144	0.0	3.60E+02
12	0.08382	0.0	3.60E+02
11	0.07620	0.0	3.60E+02
10	0.06858	3.60E+02	3.60E+02
9	0.06096	3.60E+02	3.60E+02
8	0.05334	3.60E+02	3.60E+02
7	0.04572	3.60E+02	3.60E+02
6	0.03810	3.60E+02	3.60E+02
5	0.03048	3.60E+02	3.60E+02
4	0.02286	3.60E+02	3.60E+02
3	0.01524	3.60E+02	3.60E+02
2	0.00762	3.60E+02	3.60E+02
1	0.0	3.60E+02	3.60E+02

(a) Yaw Angle

TABLE VII (Continued)

	I =	1	2
	X =	0.0	0.14935
J	Y		
20	0.14478	0.0	-8.38E-01
19	0.13716	0.0	-1.25E+01
18	0.12954	0.0	-3.57E+01
17	0.12192	0.0	0.0
16	0.11430	0.0	0.0
15	0.10668	0.0	-5.61E+01
14	0.09906	0.0	0.0
13	0.09144	0.0	-2.69E+01
12	0.08382	0.0	8.73E+00
11	0.07620	0.0	8.64E+00
10	0.06858	2.79E+00	4.47E+00
9	0.06096	1.91E+00	2.73E+00
8	0.05334	7.83E-01	1.50E+00
7	0.04572	2.69E-01	9.48E-01
6	0.03810	2.07E-01	7.78E-01
5	0.03048	1.42E-01	7.23E-01
4	0.02286	3.26E-01	8.24E-01
3	0.01524	5.50E-01	8.25E-01
2	0.00762	5.87E-01	8.80E-01
1	0.0	7.71E-01	9.71E-01

(b) Pitch Angle

TABLE VII (Continued)

	I =	1	2
	X =	0.0	0.50042
J	Y		
20	0.43511	0.0	-1.66E-01
19	0.45957	0.0	-1.67E-01
18	0.43404	0.0	-1.32E-01
17	0.40851	0.0	-1.41E-01
16	0.38298	0.0	-1.16E-01
15	0.35745	0.0	-8.16E-02
14	0.33191	0.0	1.87E-02
13	0.30638	0.0	8.74E-02
12	0.28085	0.0	2.62E-01
11	0.25532	0.0	5.35E-01
10	0.22979	1.01E+00	8.23E-01
9	0.20425	1.01E+00	9.84E-01
8	0.17872	1.01E+00	1.02E+00
7	0.15319	1.01E+00	1.02E+00
6	0.12766	1.01E+00	1.02E+00
5	0.10213	1.01E+00	1.02E+00
4	0.07650	1.01E+00	1.03E+00
3	0.05106	1.01E+00	1.03E+00
2	0.02553	1.01E+00	1.03E+00
1	0.0	1.01E+00	1.03E+00

(c) u/u_o

TABLE VII (Continued)

	I =	1	2
	X =	0.0	0.50042
J	Y		
20	0.48511	0.0	-2.43E-03
19	0.45957	0.0	-3.72E-02
18	0.43404	0.0	-5.49E-02
17	0.40851	0.0	0.0
16	0.38298	0.0	0.0
15	0.35745	0.0	-1.22E-01
14	0.33191	0.0	0.0
13	0.30638	0.0	-4.43E-02
12	0.28085	0.0	4.01E-02
11	0.25532	0.0	8.12E-02
10	0.22979	4.94E-02	6.44E-02
9	0.20425	3.37E-02	4.70E-02
8	0.17872	1.38E-02	2.67E-02
7	0.15319	4.73E-03	1.69E-02
6	0.12766	3.65E-03	1.39E-02
5	0.10213	2.50E-03	1.29E-02
4	0.07660	5.74E-03	1.48E-02
3	0.05106	9.69E-03	1.48E-02
2	0.02553	1.03E-02	1.58E-02
1	0.0	1.36E-02	1.75E-02

(d) v/u_o

TABLE VII (Continued)

	I =	1	2
	X =	0.0	0.50042
J	Y		
20	0.48511	0.0	5.80E-07
19	0.43957	0.0	5.84E-07
18	0.43404	0.0	-9.21E-03
17	0.40851	0.0	-1.23E-02
16	0.38298	0.0	-1.42E-02
15	0.35745	0.0	-1.00E-02
14	0.33191	0.0	-1.13E-07
13	0.30638	0.0	-5.26E-07
12	0.28085	0.0	-1.58E-06
11	0.25532	0.0	-3.22E-06
10	0.22979	-6.11E-06	-4.96E-06
9	0.20425	-6.10E-06	-5.93E-06
8	0.17872	-6.08E-06	-6.15E-06
7	0.15319	-6.08E-06	-6.14E-06
6	0.12766	-6.07E-06	-6.16E-06
5	0.10213	-6.08E-06	-6.17E-06
4	0.07660	-6.08E-06	-6.19E-06
3	0.05106	-6.08E-06	-6.19E-06
2	0.02553	-6.07E-06	-6.20E-06
1	0.0	-6.07E-06	-6.21E-06

(e) w/u_o

TABLE VIII

VELOCITY DATA FOR SWIRL VANE ANGLE ϕ = 45° [SIDE-WALL EXPANSION ANGLE α = 90° WITH CONTRACTION BLOCK AT L/D = 2]

	I =	1	2	3	4
	X =	0.0	0.14935	0.29845	0.44780
J	Y				
20	0.14478	0.0	1.82E+02	3.60E+02	1.90E+02
19	0.13716	0.0	1.82E+02	3.60E+02	1.90E+02
18	0.12954	0.0	1.95E+02	3.60E+02	3.60E+02
17	0.12192	0.0	1.87E+02	3.60E+02	3.60E+02
16	0.11430	0.0	1.87E+02	3.60E+02	3.60E+02
15	0.10668	0.0	1.81E+02	3.60E+02	3.60E+02
14	0.09906	0.0	3.60E+02	3.60E+02	3.60E+02
13	0.09144	0.0	3.60E+02	3.60E+02	3.60E+02
12	0.08382	0.0	3.60E+02	3.60E+02	3.60E+02
11	0.07620	0.0	3.60E+02	3.60E+02	3.60E+02
10	0.06858	3.60E+02	3.60E+02	3.60E+02	3.60E+02
9	0.06096	3.60E+02	3.60E+02	3.60E+02	3.60E+02
8	0.05334	3.60E+02	3.60E+02	3.60E+02	3.60E+02
7	0.04572	3.60E+02	3.60E+02	3.60E+02	3.60E+02
6	0.03810	3.60E+02	3.60E+02	3.60E+02	3.60E+02
5	0.03048	3.60E+02	3.60E+02	3.60E+02	3.60E+02
4	0.02286	3.60E+02	3.60E+02	3.60E+02	3.60E+02
3	0.01524	3.60E+02	3.60E+02	3.60E+02	3.60E+02
2	0.00762	3.60E+02	3.60E+02	3.60E+02	3.60E+02
1	0.0	3.60E+02	3.60E+02	3.60E+02	3.60E+02

(a) Yaw Angle

TABLE VIII (Continued)

	I =	1	2	3	4
	X =	0.0	0.14935	0.29845	0.44780
J	Y				
20	0.14478	0.0	0.0	-4.18E+01	-2.89E+01
19	0.13716	0.0	0.0	0.0	-3.59E+01
18	0.12954	0.0	0.0	-2.02E+01	5.39E+01
17	0.12192	0.0	-4.13E+01	3.87E+01	5.18E+01
16	0.11430	0.0	-4.02E+01	3.16E+01	4.32E+01
15	0.10668	0.0	0.0	3.46E+01	3.41E+01
14	0.09906	0.0	-3.00E+01	2.16E+01	2.90E+01
13	0.09144	0.0	1.09E+01	1.69E+01	1.87E+01
12	0.08382	0.0	1.12E+01	1.11E+01	1.32E+01
11	0.07620	0.0	7.89E+00	7.59E+00	1.07E+01
10	0.06858	3.83E+00	4.83E+00	5.59E+00	8.33E+00
9	0.06096	2.63E+00	2.86E+00	4.17E+00	6.53E+00
8	0.05334	1.32E+00	1.82E+00	2.89E+00	5.02E+00
7	0.04572	3.82E-01	1.28E+00	2.08E+00	4.10E+00
6	0.03810	1.16E-01	9.90E-01	1.54E+00	3.29E+00
5	0.03048	1.92E-02	8.32E-01	1.13E+00	2.58E+00
4	0.02286	2.97E-01	7.95E-01	9.83E-01	2.15E+00
3	0.01524	4.67E-01	8.64E-01	8.71E-01	1.60E+00
2	0.00762	6.01E-01	8.12E-01	8.00E-01	1.25E+00
1	0.0	8.38E-01	9.03E-01	8.27E-01	1.41E+00

(b) Pitch Angle

TABLE VIII (Continued)

	I =	1	2	3	4
	X =	0.0	0.50042	1.00000	1.50042
J	Y				
20	0.48511	0.0	-7.26E-02	3.80E-02	-8.77E-02
19	0.45957	0.0	-8.30E-02	2.01E-02	-8.18E-02
18	0.43404	0.0	-8.25E-02	4.66E-02	3.83E-02
17	0.40851	0.0	-6.32E-02	5.40E-02	6.19E-02
16	0.38298	0.0	-6.36E-02	8.74E-02	1.03E-01
15	0.35745	0.0	-4.50E-02	1.20E-01	1.66E-01
14	0.33191	0.0	1.81E-02	2.16E-01	2.18E-01
13	0.30638	0.0	1.13E-01	3.06E-01	3.25E-01
12	0.28085	0.0	2.84E-01	4.21E-01	4.09E-01
11	0.25532	0.0	5.68E-01	5.85E-01	5.09E-01
10	0.22979	1.03E+00	8.55E-01	7.54E-01	6.29E-01
9	0.20425	1.02E+00	1.03E+00	8.67E-01	7.14E-01
8	0.17872	1.01E+00	1.04E+00	9.56E-01	7.95E-01
7	0.15319	1.00E+00	1.04E+00	9.98E-01	8.71E-01
6	0.12766	1.01E+00	1.04E+00	1.01E+00	9.13E-01
5	0.10213	1.00E+00	1.04E+00	1.02E+00	9.38E-01
4	0.07660	1.01E+00	1.04E+00	1.02E+00	9.56E-01
3	0.05106	1.00E+00	1.04E+00	1.02E+00	9.61E-01
2	0.02553	1.00E+00	1.04E+00	1.02E+00	9.68E-01
1	0.0	1.01E+00	1.04E+00	1.02E+00	9.71E-01

(c) u/u_o

TABLE VIII (Continued)

	I =	1	2	3	4
	X =	0.0	0.50042	1.CCCCC	1.50042
J	Y				
20	0.48511	0.0	0.0	-3.40E-02	-4.93E-02
19	0.45957	0.0	0.0	0.0	-6.01E-02
18	0.43404	0.0	0.0	-1.72E-02	5.26E-02
17	0.40851	0.0	-5.61E-02	4.32E-02	7.87E-02
16	0.38298	0.0	-5.41E-02	5.37E-02	9.65E-02
15	0.35745	0.0	0.0	8.25E-02	1.13E-01
14	0.33191	0.0	-1.04E-02	8.55E-02	1.21E-01
13	0.30638	0.0	2.16E-02	9.32E-02	1.10E-01
12	0.28085	0.0	5.63E-02	8.26E-02	9.57E-02
11	0.25532	0.0	7.88E-02	7.79E-02	9.63E-02
10	0.22979	6.90E-02	7.22E-02	7.37E-02	9.21E-02
9	0.20425	4.68E-02	5.16E-02	6.31E-02	8.18E-02
8	0.17872	2.34E-02	3.30E-02	4.83E-02	6.98E-02
7	0.15319	6.69E-03	2.32E-02	3.62E-02	6.25E-02
6	0.12766	2.03E-03	1.79E-02	2.72E-02	5.25E-02
5	0.10213	3.36E-04	1.51E-02	2.02E-02	4.23E-02
4	0.07660	5.22E-03	1.44E-02	1.75E-02	3.59E-02
3	0.05106	8.19E-03	1.57E-02	1.56E-02	2.69E-02
2	0.02553	1.05E-02	1.47E-02	1.43E-02	2.12E-02
1	0.0	1.47E-02	1.64E-02	1.48E-02	2.38E-02

(d) v/u_o

TABLE VIII (Continued)

	I =	1	2	3	4
	X =	0.0	0.50042	1.00000	1.50042
J	Y				
20	0.46511	0.0	-2.53E-03	-2.29E-07	-1.61E-02
19	0.45957	0.0	-2.90E-03	-1.21E-07	-1.50E-02
18	0.43404	0.0	-2.21E-02	-2.81E-07	-2.31E-07
17	0.40851	0.0	-8.21E-03	-3.25E-07	-3.73E-07
16	0.38298	0.0	-8.26E-03	-5.26E-07	-6.19E-07
15	0.35745	0.0	-7.86E-04	-7.21E-07	-1.00E-06
14	0.33191	0.0	-1.09E-07	-1.30E-06	-1.31E-06
13	0.30638	0.0	-6.79E-07	-1.85E-06	-1.96E-06
12	0.28085	0.0	-1.71E-06	-2.54E-06	-2.47E-06
11	0.25532	0.0	-3.42E-06	-3.52E-06	-3.07E-06
10	0.22979	-6.21E-06	-5.15E-06	-4.54E-06	-3.79E-06
9	0.20425	-6.14E-06	-6.23E-06	-5.22E-06	-4.30E-06
8	0.17872	-6.10E-06	-6.24E-06	-5.76E-06	-4.79E-06
7	0.15319	-6.05E-06	-6.25E-06	-6.01E-06	-5.25E-06
6	0.12766	-6.06E-06	-6.25E-06	-6.10E-06	-5.50E-06
5	0.10213	-6.04E-06	-6.25E-06	-6.16E-06	-5.65E-06
4	0.07660	-6.06E-06	-6.25E-06	-6.16E-06	-5.76E-06
3	0.05106	-6.05E-06	-6.26E-06	-6.16E-06	-5.79E-06
2	0.02553	-6.05E-06	-6.26E-06	-6.17E-06	-5.83E-06
1	0.0	-6.06E-06	-6.27E-06	-6.17E-06	-5.85E-06

(e) $w/_{uo}$

TABLE IX

VELOCITY DATA FOR SWIRL VANE ANGLE
$\phi = 45^{\circ}$ [SIDE-WALL EXPANSION ANGLE
$\alpha = 90°$ WITH CONTRACTION BLOCK]
AT L/D = 1

	I =	1	2
	X =	0.0	0.14935
J	Y		
19	0.13716	0.0	2.90E+01
18	0.12954	0.0	2.58E+01
17	0.12192	0.0	2.80E+01
16	0.11430	0.0	3.46E+01
15	0.10668	0.0	5.14E+01
14	0.09906	0.0	7.76E+01
13	0.09144	0.0	1.00E+02
12	0.08382	0.0	1.12E+02
11	0.07620	0.0	1.17E+02
10	0.06858	3.30E+01	1.18E+02
9	0.06096	3.34E+01	1.17E+02
8	0.05334	3.10E+01	1.15E+02
7	0.04572	3.54E+01	1.12E+02
6	0.03810	4.14E+01	1.08E+02
5	0.03048	7.76E+01	1.04E+02
4	0.02286	9.74E+01	9.74E+01
3	0.01524	1.02E+02	8.56E+01
2	0.00762	1.08E+02	6.00E+01
1	0.0	5.40E+00	-2.00E-01

(a) Yaw Angle

TABLE IX (Continued)

	I =	1	2
	X =	0.0	0.14935
J	Y		
19	0.13716	0.0	1.32E+01
18	0.12954	0.0	5.08E+00
17	0.12192	0.0	3.64E+00
16	0.11430	0.0	-2.65E-01
15	0.10668	0.0	-7.18E+00
14	0.09906	0.0	-1.10E+01
13	0.09144	0.0	-5.81E+00
12	0.08382	0.0	-2.82E+00
11	0.07620	0.0	-3.11E+00
10	0.06858	1.19E+01	-3.30E+00
9	0.06096	1.16E+01	-3.59E+00
8	0.05334	1.01E+01	-4.39E+00
7	0.04572	6.98E+00	-6.04E+00
6	0.03810	3.59E+00	-7.58E+00
5	0.03048	-2.13E+01	-1.21E+01
4	0.02286	-1.69E+01	-1.87E+01
3	0.01524	-1.49E+01	-3.39E+01
2	0.00762	-1.87E+00	0.0
1	0.0	-1.03E+01	-4.15E+01

(b) Pitch Angle

TABLE IX (Continued)

	I =	1	2
	X =	0.0	0.50042
J	Y		
19	0.45957	0.0	7.54E-01
18	0.43404	0.0	8.17E-01
17	0.40851	0.0	7.01E-01
16	0.38298	0.0	5.06E-01
15	0.35745	0.0	2.59E-01
14	0.33191	0.0	6.80E-02
13	0.30638	0.0	-6.79E-02
12	0.28085	0.0	-1.84E-01
11	0.25532	0.0	-2.53E-01
10	0.22979	1.53E+00	-2.86E-01
9	0.20425	1.68E+00	-2.85E-01
8	0.17872	1.81E+00	-2.68E-01
7	0.15319	1.32E+00	-2.27E-01
6	0.12766	3.58E-01	-1.73E-01
5	0.10213	2.14E-02	-1.16E-01
4	0.07660	-2.18E-02	-4.67E-02
3	0.05106	-3.62E-02	1.63E-02
2	0.02553	-4.79E-02	4.43E-02
1	0.0	1.39E-01	9.80E-02

(c) u/u_o

TABLE IX (Continued)

	I =	1	2
	X =	0.0	0.50042
J	Y		
19	0.45957	0.0	2.02E-01
18	0.43404	0.0	8.06E-02
17	0.40851	0.0	5.06E-02
16	0.38298	0.0	-2.84E-03
15	0.35745	0.0	-5.23E-02
14	0.33191	0.0	-6.15E-02
13	0.30638	0.0	-3.98E-02
12	0.28085	0.0	-2.44E-02
11	0.25532	0.0	-3.02E-02
10	0.22979	3.86E-01	-3.46E-02
9	0.20425	4.12E-01	-3.94E-02
8	0.17872	3.76E-01	-4.90E-02
7	0.15319	1.99E-01	-6.47E-02
6	0.12766	2.99E-02	-7.51E-02
5	0.10213	-3.88E-02	-1.03E-01
4	0.07660	-5.15E-02	-1.23E-01
3	0.05106	-4.63E-02	-1.43E-01
2	0.02553	-5.02E-03	0.0
1	0.0	-2.54E-02	-8.68E-02

(d) v/u_o

TABLE IX (Continued)

	I =	1	2
	X =	0.0	0.50042
J	Y		
19	0.45957	0.0	4.18E-01
18	0.43404	0.0	3.95E-01
17	0.40851	0.0	3.73E-01
16	0.38298	0.0	3.49E-01
15	0.35745	0.0	3.24E-01
14	0.33191	0.0	3.09E-01
13	0.30638	0.0	3.85E-01
12	0.28085	0.0	4.59E-01
11	0.25532	0.0	4.96E-01
10	0.22979	9.95E-01	5.29E-01
9	0.20425	1.11E+00	5.58E-01
8	0.17872	1.09E+00	5.80E-01
7	0.15319	9.40E-01	5.68E-01
6	0.12766	3.10E-01	5.38E-01
5	0.10213	9.72E-02	4.63E-01
4	0.07660	1.63E-01	3.59E-01
3	0.05106	1.70E-01	2.12E-01
2	0.02553	1.46E-01	7.67E-02
1	0.0	1.31E-02	-3.42E-04

(e) w/u_o

TABLE X

VELOCITY DATA FOR SWIRL VANE ANGLE ϕ = 45° [SIDE-WALL EXPANSION ANGLE α = 90° WITH CONTRACTION BLOCK AT L/D = 2]

	I =	1	2	3	4
	X =	0.0	0.14935	0.29845	0.44780
J	Y				
19	0.13716	0.0	2.50E+01	3.60E+01	6.30E+01
18	0.12954	0.0	2.32E+01	4.06E+01	6.26E+01
17	0.12192	0.0	2.62E+01	4.76E+01	6.26E+01
16	0.11430	0.0	3.48E+01	5.44E+01	6.18E+01
15	0.10668	0.0	4.00E+01	6.14E+01	6.22E+01
14	0.09906	0.0	9.26E+01	6.92E+01	6.22E+01
13	0.09144	0.0	1.13E+02	7.60E+01	6.28E+01
12	0.08382	0.0	1.21E+02	8.10E+01	6.36E+01
11	0.07620	0.0	1.24E+02	8.40E+01	6.40E+01
10	0.06858	3.24E+01	1.24E+02	8.60E+01	6.58E+01
9	0.06096	3.28E+01	1.24E+02	8.72E+01	6.64E+01
8	0.05334	3.22E+01	1.23E+02	8.62E+01	6.70E+01
7	0.04572	3.36E+01	1.20E+02	8.64E+01	6.80E+01
6	0.03810	3.76E+01	1.16E+02	8.70E+01	6.92E+01
5	0.03048	8.76E+01	1.14E+02	8.40E+01	6.80E+01
4	0.02286	1.29E+02	1.10E+02	8.04E+01	6.56E+01
3	0.01524	1.45E+02	1.02E+02	7.38E+01	5.96E+01
2	0.00762	1.56E+02	9.90E+01	6.28E+01	4.72E+01
1	0.0	1.93E+02	1.28E+02	4.56E+01	1.56E+01

(a) Yaw Angle

TABLE X (Continued)

	I =	1	2	3	4
	X =	0.0	0.14935	0.29845	0.44780
J	Y				
19	0.13716	0.0	8.00E+00	2.36E+00	1.58E+00
18	0.12954	0.0	2.56E+00	7.18E+00	6.10E 01
17	0.12192	0.0	1.06E+00	1.02E+01	2.20E+00
16	0.11430	0.0	-5.32E+00	-1.35E+01	-3.17E+00
15	0.10668	0.0	-1.81E+01	-1.51E+01	4.40E+00
14	0.09906	0.0	-3.00E+00	-1.55E+01	-4.04E+00
13	0.09144	0.0	1.52E+00	-1.53E+01	-4.31E+00
12	0.08382	0.0	3.14E+00	1.36E+01	4.32E+00
11	0.07620	0.0	2.68E+00	-1.26E+01	-3.99E+00
10	0.06858	1.23E+01	1.65E+00	-1.03E+01	3.94E+00
9	0.06096	1.20E+01	1.08E+00	8.71E+00	-3.83E+00
8	0.05334	1.04E+01	4.58E- 01	-7.87E+00	-4.53E+00
7	0.04572	7.75E+00	2.09E+00	6.87E+00	5.04E+00
6	0.03810	5.05E+00	5.03E+00	-7.31E+00	-5.18E+00
5	0.03048	2.13E+01	-8.78E+00	-7.10E+00	7.46E+00
4	0.02286	3.13E+01	1.12E+01	1.25E+01	8.24E+00
3	0.01524	-3.41E+01	-3.00E+01	-1.50E+01	-1.24E+01
2	0.00762	5.27E+01	0.0	2.86E+01	1.79E+01
1	0.0	3.00E+01	0.0	-3.48E+01	-1.46E+01

(b) Pitch Angle

TABLE X (Continued)

	I =	1	2	3	4
	X =	0.0	0.50042	1.00000	1.50042
J	Y				
19	0.45957	0.0	8.08E-01	6.27E-01	2.56E 01
18	0.43404	0.0	8.20E-01	5.29E-01	2.72E 01
17	0.40851	0.0	6.68E-01	4.33E-01	2.79E-01
16	0.38298	0.0	4.15E 01	3.40E 01	2.87E 01
15	0.35745	0.0	1.98E-01	2.58E-01	2.90E-01
14	0.33191	0.0	1.26E-02	1.84E 01	3.00E-01
13	0.30638	0.0	1.49E 01	1.24E 01	3.04E 01
12	0.28085	0.0	2.34E 01	8.19E-02	3.04E 01
11	0.25532	0.0	2.82E-01	5.61E-02	3.10E-01
10	0.22979	1.53E+00	2.96E-01	3.93E 02	3.04E-01
9	0.20425	1.57E+00	3.01E 01	2.9.E 02	3.07E 01
8	0.17872	1.76E+00	2.89E 01	4.11E-02	3.05E 01
7	0.15319	1.27E+00	2.55E-01	4.07E-02	2.94E 01
6	0.12766	3.28E 01	1.91E-01	3.43E-02	2.87E-01
5	0.10213	2.65E-03	1.54E-01	6.91E-02	2.84E-01
4	0.07660	-8.01E-02	1.03E 01	8.85E 02	2.71E 01
3	0.05106	-9.80E-02	3.60E-02	1.24E-01	2.60E-01
2	0.02553	-5.90E-02	9.07E 03	1.32E 01	2.24E-01
1	0.0	6.05E-02	2.90E 02	1.40E-01	2.20E-01

(c) u/u_o

TABLE X (Continued)

	I =	1	2	3	4
	X =	0.0	0.50042	1.00000	1.50042
J	Y				
19	0.45957	0.0	1.25E 01	3.19E-02	1.56E 02
18	0.43404	0.0	3.99E-02	-6.78E-02	-6.29E-03
17	0.40851	0.0	1.38E-02	-1.16E-01	-2.32E-02
16	0.38298	0.0	4.70E 02	1.40E 01	3.36E 02
15	0.35745	0.0	-8.48E-02	-1.45E-01	-4.79E-02
14	0.33191	0.0	-1.46E-02	1.43E-01	4.54E 02
13	0.30638	0.0	1.03E 02	1.41E 01	5.00E 02
12	0.28085	0.0	2.48E-02	-1.27E-01	-5.16E 02
11	0.25532	0.0	2.33E-02	-1.20E-01	-4.93E 02
10	0.22979	5.95E-01	1.50E-02	-1.02E-01	-5.10E-02
9	0.20425	4.22E-01	1.01E-02	-9.25E-02	-5.13E-02
8	0.17872	3.32E 01	4.25E 03	8.58E 02	6.19E 02
7	0.15319	2.08E-01	-1.88E-02	-7.81E-02	-6.92E-02
6	0.12766	4.40E-02	3.81E-02	8.42E-02	7.32E-02
5	0.10213	2.47E 02	5.85E 02	8.23E 02	9.24E-02
4	0.07660	-7.74E-02	-5.88E-02	-1.17E-01	-9.49E-02
3	0.05106	-8.07E-02	-9.98E-02	-1.18E-01	1.13E 01
2	0.02553	-8.49E-02	0.0	-1.58E-01	-1.06E-01
1	0.0	3.58E-02	0.0	1.40E 01	5.97E 02

(d) v/u_o

TABLE X (Continued)

	I =	1	2	3	4
	λ =	0.0	0.50042	1.00000	1.50042
J	Y				
19	0.45957	0.0	3.77E-01	4.56E-01	5.02E-01
18	0.43404	0.0	3.52E 01	4.54E 01	5.25E 01
17	0.40851	0.0	3.29E-01	4.75E-01	5.38E-01
16	0.38298	0.0	2.88E 01	4.75E-01	5.35E 01
15	0.35745	0.0	1.55E 01	4.73E 01	5.51E 01
14	0.33191	0.0	2.77E-01	4.83E-01	5.68E-01
13	0.30638	0.0	3.57E-01	4.99E-01	5.91E 01
12	0.28085	0.0	3.87E-01	5.17E-01	6.12E-01
11	0.25532	0.0	4.11E-01	5.34E-01	6.36E 01
10	0.22979	9.58E 01	4.32E 01	5.62E 01	6.76E 01
9	0.20425	1.07E+00	4.46E-01	6.05E-01	7.02E-01
8	0.17872	1.11E+00	4.46E-01	6.19E-01	7.19E-01
7	0.15319	8.43E 01	4.45E 01	6.47E-01	7.27E-01
6	0.12766	2.53E-01	3.89E-01	6.55E-01	7.55E-01
5	0.10213	5.33E-02	3.46E 01	6.57E 01	6.54E 01
4	0.07660	9.89E-02	2.79E-01	5.23E-01	5.96E-01
3	0.05106	6.70E-02	1.69E-01	4.26E 01	4.43E-01
2	0.02553	2.67E 02	5.73E 02	2.58E 01	2.42E 01
1	0.0	-1.40E-02	3.74E-02	1.43E-01	6.14E-02

(e) w/u_o

TABLE XI

VELOCITY DATA FOR SWIRL VANE ANGLE
ϕ = 70° [SIDE-WALL EXPANSION ANGLE
α = 90° WITH CONTRACTION
BLOCK AT L/D = 1]

	I =	1	2
	X =	0.0	0.14935
J	Y		
19	0.13716	0.0	5.48E+01
18	0.12954	0.0	6.04E+01
17	0.12192	0.0	6.74E+01
16	0.11430	0.0	7.44E+01
15	0.10668	0.0	8.18E+01
14	0.09906	0.0	8.76E+01
13	0.09144	0.0	9.18E+01
12	0.08382	0.0	9.40E+01
11	0.07620	0.0	9.56E+01
10	0.06858	4.36E+01	9.40E+01
9	0.06096	3.86E+01	9.38E+01
8	0.05334	5.44E+01	9.34E+01
7	0.04572	9.54E+01	9.38E+01
6	0.03810	1.16E+02	9.52E+01
5	0.03048	1.13E+02	9.78E+01
4	0.02286	1.02E+02	1.04E+02
3	0.01524	9.72E+01	1.16E+02
2	0.00762	1.02E+02	1.36E+02
1	0.0	1.20E+02	1.63E+02

(a) Yaw Angle

TABLE XI (Continued)

	I =	1	2
	X =	0.0	0.14935
J	Y		
19	0.13716	0.0	5.93E+00
18	0.12954	0.0	-1.43E+00
17	0.12192	0.0	-3.81E+00
16	0.11430	0.0	-5.45E+00
15	0.10668	0.0	-7.11E+00
14	0.09906	0.0	-7.98E+00
13	0.09144	0.0	-7.83E+00
12	0.08382	0.0	-7.63E+00
11	0.07620	0.0	-6.30E+00
10	0.06858	4.42E+00	-5.69E+00
9	0.06096	1.46E+00	-5.10E+00
8	0.05334	-8.60E+00	4.81E+00
7	0.04572	-1.43E+01	-5.35E+00
6	0.03810	-6.23E+00	-6.16E+00
5	0.03048	-6.92E+00	-7.34E+00
4	0.02286	-1.51E+01	-1.05E+01
3	0.01524	-2.11E+01	-1.47E+01
2	0.00762	-2.83E+01	-1.79E+01
1	0.0	-4.39E+01	-1.58E+01

(b) Pitch Angle

TABLE XI (Continued)

	I =	1	2
	X =	0.0	0.50042
J	Y		
19	0.45957	0.0	8.01E-01
18	0.43404	0.0	6.29E-01
17	0.40851	0.0	4.70E-01
16	0.38298	0.0	3.21E-01
15	0.35745	0.0	1.70E-01
14	0.33191	0.0	5.02E-02
13	0.30638	0.0	-4.00E-02
12	0.28085	0.0	-9.36E-02
11	0.25532	0.0	-1.41E-01
10	0.22979	3.14E+00	-1.05E-01
9	0.20425	2.72E+00	-1.02E-01
8	0.17872	9.99E-01	-9.12E-02
7	0.15319	-8.40E-02	-9.64E-02
6	0.12766	-3.79E-01	-1.15E-01
5	0.10213	-2.68E-01	-1.41E-01
4	0.07660	-1.06E-01	-1.94E-01
3	0.05106	-5.49E-02	-2.44E-01
2	0.02553	-6.98E-02	-3.06E-01
1	0.0	-7.83E-02	-3.71E-01

(c) u/u_o

TABLE XI (Continued)

	I =	1	2
	X =	0.0	0.50042
J	Y		
19	0.45957	0.0	1.44E-01
18	0.43404	0.0	-3.17E-02
17	0.40851	0.0	-8.16E-02
16	0.38298	0.0	-1.14E-01
15	0.35745	0.0	-1.49E-01
14	0.33191	0.0	-1.68E-01
13	0.30638	0.0	-1.75E-01
12	0.28085	0.0	-1.80E-01
11	0.25532	0.0	-1.59E-01
10	0.22979	3.36E-01	-1.50E-01
9	0.20425	8.85E-02	-1.37E-01
8	0.17872	-2.60E-01	-1.29E-01
7	0.15319	-2.27E-01	-1.36E-01
6	0.12766	-9.38E-02	-1.37E-01
5	0.10213	-8.32E-02	-1.33E-01
4	0.07660	-1.40E-01	-1.44E-01
3	0.05106	-1.69E-01	-1.47E-01
2	0.02553	-1.81E-01	-1.37E-01
1	0.0	-1.52E-01	-1.10E-01

(d) v/u_o

TABLE XI (Continued)

	I =	1	2
	X =	0.0	0.50042
J	Y		
19	0.45957	0.0	1.14E+00
18	0.43404	0.0	1.11E+00
17	0.40851	0.0	1.13E+00
16	0.38298	0.0	1.15E+00
15	0.35745	0.0	1.18E+00
14	0.33191	0.0	1.20E+00
13	0.30638	0.0	1.27E+00
12	0.28085	0.0	1.34E+00
11	0.25532	0.0	1.44E+00
10	0.22979	2.99E+00	1.50E+00
9	0.20425	2.17E+00	1.54E+00
8	0.17872	1.40E+00	1.53E+00
7	0.15319	8.88E-01	1.45E+00
6	0.12766	7.70E-01	1.27E+00
5	0.10213	6.31E-01	1.03E+00
4	0.07660	5.06E-01	7.54E-01
3	0.05106	4.34E-01	5.04E-01
2	0.02553	3.28E-01	2.95E-01
1	0.0	1.37E-01	1.16E-01

(e) w/u_o

TABLE XII

VELOCITY DATA FOR SWIRL VANE ANGLE ϕ = 70°
[SIDE-WALL EXPANSION ANGLE α = 90° WITH
CONTRACTION BLOCK AT L/D = 2]

	I =	1	2	3	4
	X =	0.0	0.14935	0.29845	0.44780
J	Y				
19	0.13716	0.0	4.96E+01	7.18E+01	7.10E+01
18	0.12954	0.0	5.74E+01	7.18E+01	7.10E+01
17	0.12192	0.0	6.46E+01	7.30E+01	7.26E+01
16	0.11430	0.0	7.38E+01	7.40E+01	7.40E+01
15	0.10668	0.0	8.16E+01	7.54E+01	7.44E+01
14	0.09906	0.0	8.88E+01	7.62E+01	7.58E+01
13	0.09144	0.0	9.36E+01	7.76E+01	7.74E+01
12	0.08382	0.0	9.62E+01	7.90E+01	7.88E+01
11	0.07620	0.0	9.76E+01	8.02E+01	8.00E+01
10	0.06858	4.36E+01	9.80E+01	8.18E+01	8.18E+01
9	0.06096	3.84E+01	9.80E+01	8.40E+01	8.38E+01
8	0.05334	5.24E+01	9.80E+01	8.72E+01	8.56E+01
7	0.04572	9.38E+01	9.90E+01	8.98E+01	8.76E+01
6	0.03810	1.17E+02	9.96E+01	9.36E+01	9.14E+01
5	0.03048	1.14E+02	1.01E+02	9.70E+01	9.88E+01
4	0.02286	1.03E+02	1.03E+02	1.02E+02	1.09E+02
3	0.01524	9.26E+01	1.05E+02	1.10E+02	1.29E+02
2	0.00762	8.80E+01	1.12E+02	1.23E+02	1.56E+02
1	0.0	9.00E+01	1.33E+02	1.54E+02	1.84E+02

(a) Yaw Angle

TABLE XII (Continued)

	I =	1	2	3	4
	X =	0.0	0.14935	0.29845	0.44780
J	Y				
19	0.13716	0.0	3.70E+00	3.16E+00	4.09E+00
18	0.12954	0.0	-2.41E+00	-1.11E+00	8.67E-01
17	0.12192	0.0	-4.61E+00	-2.13E+00	-2.35E-01
16	0.11430	0.0	-6.11E+00	-2.77E+00	-8.45E-01
15	0.10668	0.0	-7.58E+00	-2.85E+00	-1.71E+00
14	0.09906	0.0	-8.04E+00	-3.21E+00	-2.35E+00
13	0.09144	0.0	-7.48E+00	-3.52E+00	-3.44E+00
12	0.08382	0.0	-6.88E+00	-3.83E+00	-4.18E+00
11	0.07620	0.0	-6.16E+00	-4.34E+00	-5.43E+00
10	0.06858	5.42E+00	-5.44E+00	-4.49E+00	-6.32E+00
9	0.06096	2.53E+00	-5.05E+00	-5.78E+00	-6.70E+00
8	0.05334	-6.99E+00	-5.08E+00	-7.14E+00	-8.11E+00
7	0.04572	-1.33E+01	-5.47E+00	-8.93E+00	-1.06E+01
6	0.03810	-6.38E+00	-6.41E+00	-1.17E+01	-1.55E+01
5	0.03048	-7.35E+00	-8.10E+00	-1.56E+01	-2.02E+01
4	0.02286	-1.51E+01	-1.23E+01	-1.72E+01	-2.93E+01
3	0.01524	-2.26E+01	-1.95E+01	-2.48E+01	-3.30E+01
2	0.00762	-2.93E+01	-3.00E+01	-3.64E+01	-3.65E+01
1	0.0	-3.84E+01	-4.84E+01	-4.91E+01	-3.73E+01

(b) Pitch Angle

TABLE XII (Continued)

	I =	1	2	3	4
	X =	0.0	0.50042	1.00000	1.50042
J	Y				
19	0.45957	0.0	8.94E-01	3.79E-01	3.98E-01
18	0.43404	0.0	6.86E-01	3.99E-01	4.09E-01
17	0.40851	0.0	5.08E-01	3.82E-01	3.83E-01
16	0.38298	0.0	3.20E-01	3.66E-01	3.68E-01
15	0.35745	0.0	1.65E-01	3.47E-01	3.66E-01
14	0.33191	0.0	2.39E-02	3.36E-01	3.45E-01
13	0.30638	0.0	-7.65E-02	3.13E-01	3.16E-01
12	0.28085	0.0	-1.39E-01	2.89E-01	2.87E-01
11	0.25532	0.0	-1.78E-01	2.60E-01	2.64E-01
10	0.22979	3.10E+00	-1.94E-01	2.21E-01	2.17E-01
9	0.20425	2.71E+00	-2.00E-01	1.61E-01	1.63E-01
8	0.17872	1.07E+00	-1.99E-01	7.18E-02	1.09E-01
7	0.15319	-5.94E-02	-2.15E-01	4.74E-03	5.30E-02
6	0.12766	-3.85E-01	-2.06E-01	-7.44E-02	-2.49E-02
5	0.10213	-2.89E-01	-2.00E-01	-1.20E-01	-1.18E-01
4	0.07660	-1.18E-01	-1.79E-01	-1.63E-01	-1.72E-01
3	0.05106	-1.91E-02	-1.48E-01	-1.89E-01	-2.72E-01
2	0.02553	1.24E-02	-1.27E-01	-1.95E-01	-3.18E-01
1	0.0	7.04E-07	-1.17E-01	-2.11E-01	-3.26E-01

(c) u/u_o

TABLE XII (Continued)

	I =	1	2	3	4
	X =	0.0	0.50042	1.00000	1.50042
J	Y				
19	0.45957	0.0	8.93E-02	6.70E-02	6.74E-02
18	0.43404	0.0	-5.36E-02	-2.48E-02	1.90E-02
17	0.40851	0.0	-9.55E-02	-4.86E-02	-5.25E-03
16	0.38298	0.0	-1.23E-01	-6.42E-02	-1.97E-02
15	0.35745	0.0	-1.50E-01	-6.85E-02	-4.07E-02
14	0.33191	0.0	-1.62E-01	-7.89E-02	-5.77E-02
13	0.30638	0.0	-1.60E-01	-8.98E-02	-8.73E-02
12	0.28085	0.0	-1.55E-01	-1.02E-01	-1.08E-01
11	0.25532	0.0	-1.45E-01	-1.16E-01	-1.44E-01
10	0.22979	4.06E-01	-1.33E-01	-1.22E-01	-1.69E-01
9	0.20425	1.53E-01	-1.27E-01	-1.56E-01	-1.77E-01
8	0.17872	-2.15E-01	-1.27E-01	-1.84E-01	-2.02E-01
7	0.15319	-2.12E-01	-1.31E-01	-2.13E-01	-2.38E-01
6	0.12766	-9.62E-02	-1.39E-01	-2.45E-01	-2.82E-01
5	0.10213	-9.31E-02	-1.49E-01	-2.74E-01	-2.84E-01
4	0.07660	-1.42E-01	-1.79E-01	-2.35E-01	-2.98E-01
3	0.05106	-1.75E-01	-1.98E-01	-2.54E-01	-2.80E-01
2	0.02553	-1.99E-01	-1.98E-01	-2.61E-01	-2.59E-01
1	0.0	-1.76E-01	-1.93E-01	-2.71E-01	-2.49E-01

(d) v/u_o

TABLE XII (Continued)

	I =	1	2	3	4
	X =	0.0	0.50042	1.00000	1.50042
J	Y				
19	0.45957	0.0	1.05E+00	1.15E+00	1.16E+00
18	0.43404	0.0	1.07E+00	1.21E+00	1.19E+00
17	0.40851	0.0	1.07E+00	1.25E+00	1.22E+00
16	0.38298	0.0	1.10E+00	1.28E+00	1.28E+00
15	0.35745	0.0	1.12E+00	1.33E+00	1.31E+00
14	0.33191	0.0	1.14E+00	1.37E+00	1.36E+00
13	0.30638	0.0	1.22E+00	1.42E+00	1.42E+00
12	0.28085	0.0	1.28E+00	1.49E+00	1.45E+00
11	0.25532	0.0	1.33E+00	1.50E+00	1.50E+00
10	0.22979	2.95E+00	1.38E+00	1.53E+00	1.51E+00
9	0.20425	2.15E+00	1.42E+00	1.53E+00	1.50E+00
8	0.17872	1.39E+00	1.42E+00	1.47E+00	1.41E+00
7	0.15319	8.94E-01	1.36E+00	1.36E+00	1.27E+00
6	0.12766	7.70E-01	1.22E+00	1.18E+00	1.02E+00
5	0.10213	6.62E-01	1.03E+00	9.74E-01	7.65E-01
4	0.07660	5.12E-01	7.99E-01	7.42E-01	5.00E-01
3	0.05106	4.22E-01	5.39E-01	5.18E-01	3.36E-01
2	0.02553	3.54E-01	3.19E-01	2.96E-01	1.44E-01
1	0.0	2.22E-01	1.26E-01	1.05E-01	-2.05E-02

(e) w/u_o

TABLE XIII

CHARACTERISTICS OF FLOWFIELDS IN TERMS OF THE EFFECTS OF SWIRL VANE ANGLE FOR SIDE-WALL EXPANSION ANGLE $\alpha = 90°$

Vane Angle (deg.)	U_{in} (m/sec)	Re_d	CTRZ (x/D)	CRZ (x/D)	W_{max} (r/D)
0	15.7	150,000		2.1	
38	10.5	100,000	1.6		0.2
45	12.6	120,000	1.5		0.2
60	8.84	84,000	1.3		0.25
70	5.57	53,000	1.2		0.3

TABLE XIV

SAMPLE ALPHANUMERIC HEADINGS

10000	COMPUTED MASS FLOW RATE
10040	COMPUTED MEAN AXIAL VELOCITY
10050	U VELOCITY
10060	V VELOCITY
10070	W VELOCITY
10080	TOTAL VELOCITY MAGNITUDE
10090	DIMENSIONLESS U VELOCITY
10100	DIMENSIONLESS V VELOCITY
10110	DIMENSIONLESS W VELOCITY
10120	DIMENSIONLESS TOTAL VELOCITY
10121	PROBE PITCH ANGLE (DEG.)
10123	PROBE YAW ANGLE (DEG.)
10125	P(NORTH) - P(SOUTH) (VOLTS)
10127	P(CENTER) - P(WEST) (VOLTS)
10128	MEAS. INLET MASS FLOW RATE
10129	MEAS. INLET AXIAL VELOCITY
10130	MEAS. INLET DYNAMIC PRESSURE
10131	MEAS. PITCH PRESSURE COEFF.
10132	AXIAL FLUX OF ANGULAR MOMENTUM

TABLE XV

SAMPLE CALIBRATION DATA

10133	-3.76	58.	2.42
10140	-2.81	54.	1.86
10150	-2.23	50.	1.59
10160	-1.72	45.	1.35
10170	-1.31	40.	1.19
10180	-1.00	35.	1.11
10190	-.75	30.	1.02
10200	-.59	25.	.95
10210	-.47	20.	.91
10220	-.35	15.	.87
10230	-.21	10.	.85
10240	-.063	5.	.88
10250	.09	0.	.89
10260	.23	-5.	.89
10270	.38	-10.	.89
10280	.52	-15.	.89
10290	.66	-20.	.90
10300	.82	-25.	.93
10310	1.00	-30.	.96
10320	1.23	-35.	1.04
10330	1.49	-40.	1.10
10340	1.83	-45.	1.24
10350	2.24	-50.	1.40
10360	2.65	-54.	1.59
10370	3.4	-58.	2.04

TABLE XVI

SAMPLE MEASUREMENT DATA

10380	0.0	19	.335	
10390	0.0	354.6	-.007	-.018
10400	.3	251.8	.003	.021
10410	.6	258.0	.015	.029
10420	.9	262.6	.016	.028
10430	1.2	282.4	.007	.010
10440	1.5	318.6	-.004	.205
10450	1.8	324.6	-.299	2.450
10460	2.1	329.0	-.917	4.308
10470	2.4	326.6	-1.010	3.953
10480	2.7	327.0	-.865	3.255
10490	3.0			
10500	3.3			
10510	3.6			
10520	3.9			
10530	4.2			
10540	4.5			
10550	4.8			
10560	5.1			
10570	5.4			
10580	5.88	19	.335	
10590	0.0	360.2	.019	.012
10600	.3	300.0	.036	.007
10610	.6	274.4	.060	.051
10620	.9	262.6	.081	.130
10630	1.2	256.0	.094	.213
10640	1.5	252.2	.089	.290
10650	1.8	248.2	.088	.338
10660	2.1	245.2	.078	.367
10670	2.4	243.0	.067	.352
10680	2.7	241.6	.059	.324
10690	3.0	243.0	.049	.277
10700	3.3	248.2	.037	.219
10710	3.6	260.0	.035	.138
10720	3.9	282.4	.038	.093
10730	4.2	308.6	.046	.156
10740	4.5	325.4	.033	.338
10750	4.8	332.0	-.012	.568
10760	5.1	334.2	-.049	.749
10770	5.4	331.0	-.219	.727
10780 //				
END OF DATA				

TABLE XVII

SAMPLE AUXILIARY GEOMETRIC QUANTITY OUTPUT

```
EXPANSION ANGLE(DEG.) =                     9.000E+01

SWIRL VANE ANGLE(DEG.) =                    4.500E+01

INLET RADIUS(M) =                           7.461E-02

COMBUSTOR RADIUS(M) =                       1.492E-01

LAMINAR VISCOSITY(KG/M/SEC) =               1.800E-05

DENSITY(KG/CU. M) =                         1.168E+00

*-*-*-*-*-*-*-*-*-*-*-*-*-*-*-*-*     MEAS. INLET MASS FLOW RATE

 I =      1           2
 X =   0.0         0.14935
        2.76E-01  2.76E-01

*-*-*-*-*-*-*-*-*-*-*-*-*-*-*-*-*   COMPUTED MASS FLOW RATE

 I =      1           2
 X =   0.0         0.14935
        2.85E-01  2.91E-01

*-*-*-*-*-*-*-*-*-*-*-*-*-*-*-*-*     MEAS. INLET AXIAL VELOCITY

 I =      1           2
 X =   0.0         0.14935
        1.35E+01  1.35E+01

*-*-*-*-*-*-*-*-*-*-*-*-*-*-*-*-*   COMPUTED MEAN AXIAL VELOCITY

 I =      1           2
 X =   0.0         0.14935
        3.49E+00  3.57E+00

*-*-*-*-*-*-*-*-*-*-*-*-*-*-*-*-*  AXIAL FLUX OF ANGULAR MOMENTUM

 I =      1           2
 X =   0.0         0.14935
        3.65E-02  3.47E-02
```

APPENDIX B

FIGURES

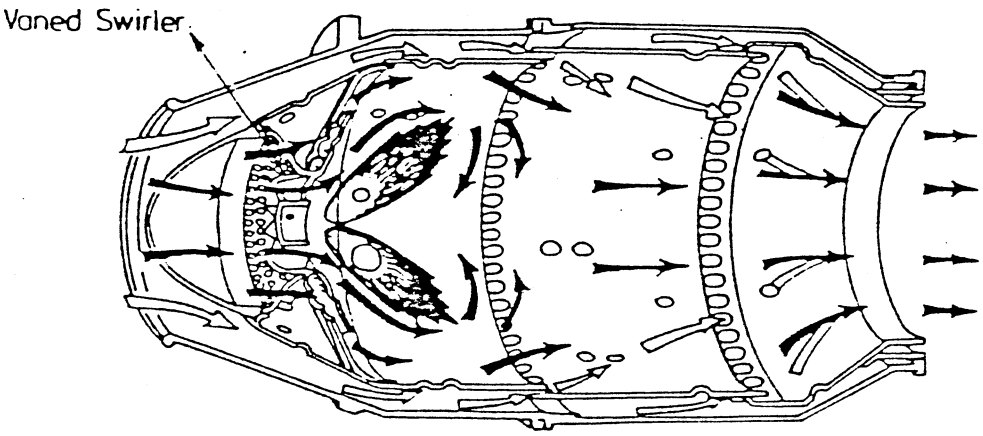

(a). Typical Axisymmetric Combustion Chamber of a Gas Turbine Engine

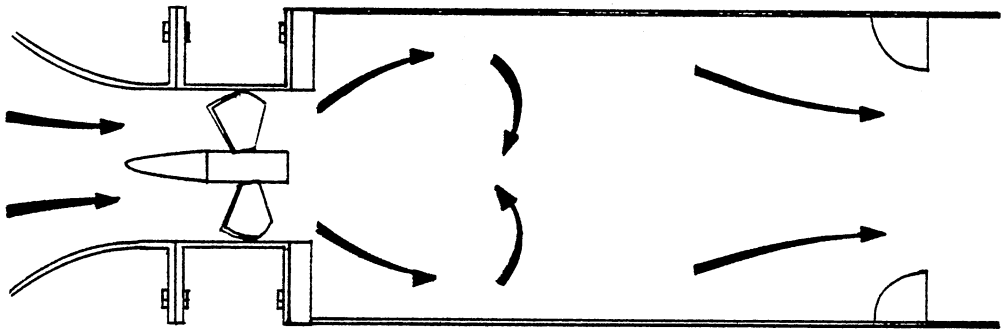

(b). Simplified Test Section

Figure 1. Typical Axisymmetric Gas Turbine Combustion Chamber

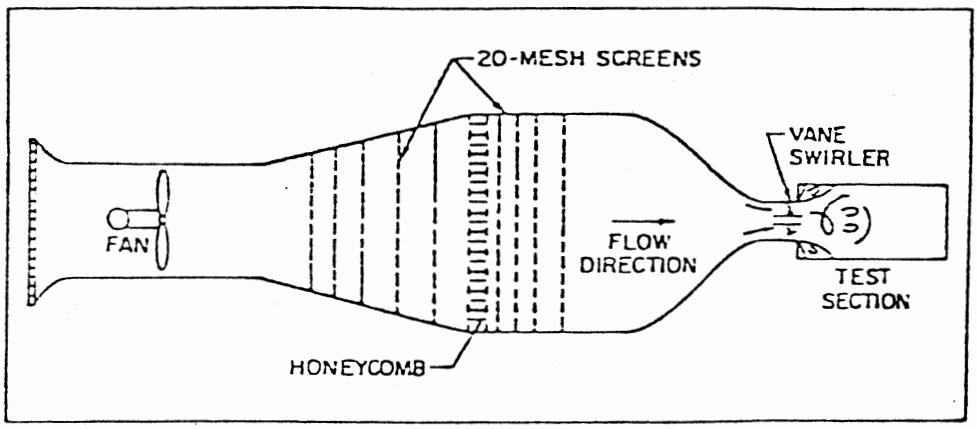

Figure 2. Schematic of Overall Flow Facility

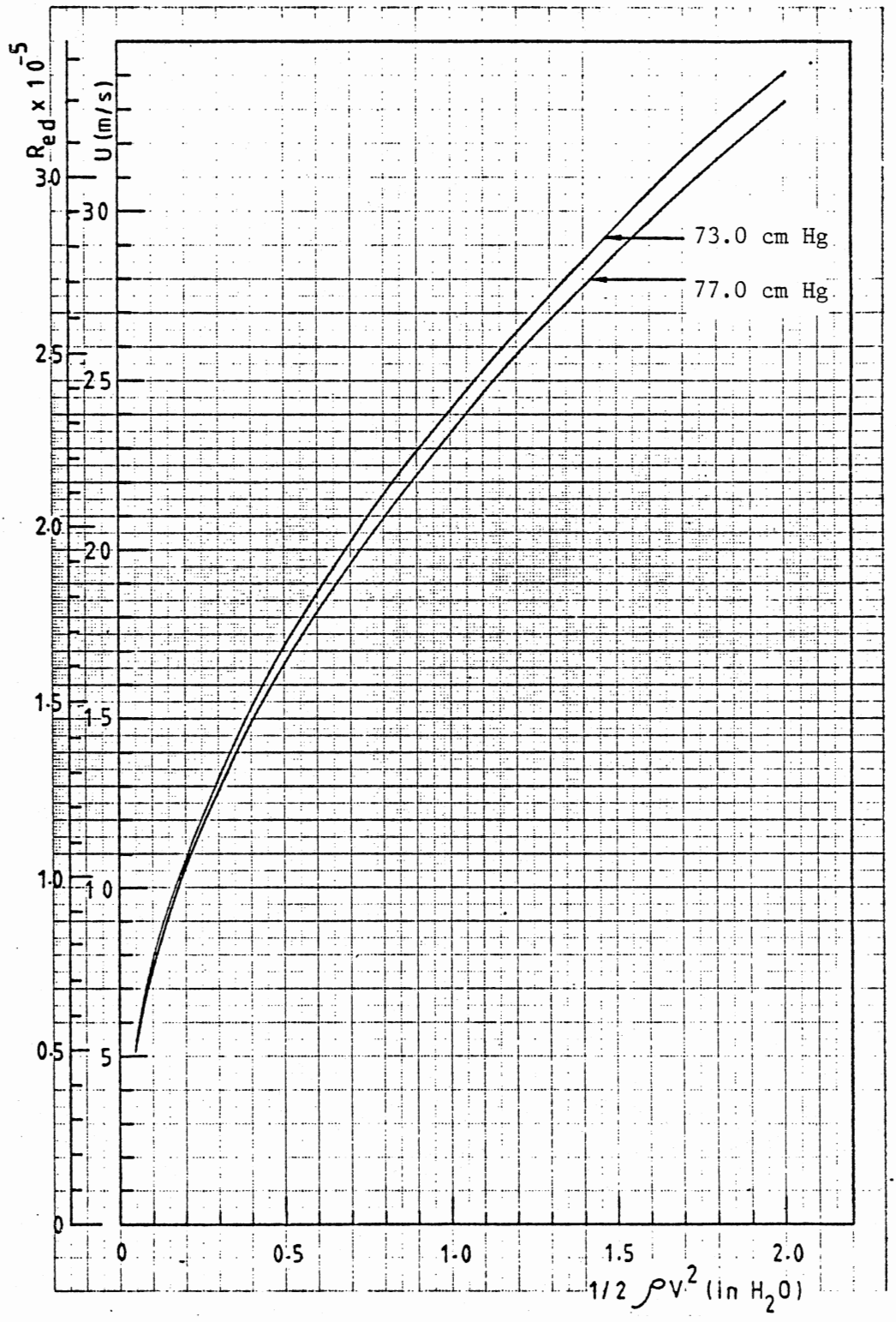

Figure 3. Dynamic Pressure Conversion Characteristic

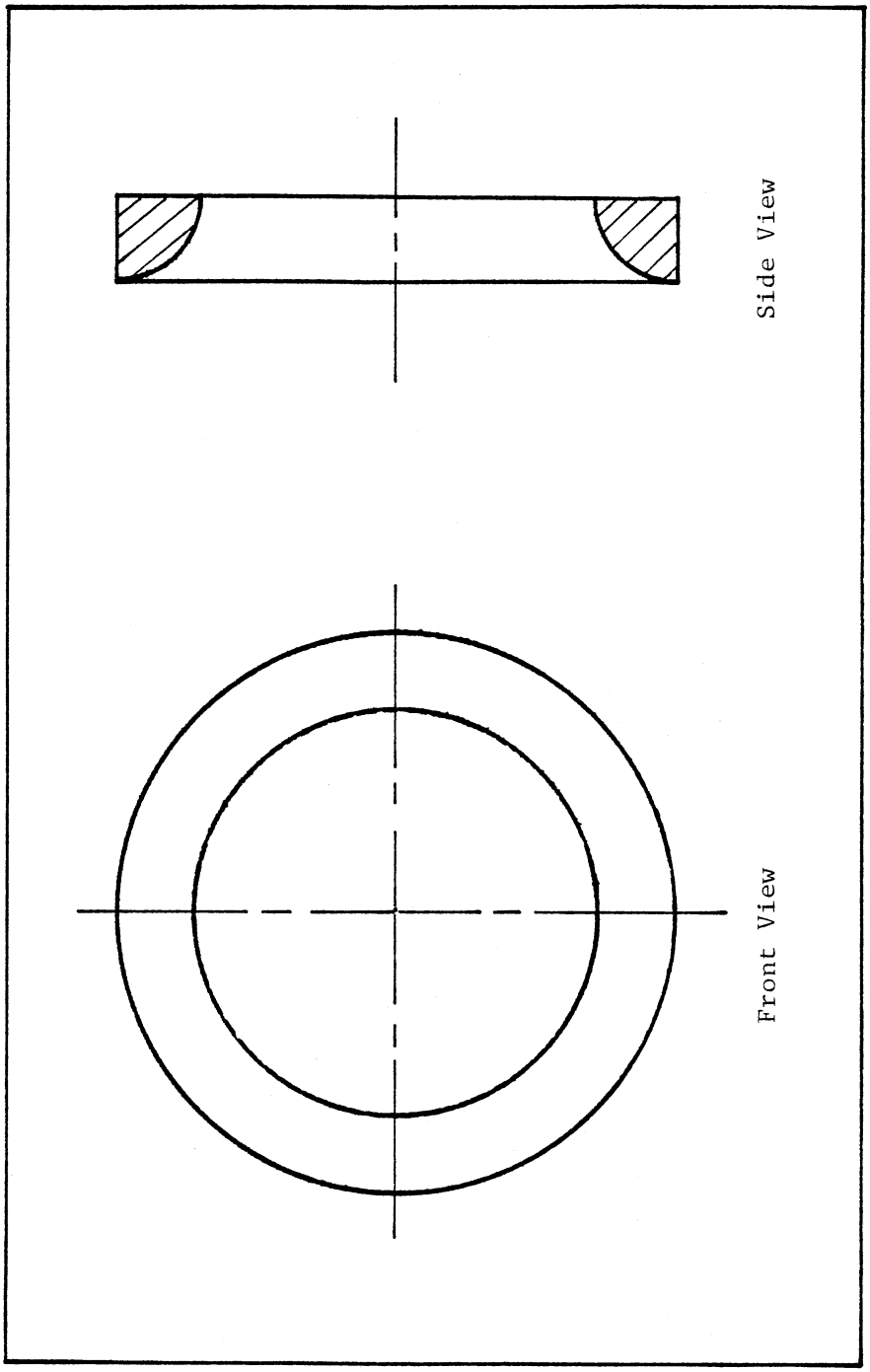

Figure 4. Contraction Block

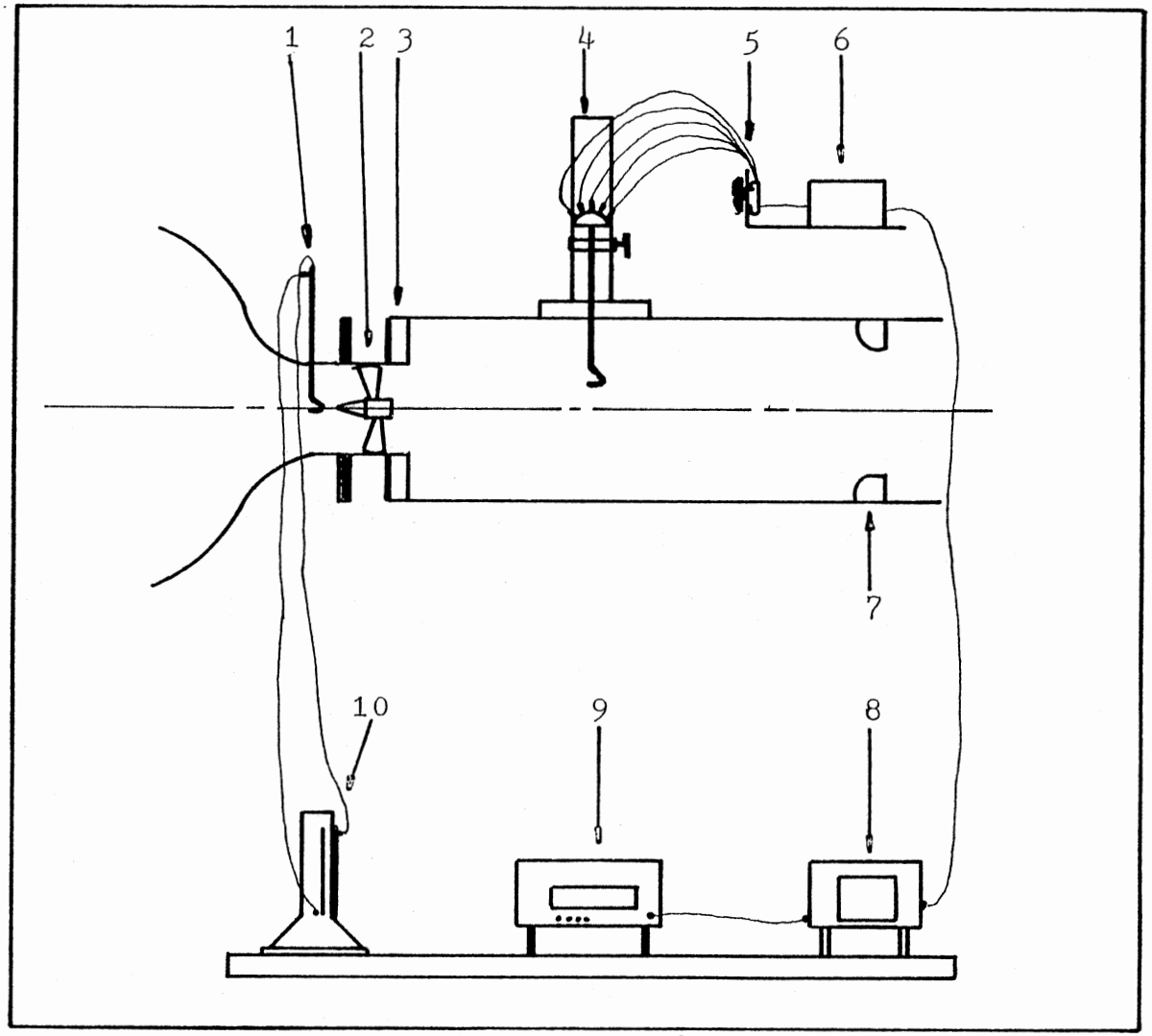

Notation

1. Pitot static probe
2. Swirler
3. Expansion block
4. Five-hole pitot probe
5. Switching valve
6. Pressure transformer
7. Contraction block
8. Voltmeter
9. Integrating voltmeter
10. Micro-manometer

Figure 5 Apparatus for Mean Velocity Measurements

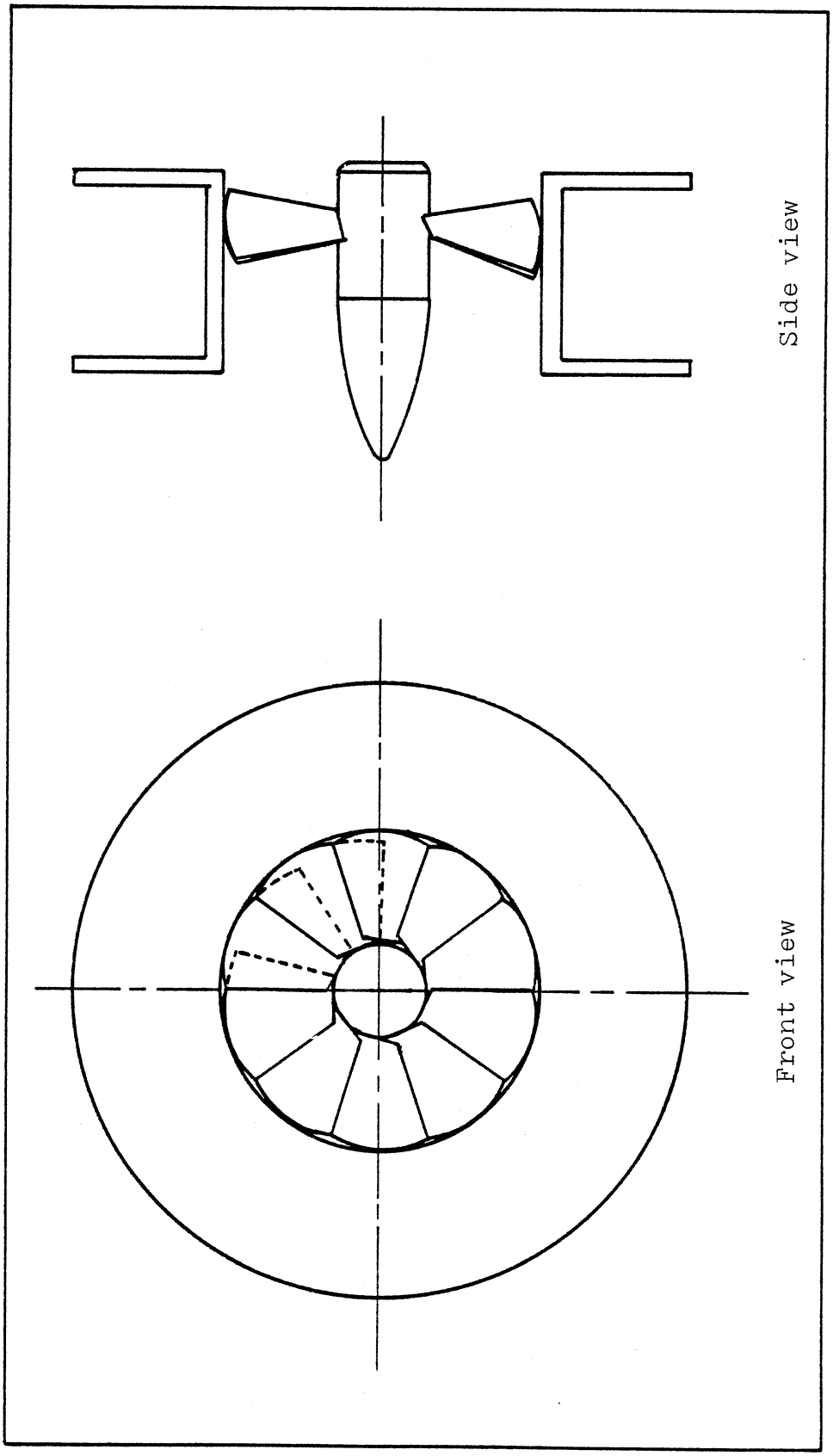

Figure 6. Swirler

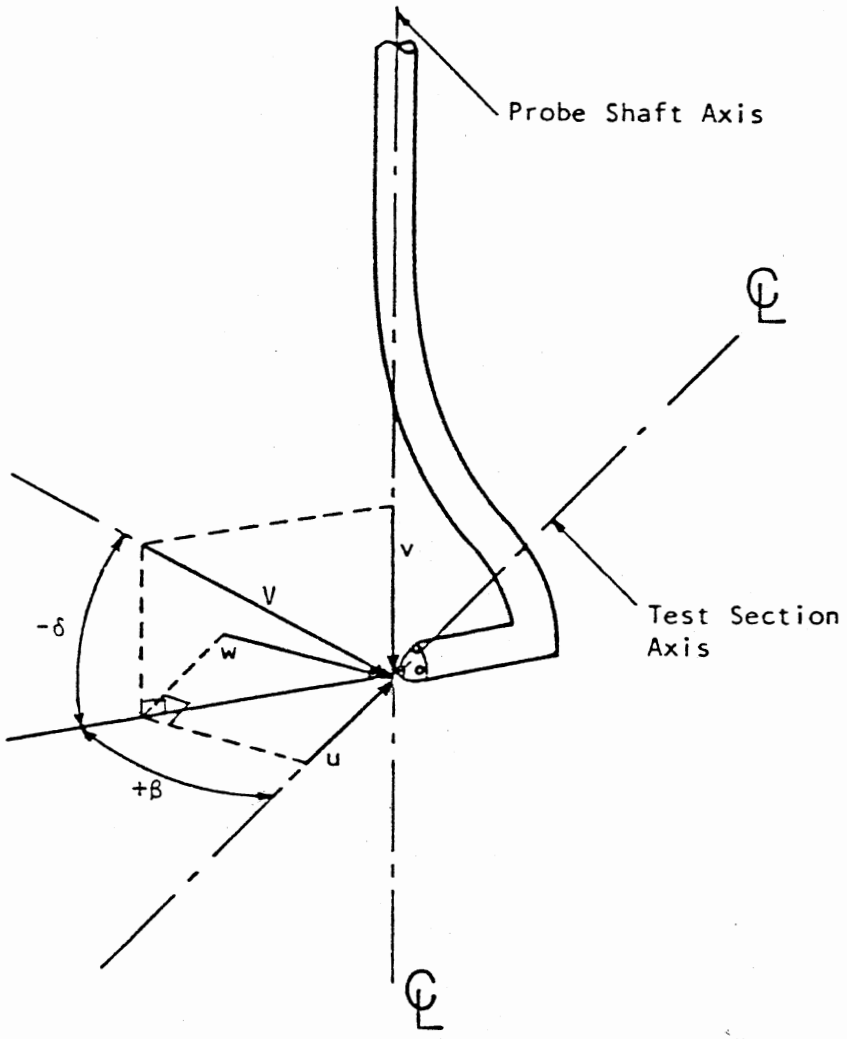

Figure 7. Velocity Components and Flow Direction Angles Associated with Five-Hole Pitot Measurements

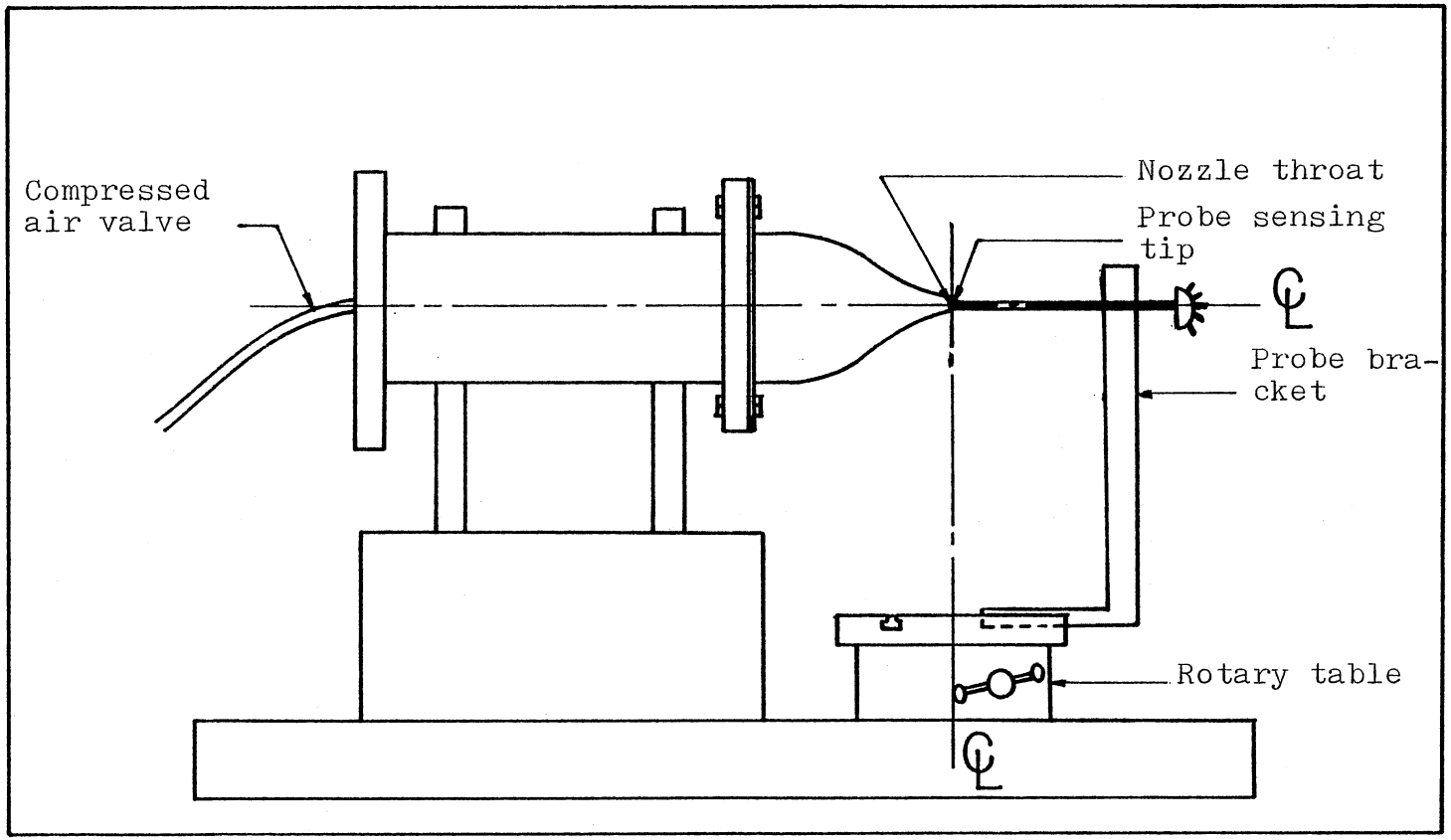

Figure 8. Calibration Apparatus

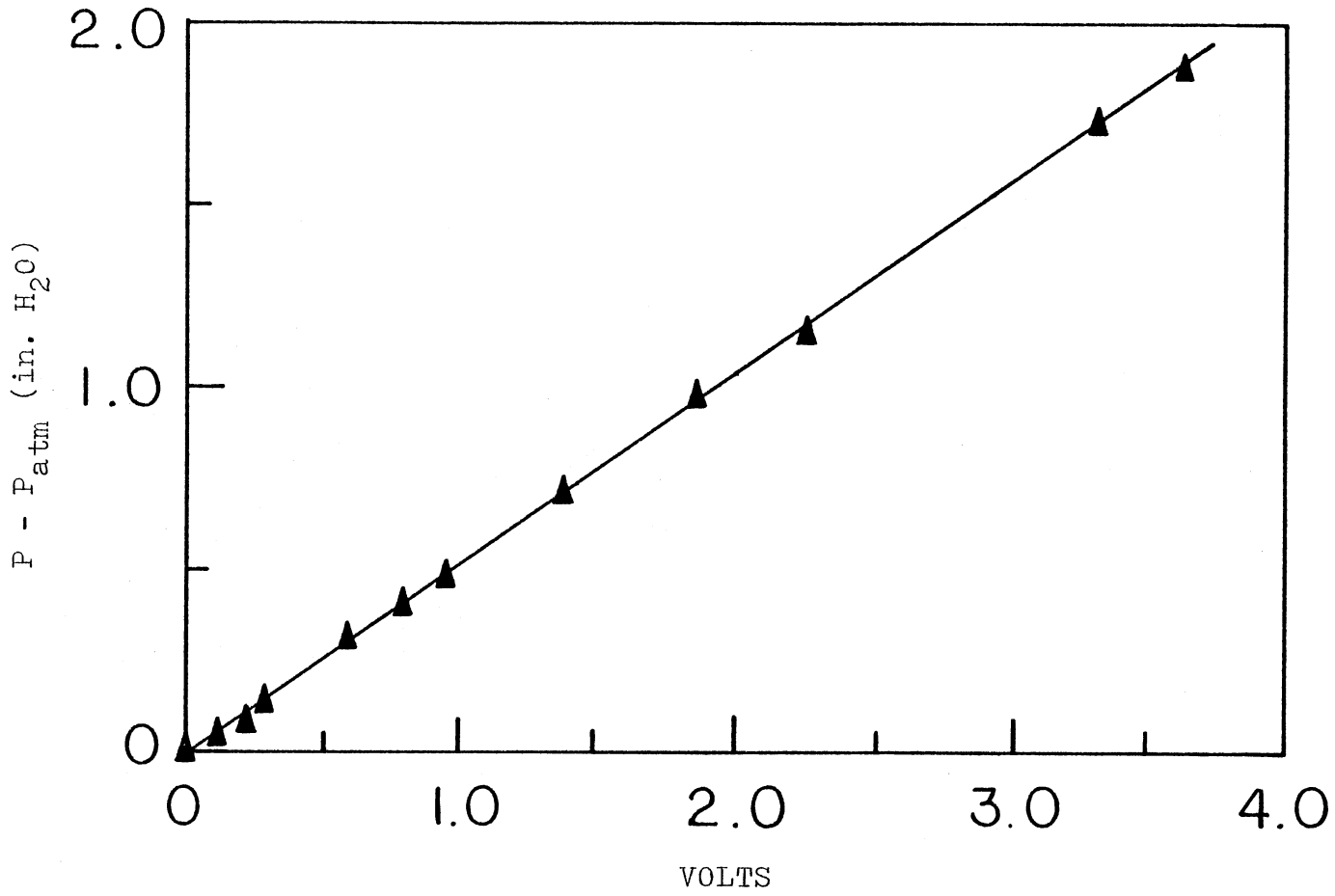

Figure 9. Voltage Output Calibration Characteristic for Voltmeter

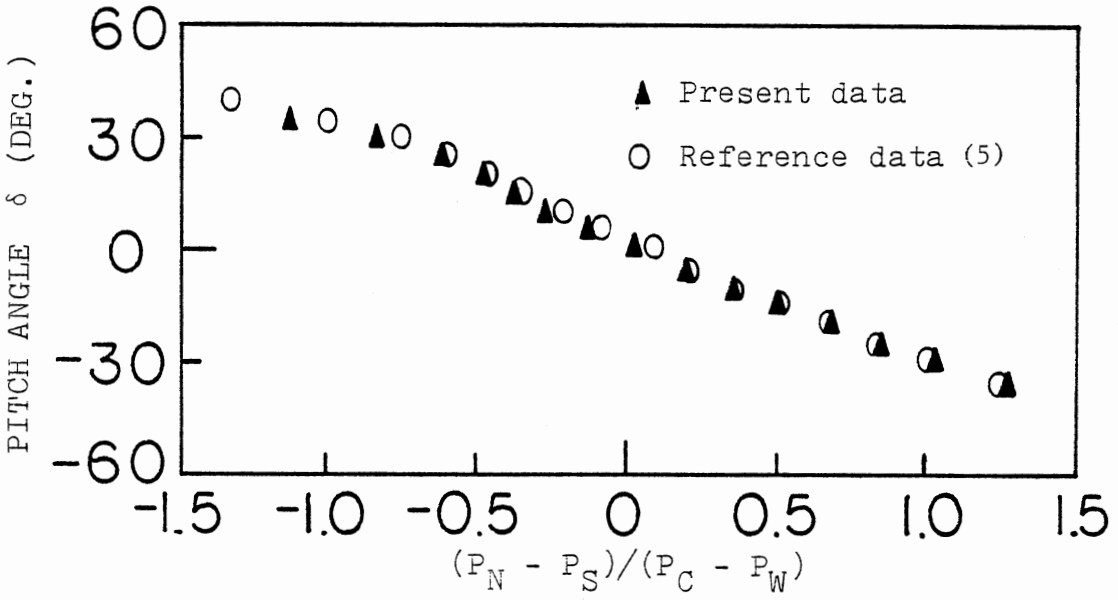

(a) Pitch Angle Calibration Characteristic

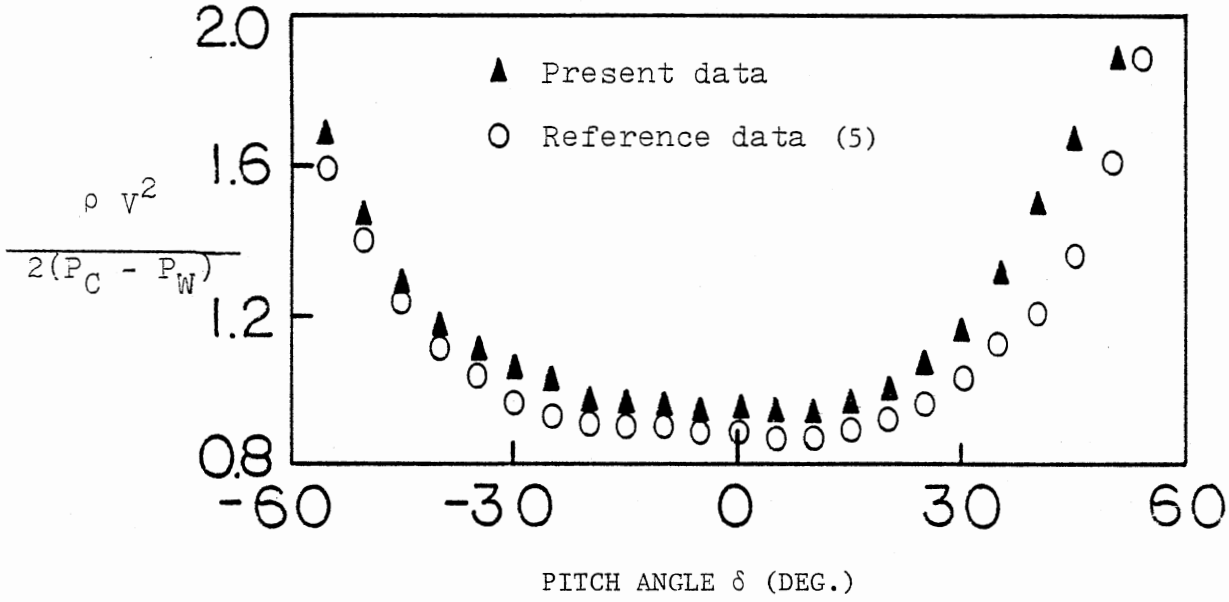

(b) Velocity Coefficient Calibration Characteristic

Figure 10. Calibration Characteristics for Five-Hole Pitot Probe

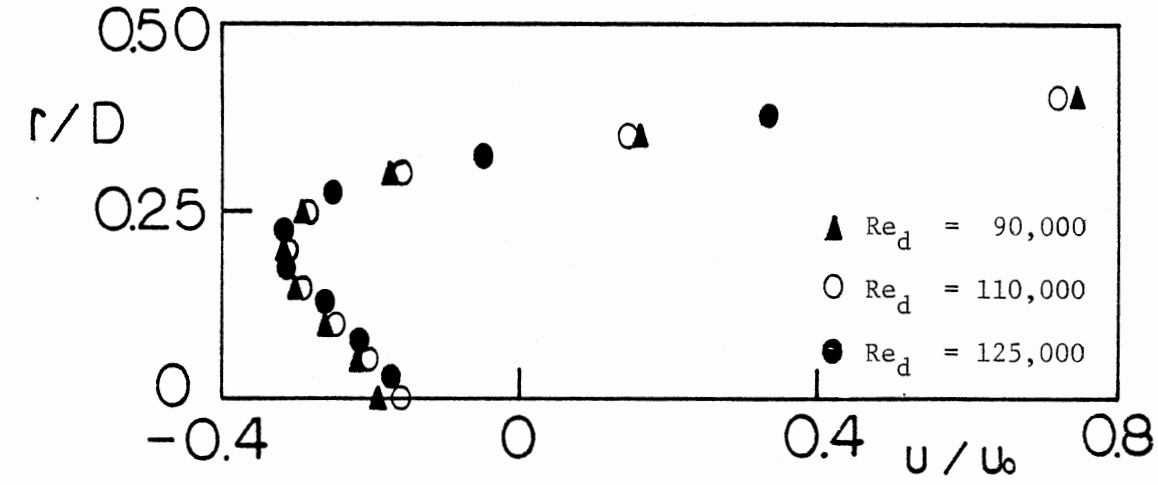

(a) Axial Velocity

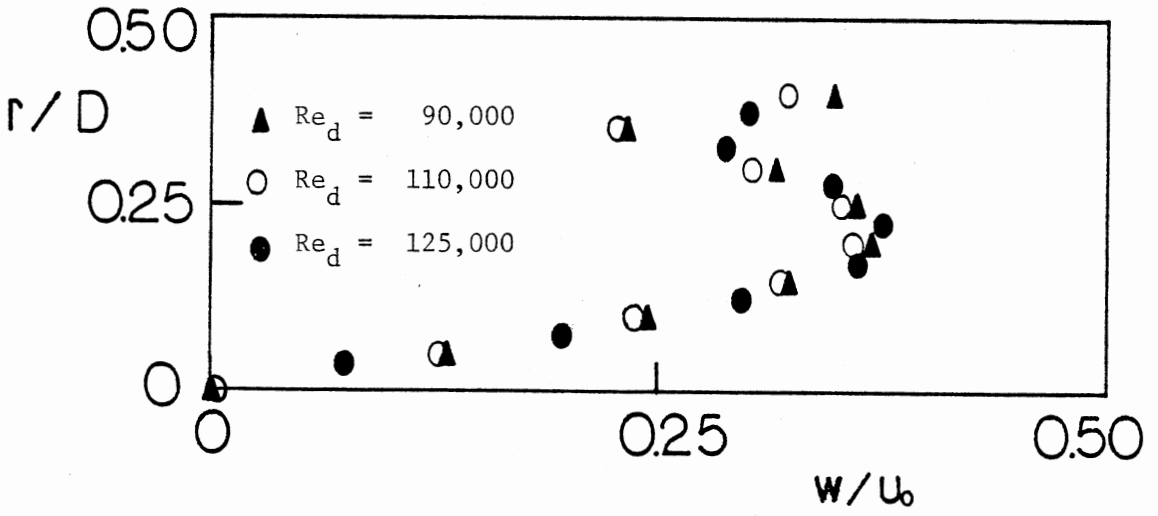

(b) Swirl Velocity

Figure 11. Flowfield Independence of Reynolds Number for Side-Wall Expansion. Angle $\alpha = 90°$ and Swirl Vane Angle $\phi = 45°$ at Axial Station $x/D = 0.5$.

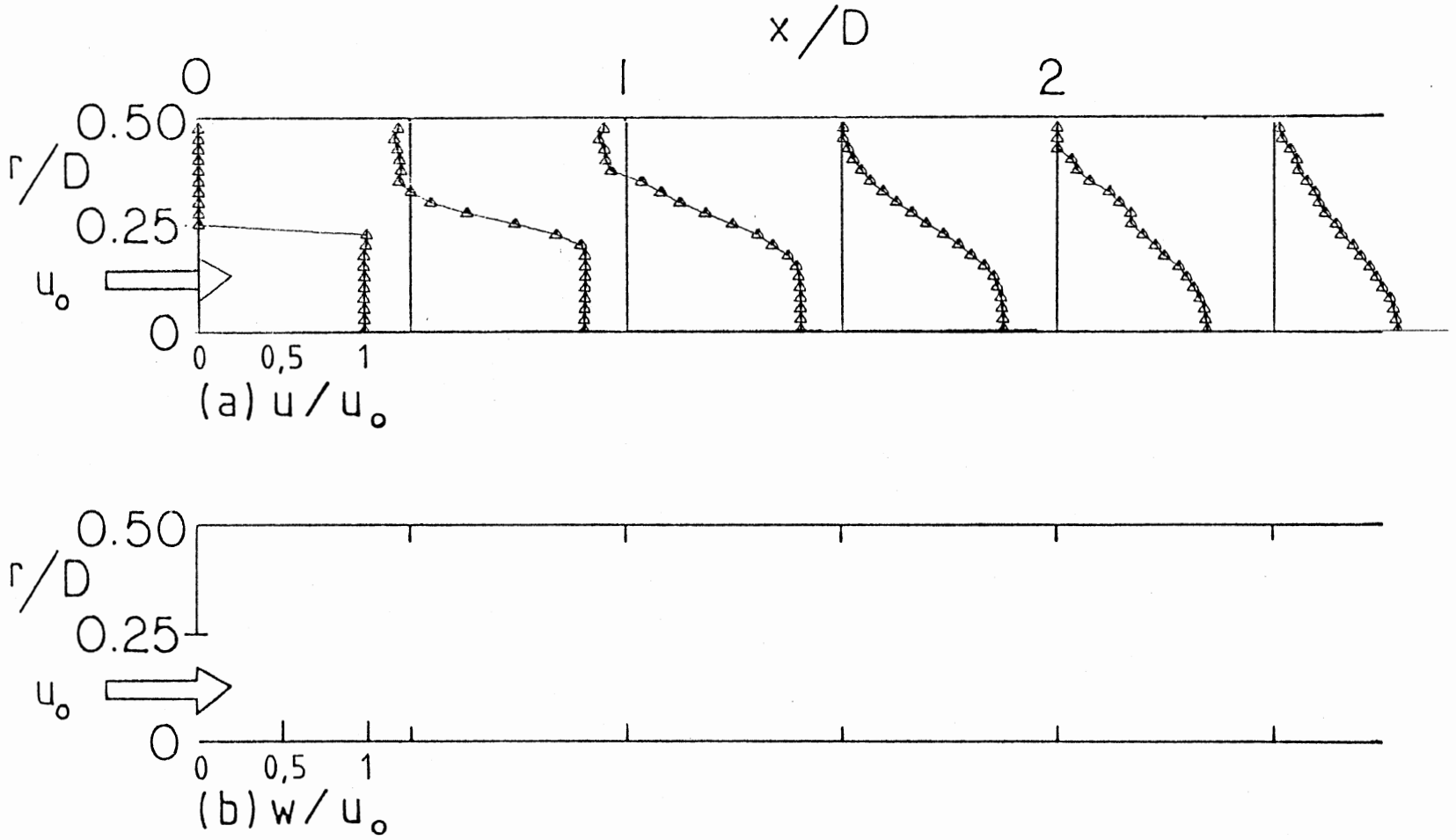

(a) Swirl Vane Angle $\phi = 0°$

Figure 12. Velocity Profiles for Side-Wall Expansion Angle $\alpha = 90°$ without Contraction Block

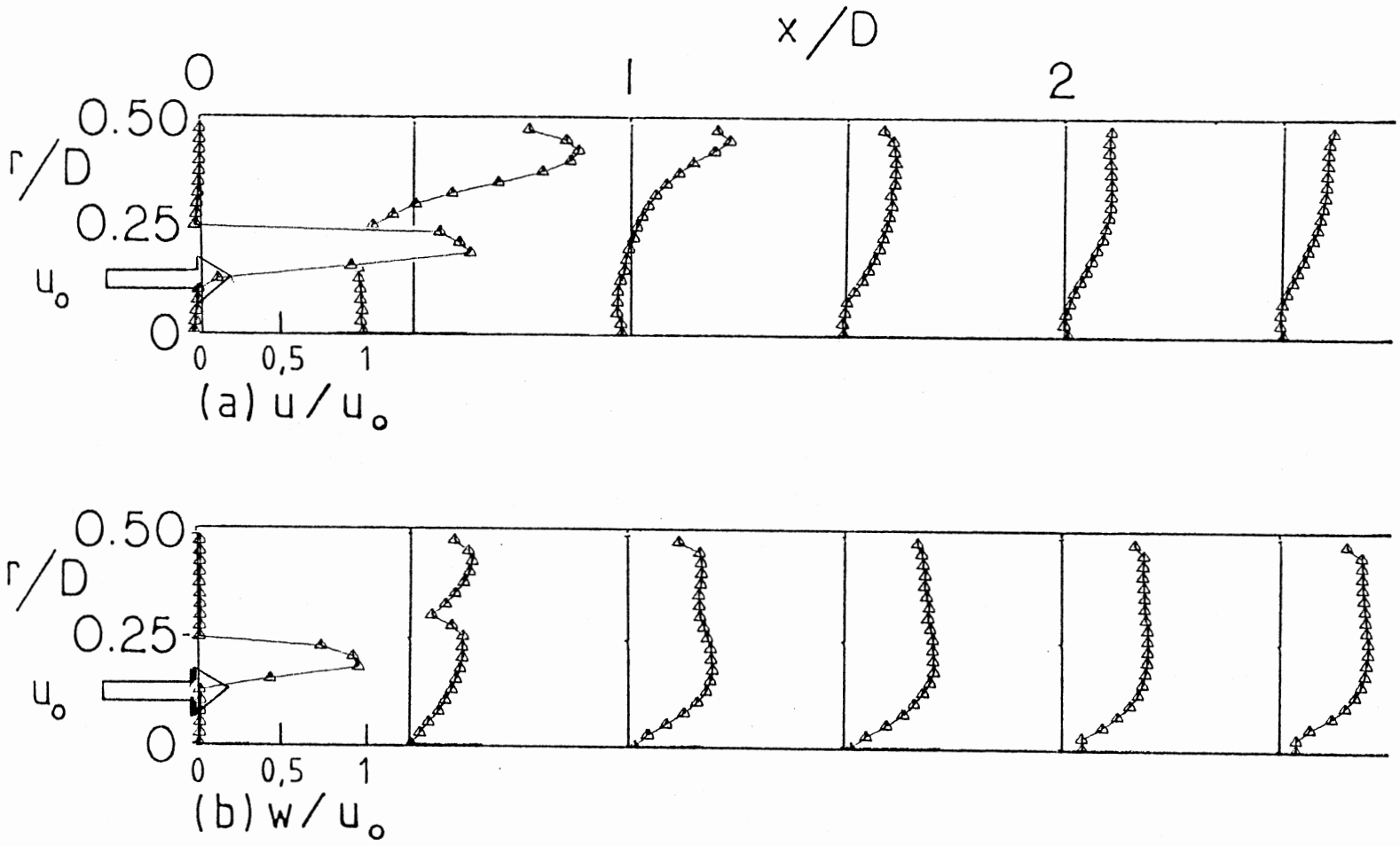

(b) Swirl Vane Angle ϕ = 38°

Figure 12 (Continued)

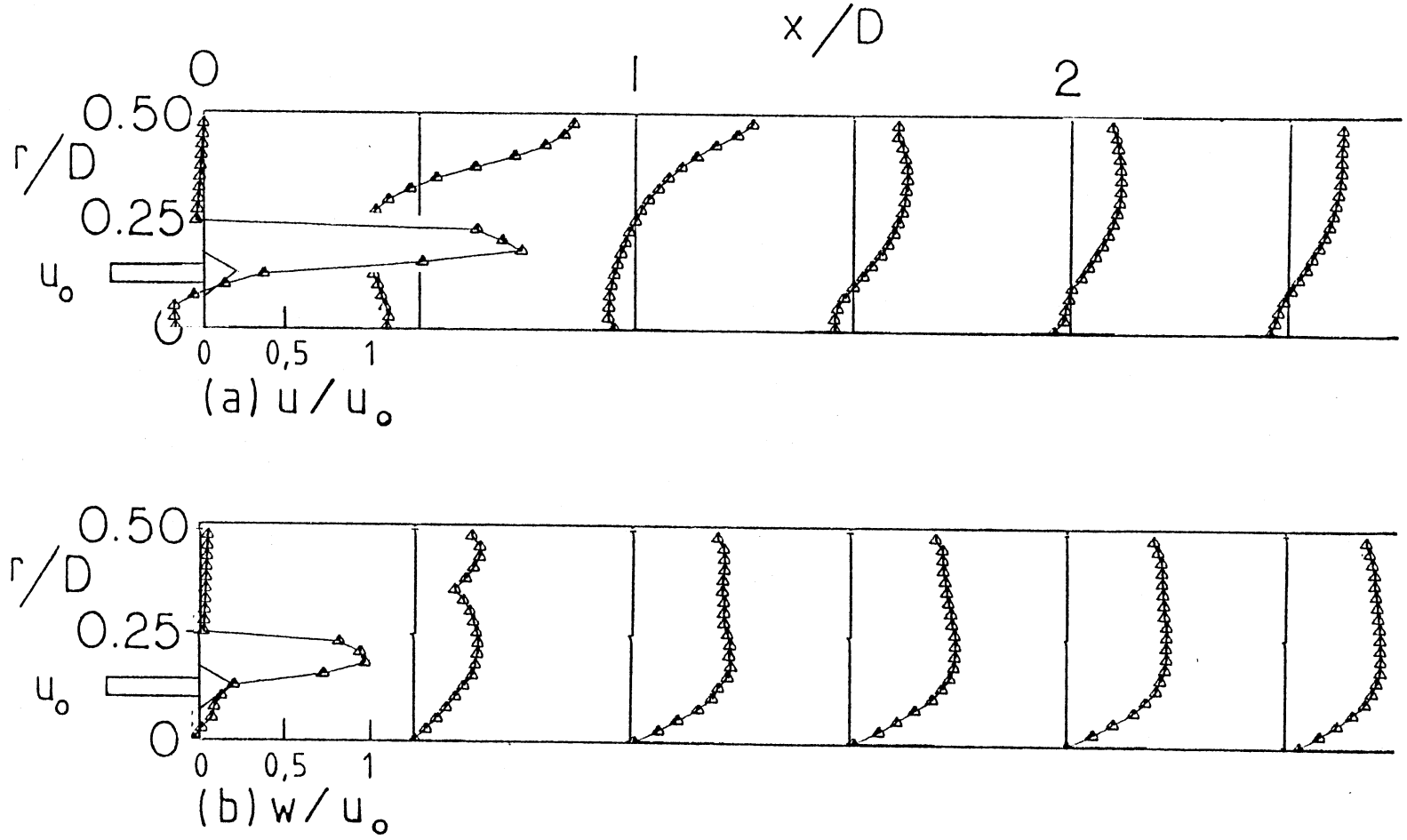

(c) Swirl Vane Angle ϕ = 45°

Figure 12 (Continued)

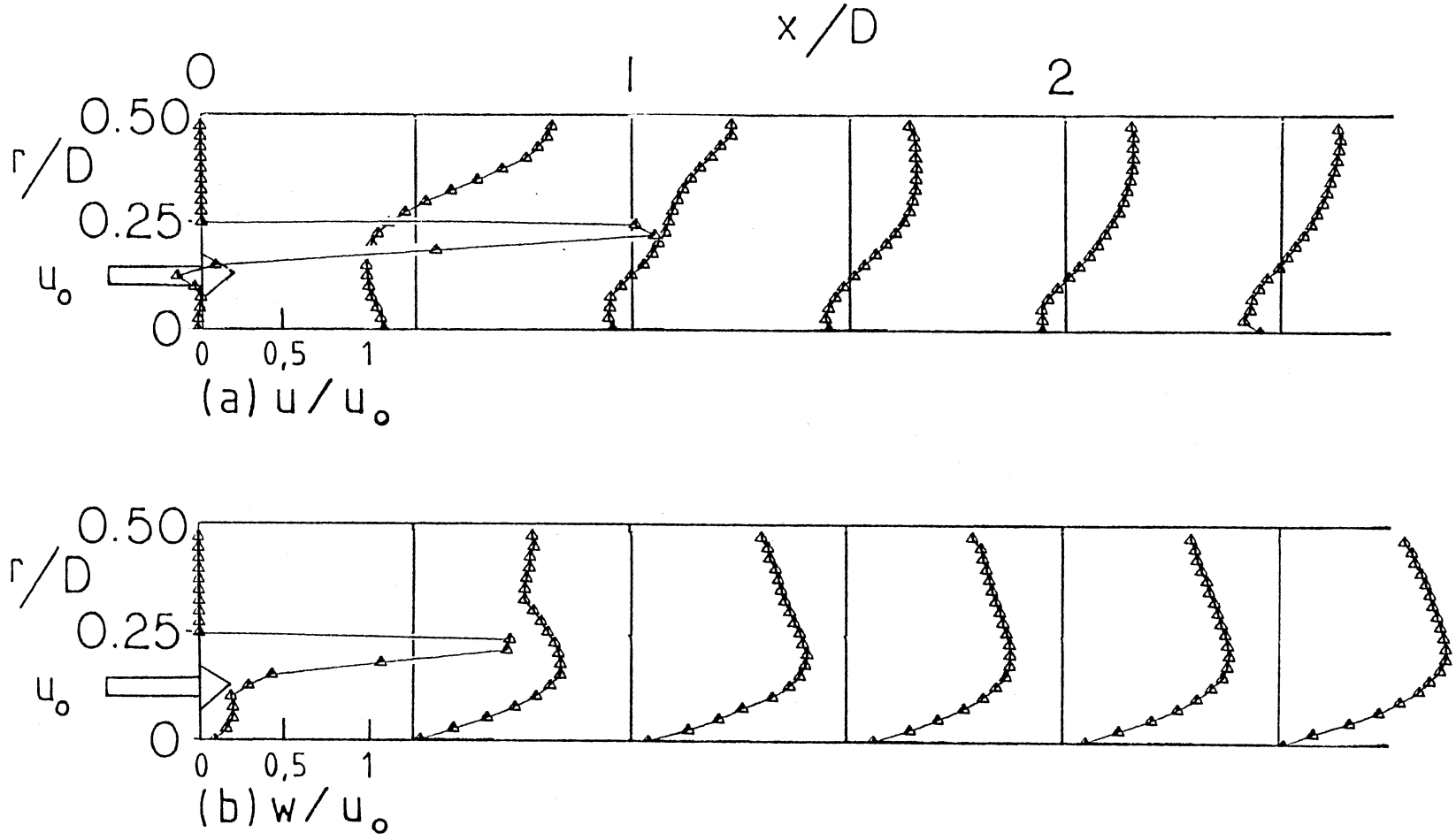

(d) Swirl Vane Angle $\phi = 60°$

Figure 12 (Continued)

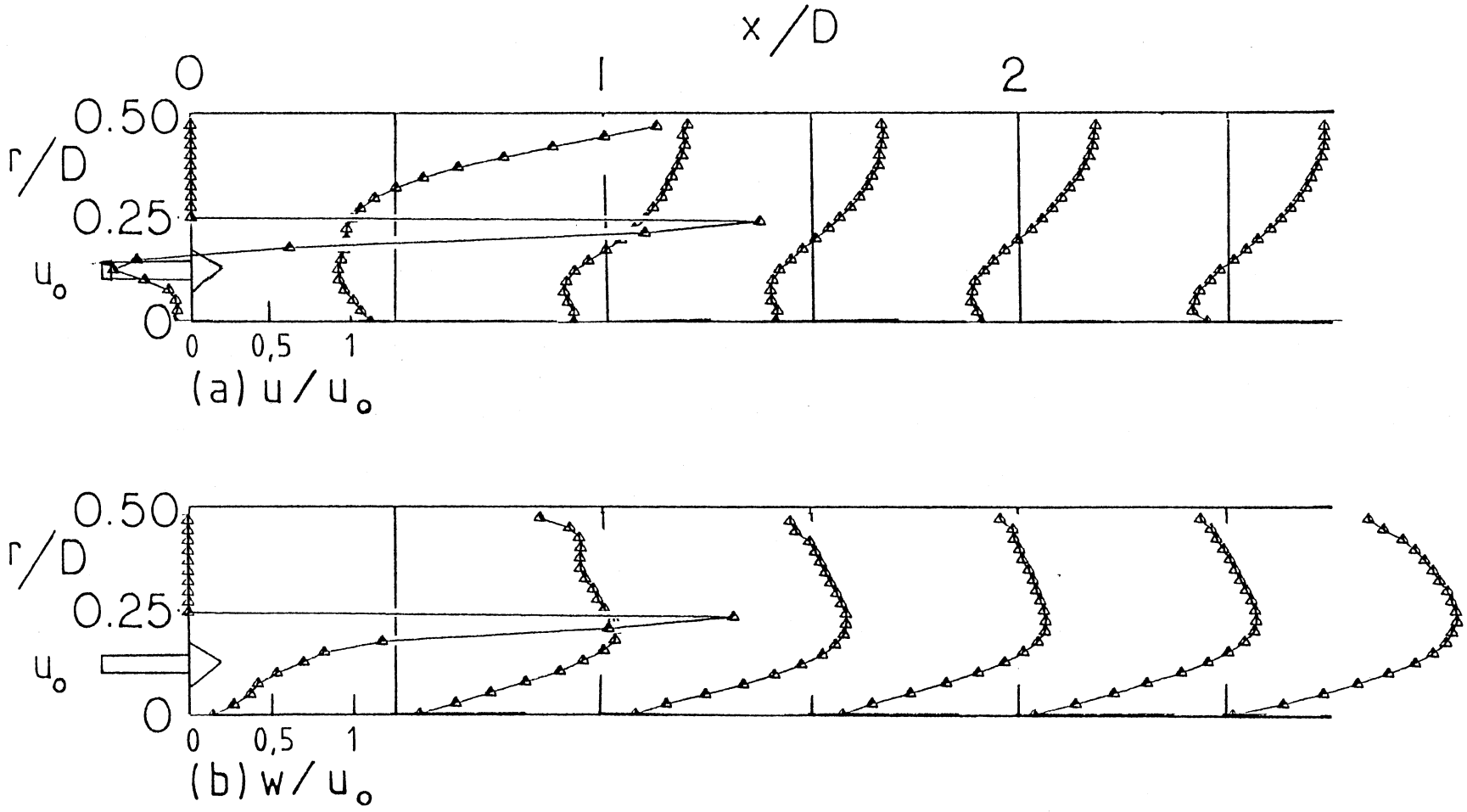

(e) Swirl Vane Angle ϕ = 70°

Figure 12 (Continued)

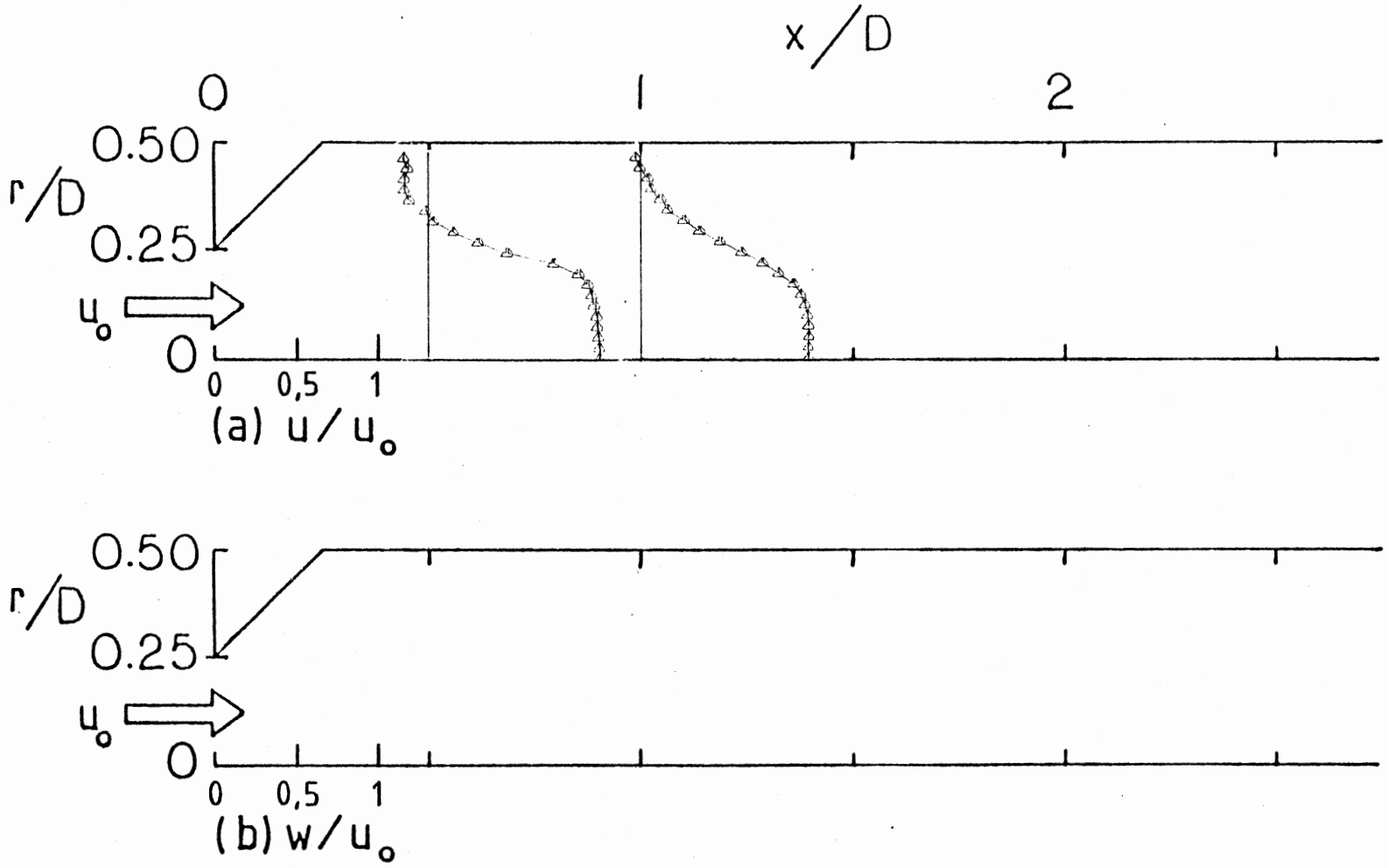

(a) Swirl Vane Angle $\phi = 0°$

Figure 13. Velocity Profiles for Side-Wall Expansion Angle $\alpha = 45°$ without Contraction Block

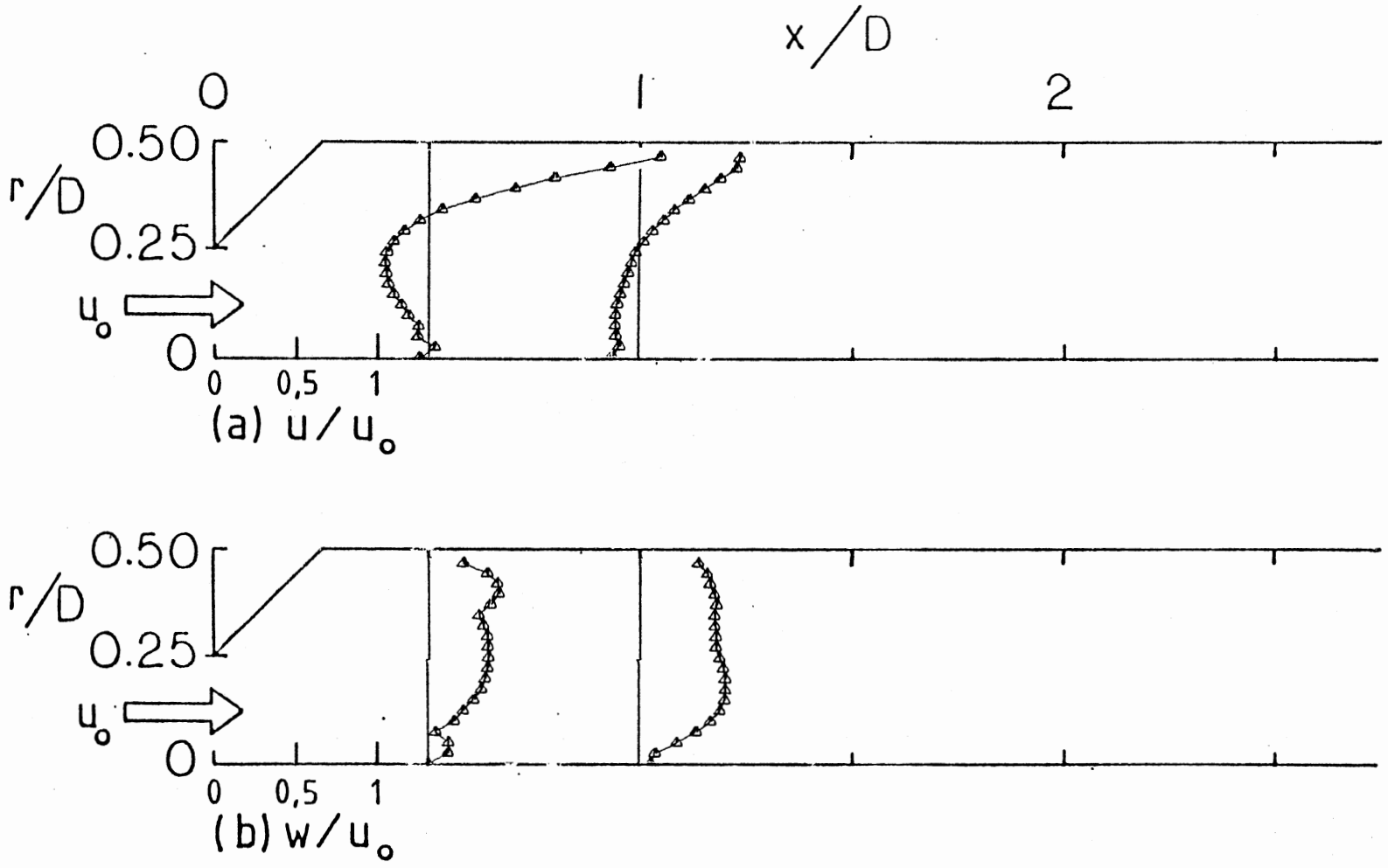

(b) Swirl Vane Angle ϕ = 38°

Figure 13 (Continued)

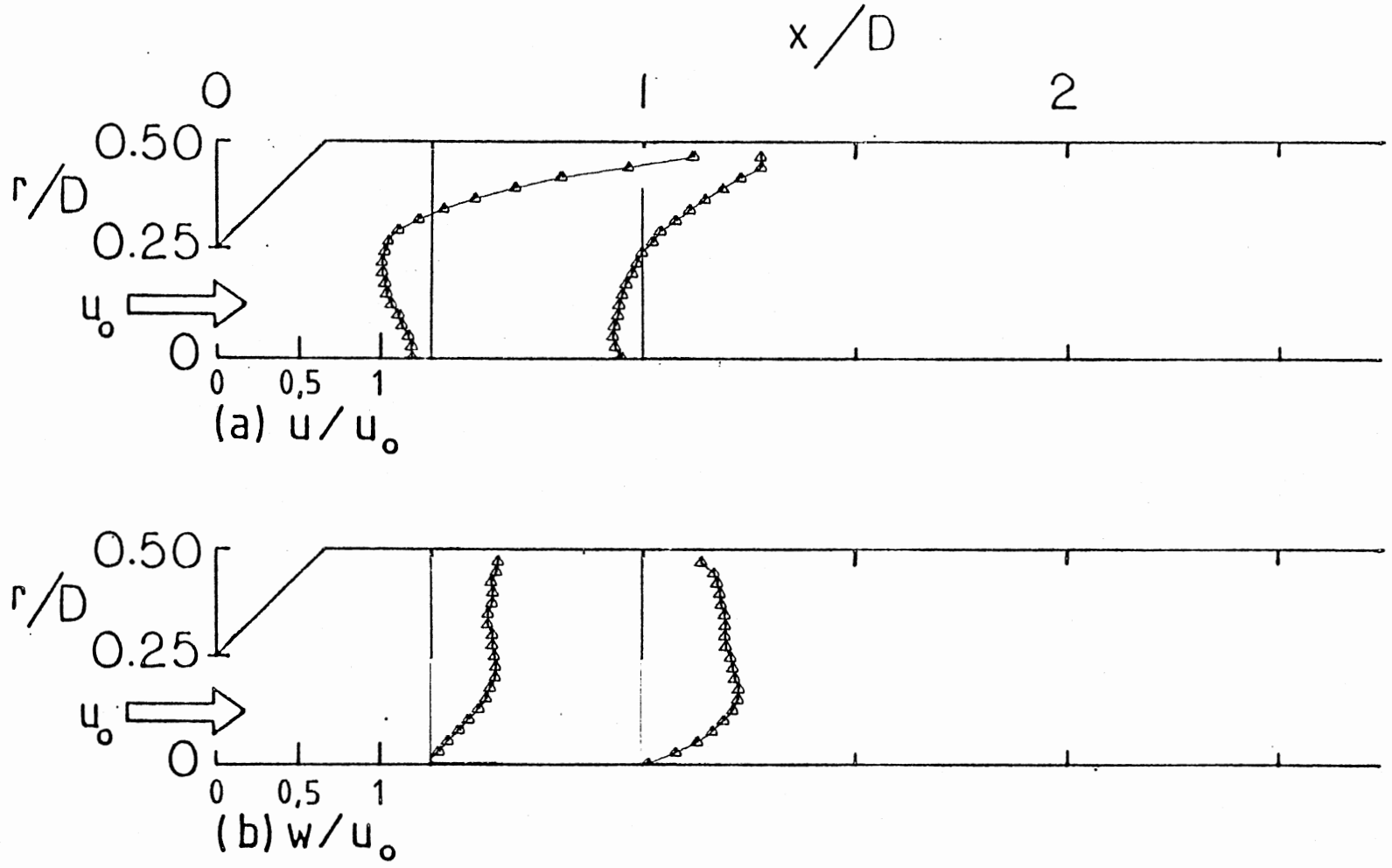

(c) Swirl Vane Angle $\phi = 45°$

Figure 13 (Continued)

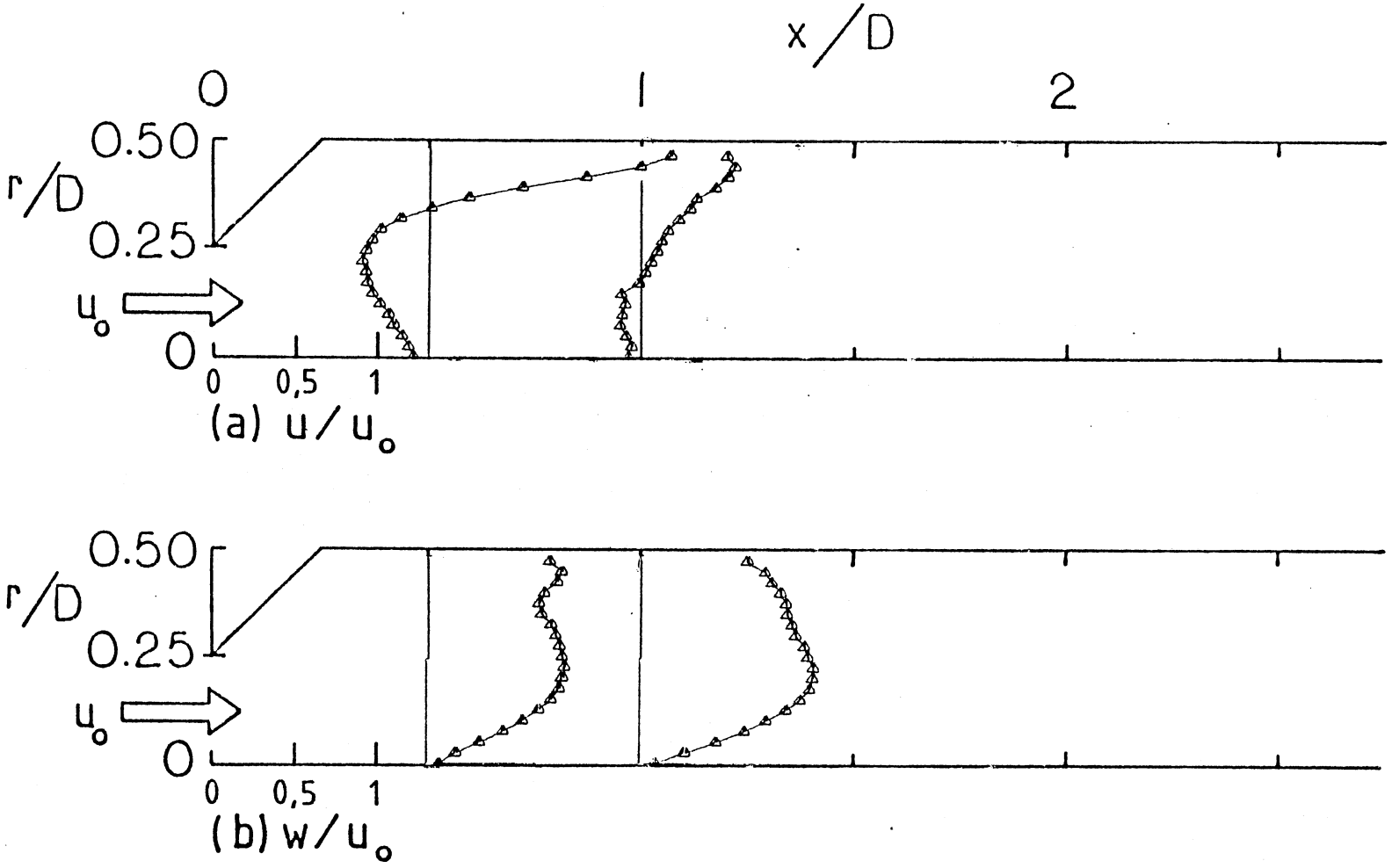

(d) Swirl Vane Angle ϕ = 60°

Figure 13 (Continued)

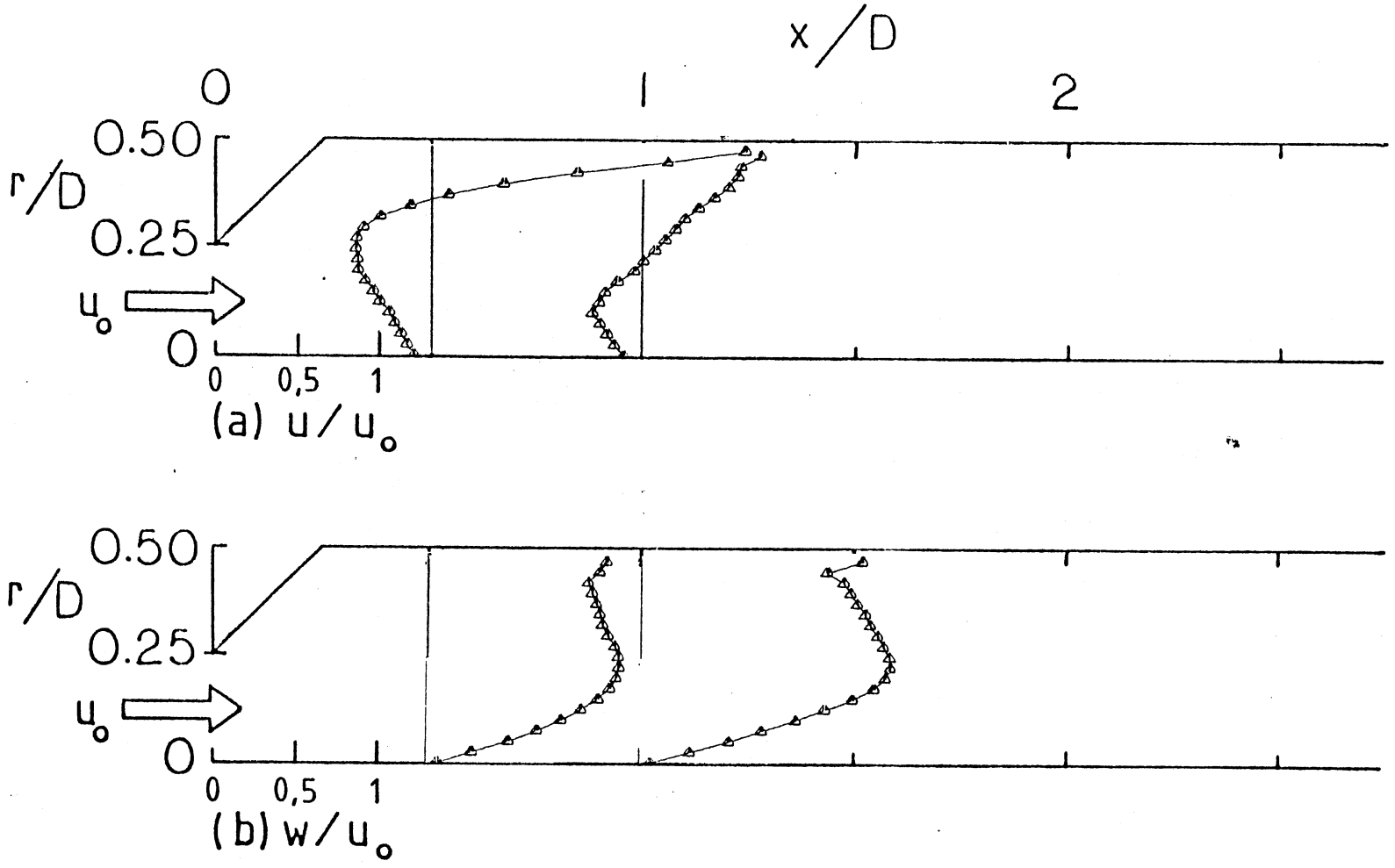

(e) Swirl Vane Angle $\phi = 70°$

Figure 13 (Continued)

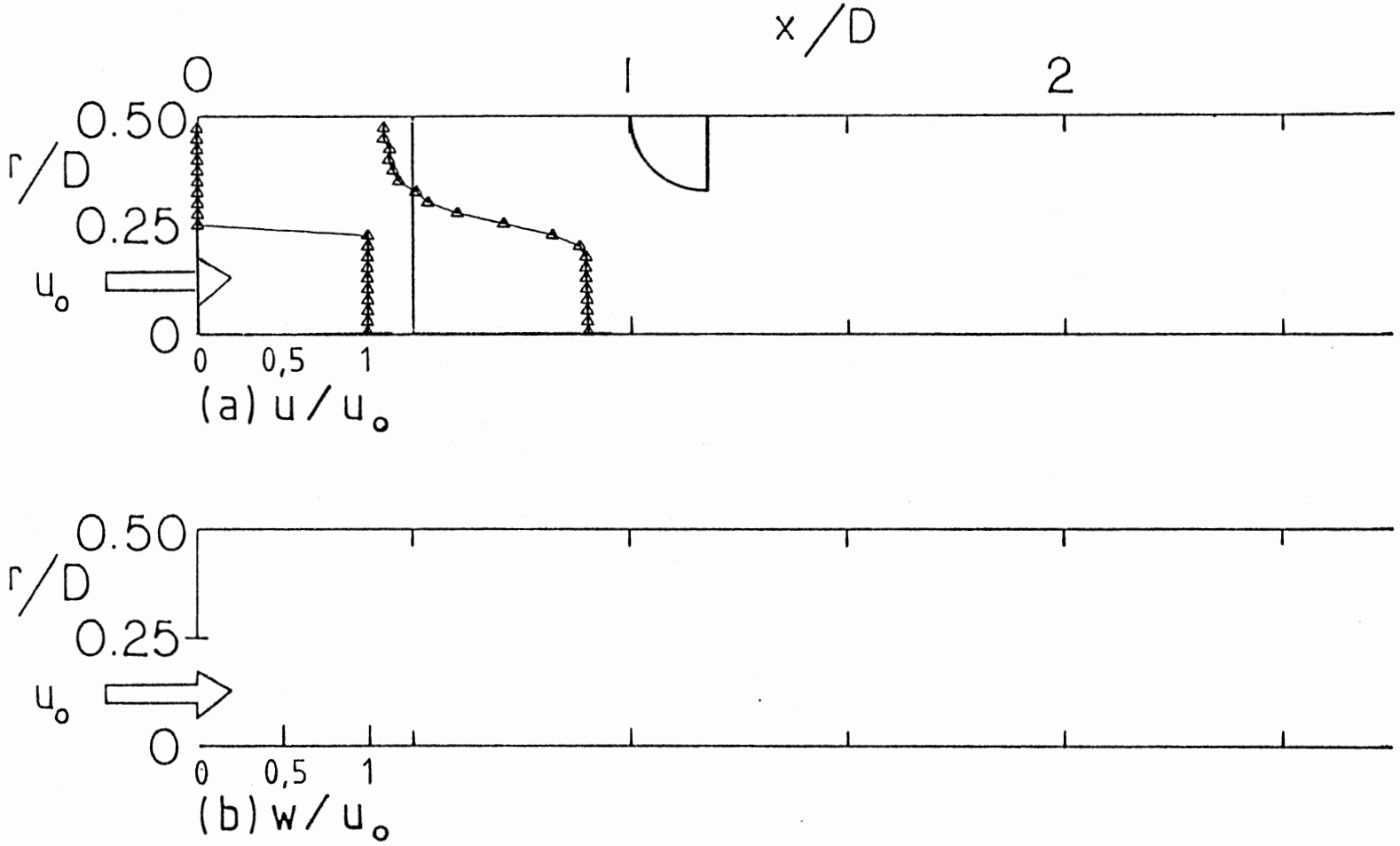

(a) L/D = 1.0

Figure 14. Velocity Profiles for Swirl Vane Angle ϕ = 0° with Contraction Block

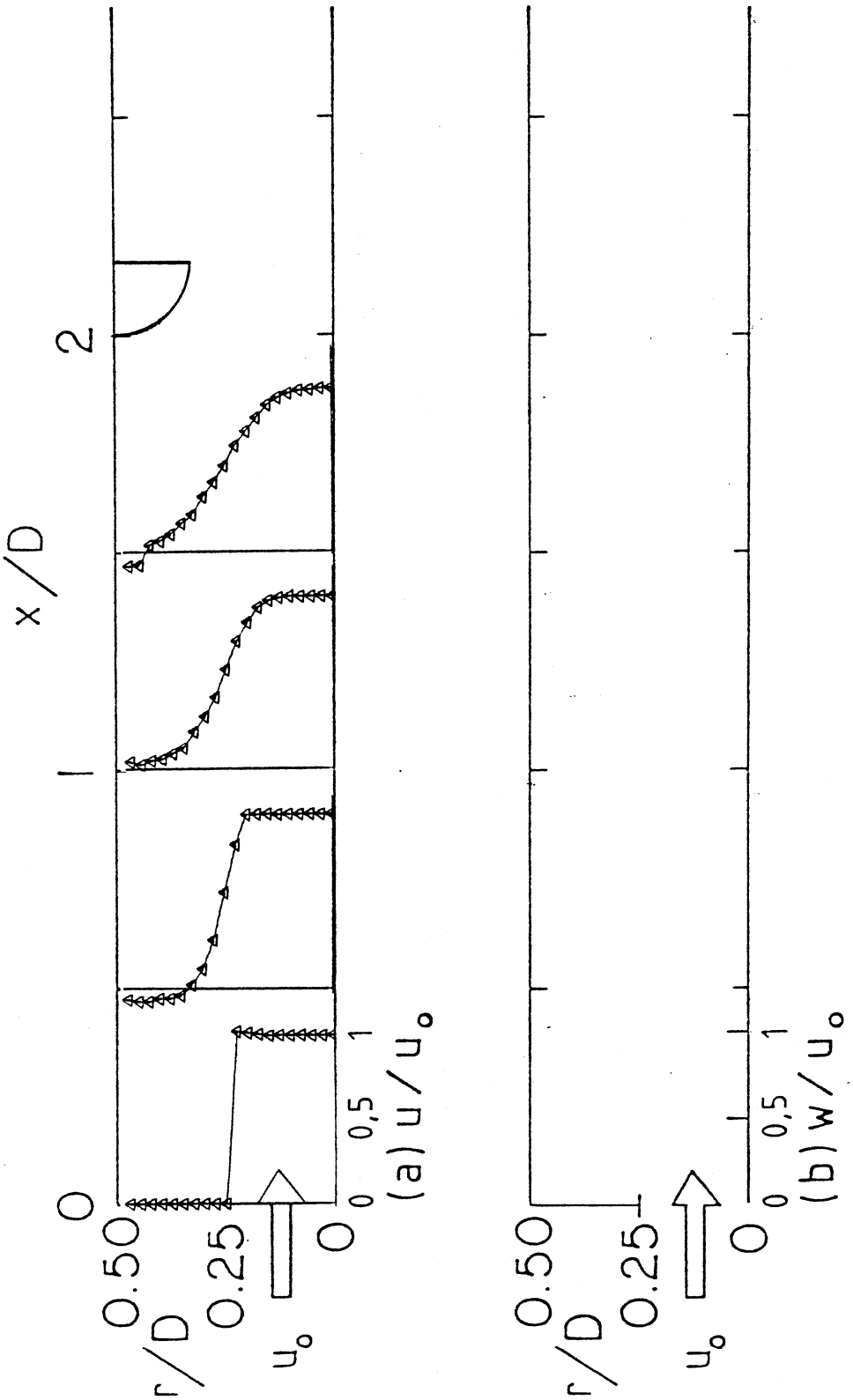

(b) L/D = 2.0

Figure 14 (Continued)

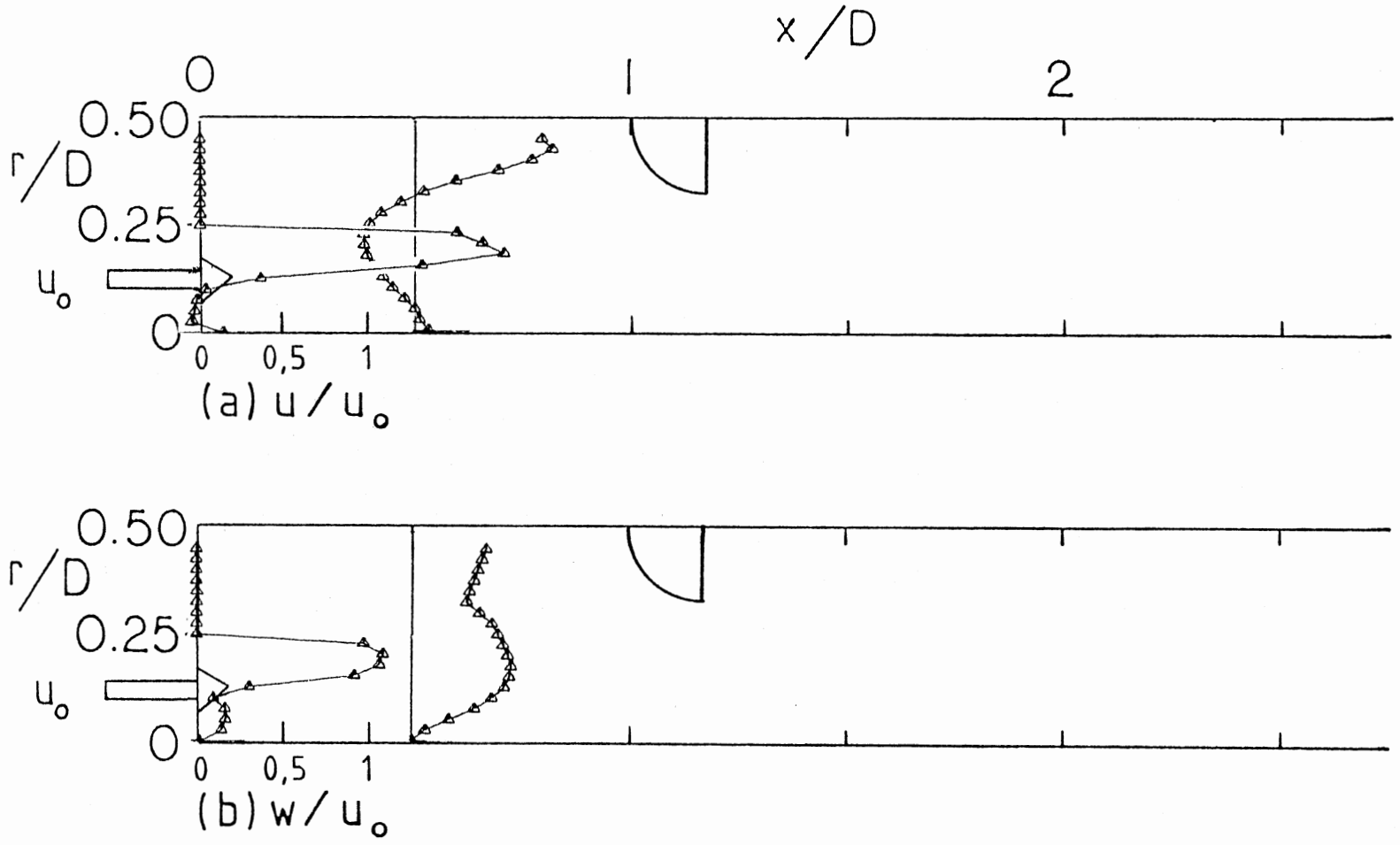

(a) L/D = 1.0

Figure 15. Velocity Profiles for Swirl Vane Angle ϕ = 45° with Contraction Block

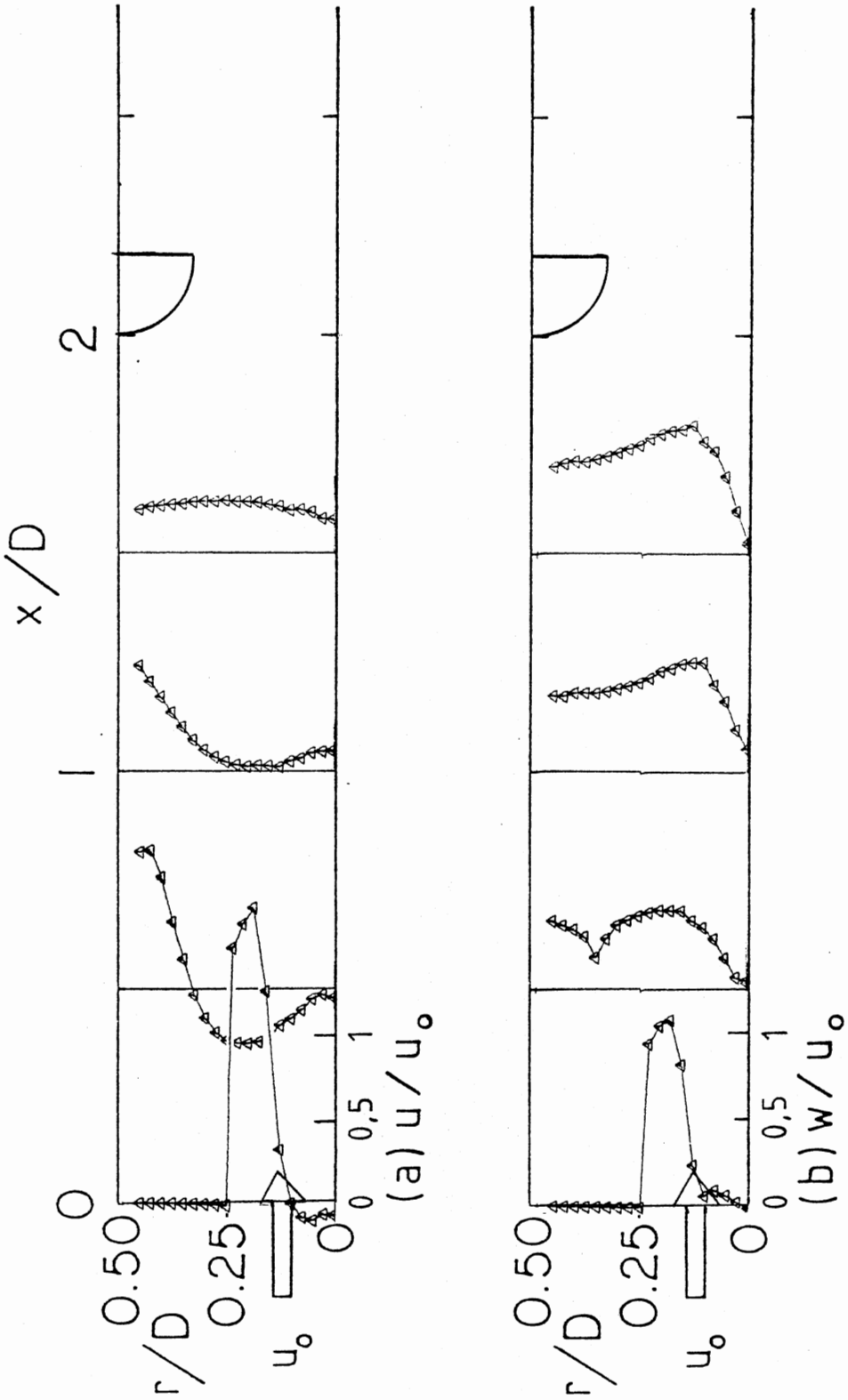

(b) L/D = 2.0

Figure 15 (Continued)

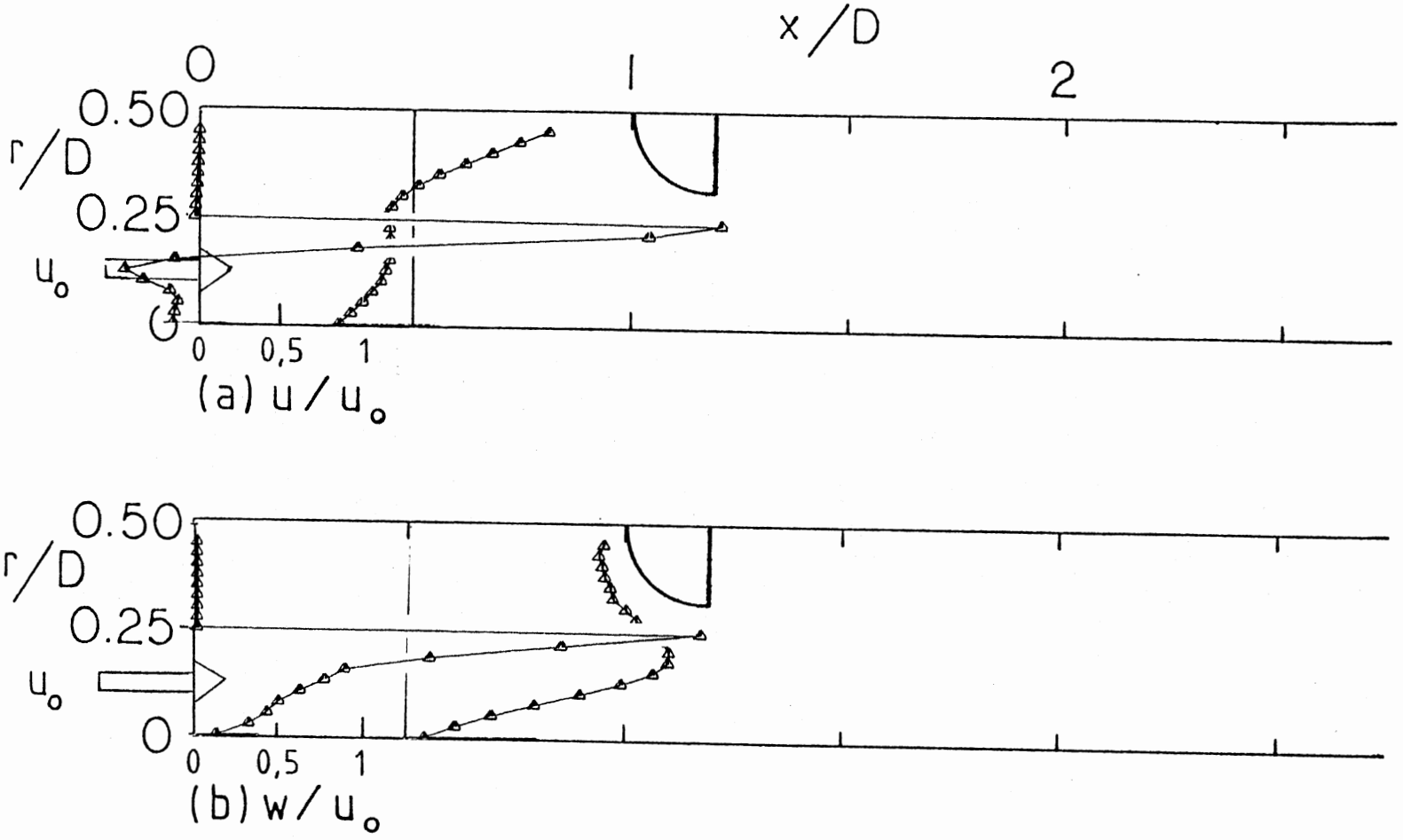

(a) L/D = 1.0

Figure 16. Velocity Profiles for Swirl Vane Angle $\phi = 70°$ with Contraction Block

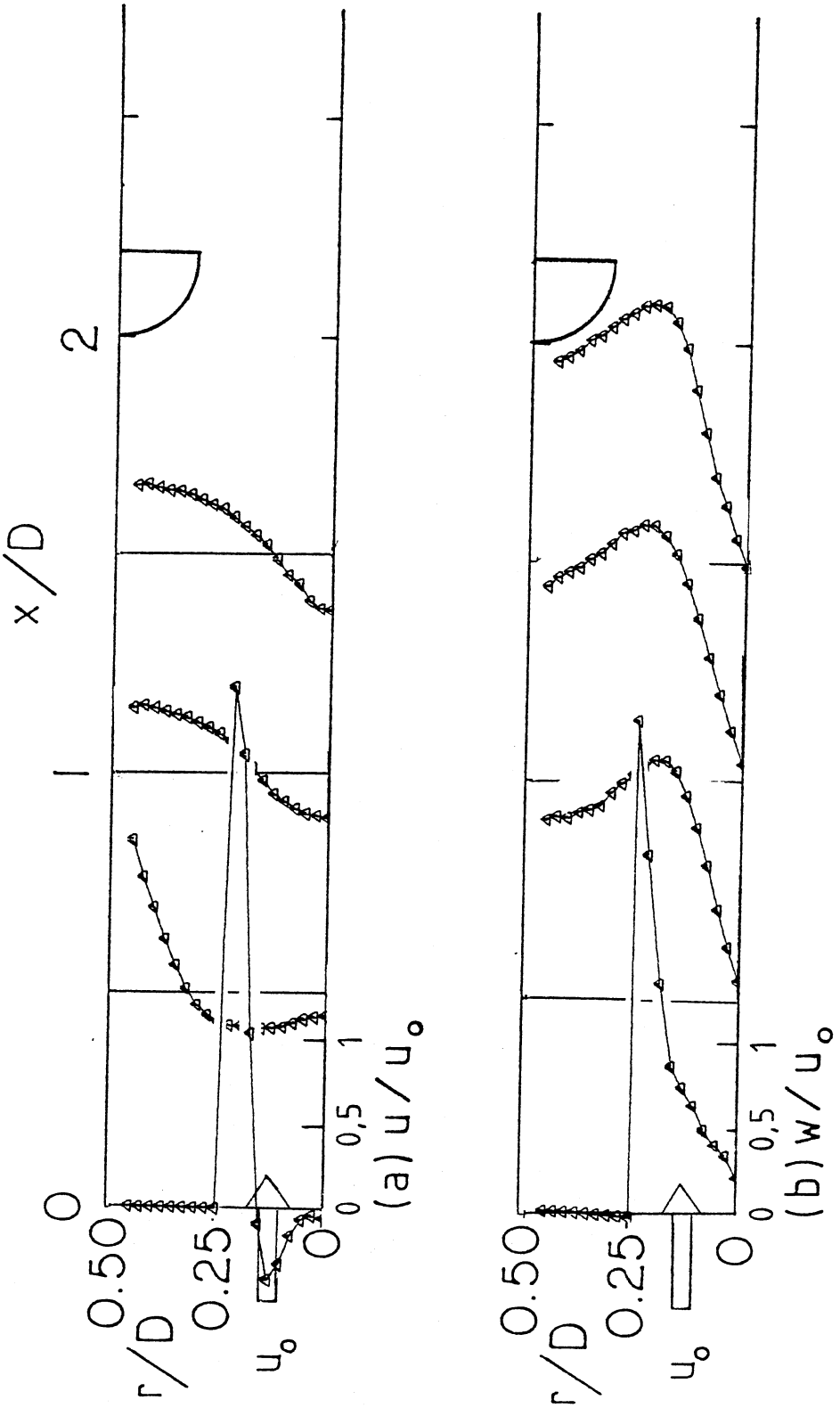

(b) L/D = 2.0

Figure 16 (Continued)

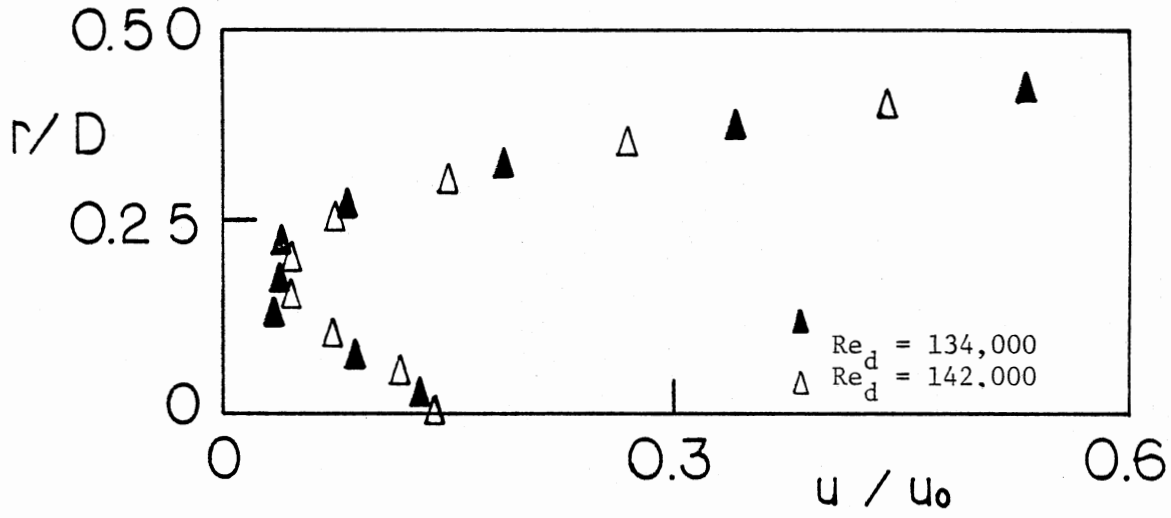

(a) Axial Velocity

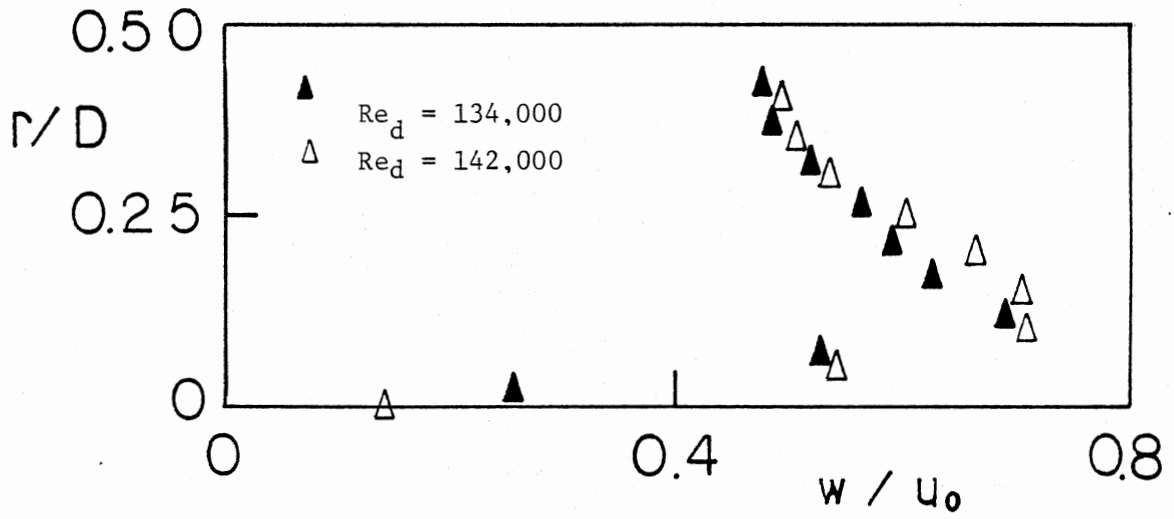

(b) Swirl Velocity

Figure 17. Repeatability of Five-Hole Pitot Probe Measurement for Side-Wall Expansion Angle α = 90° and Swirl Vane Angle ϕ = 45° with Contraction Block at L/D = 2.0 at x/D = 1.0

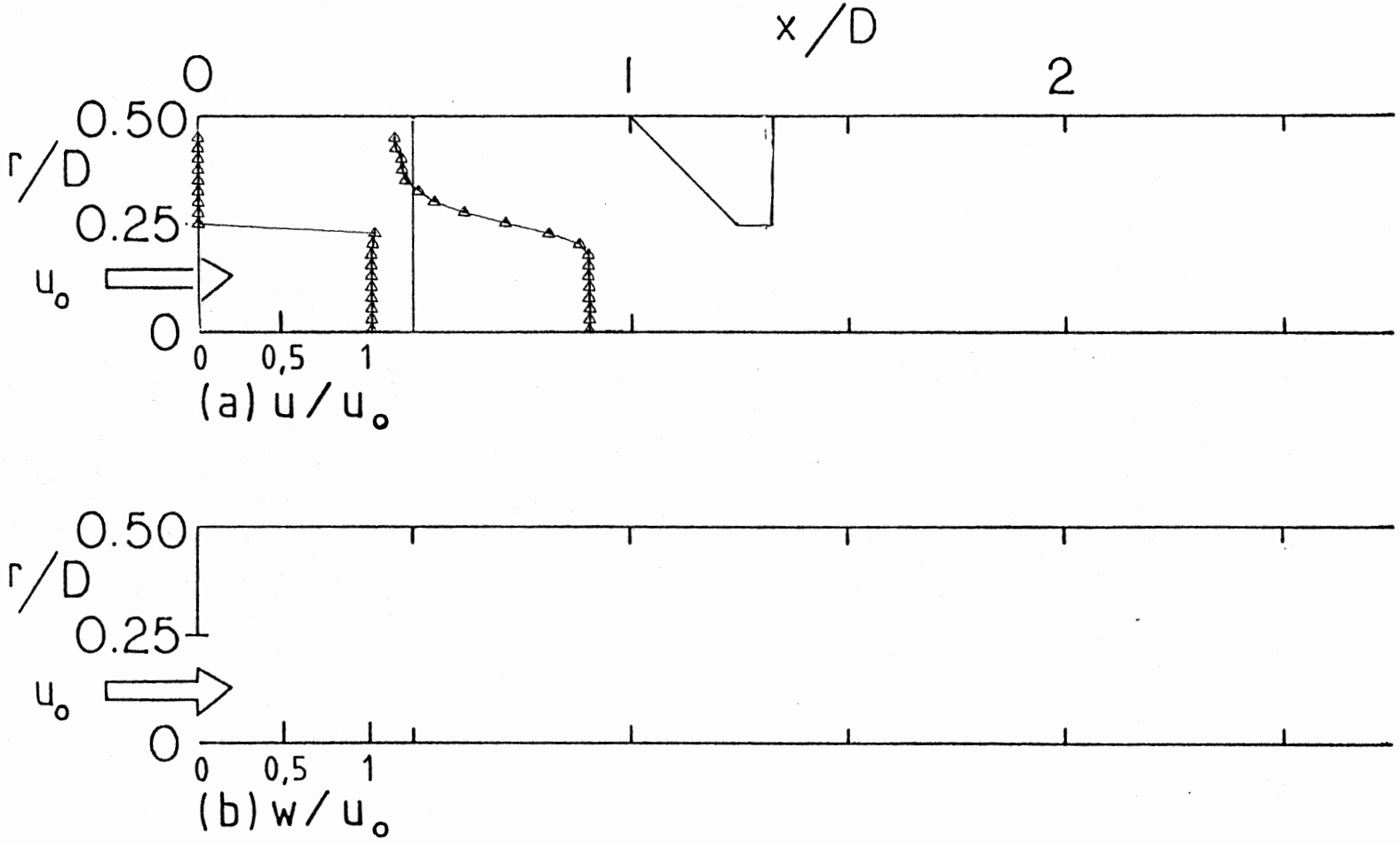

(a) L/D = 1.0

Figure 18. Velocity Profiles for Swirl Vane Angle ϕ = 0° with Strong Contraction Nozzle.

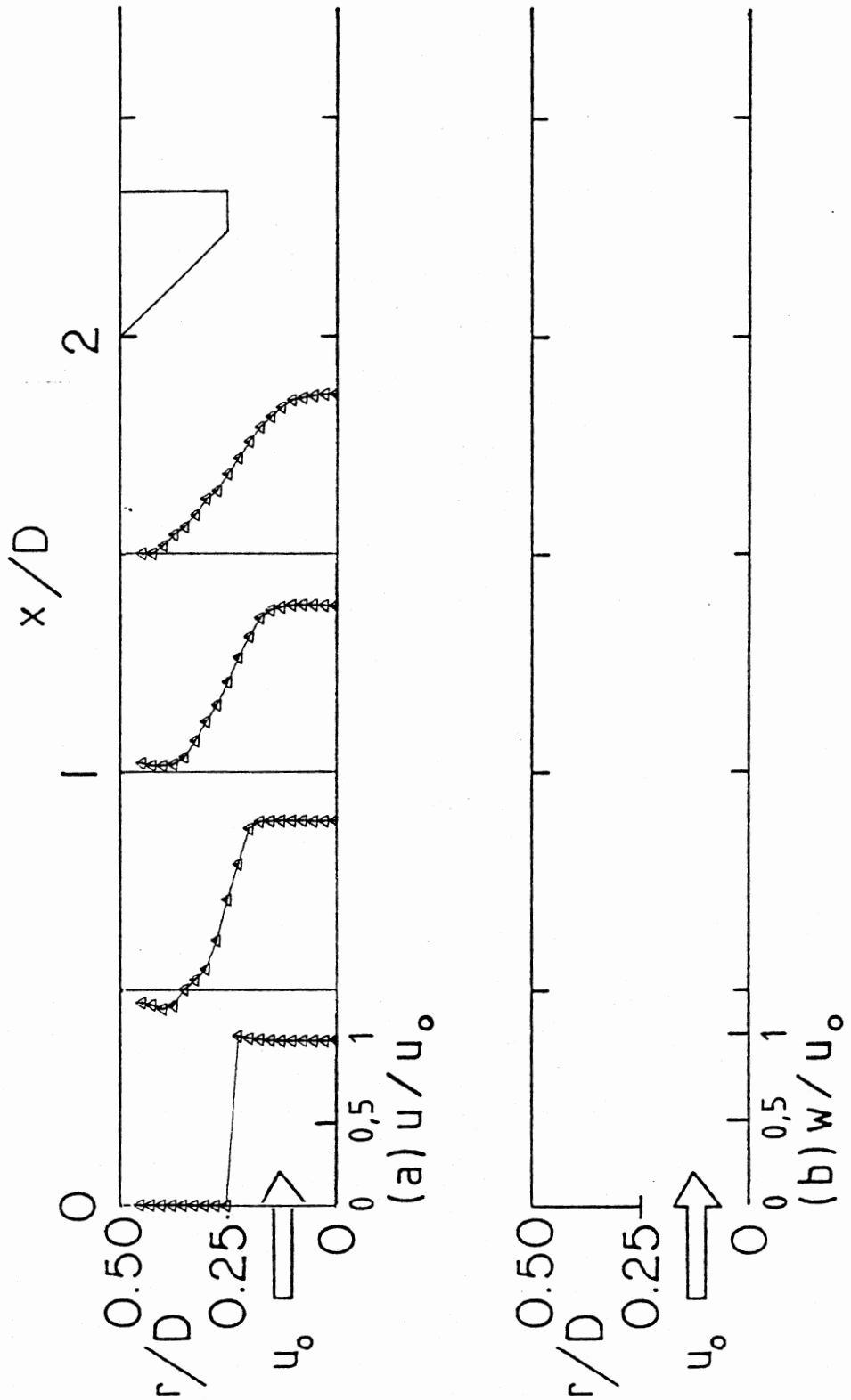

(b) L/D = 2.0

Figure 18 (Continued)

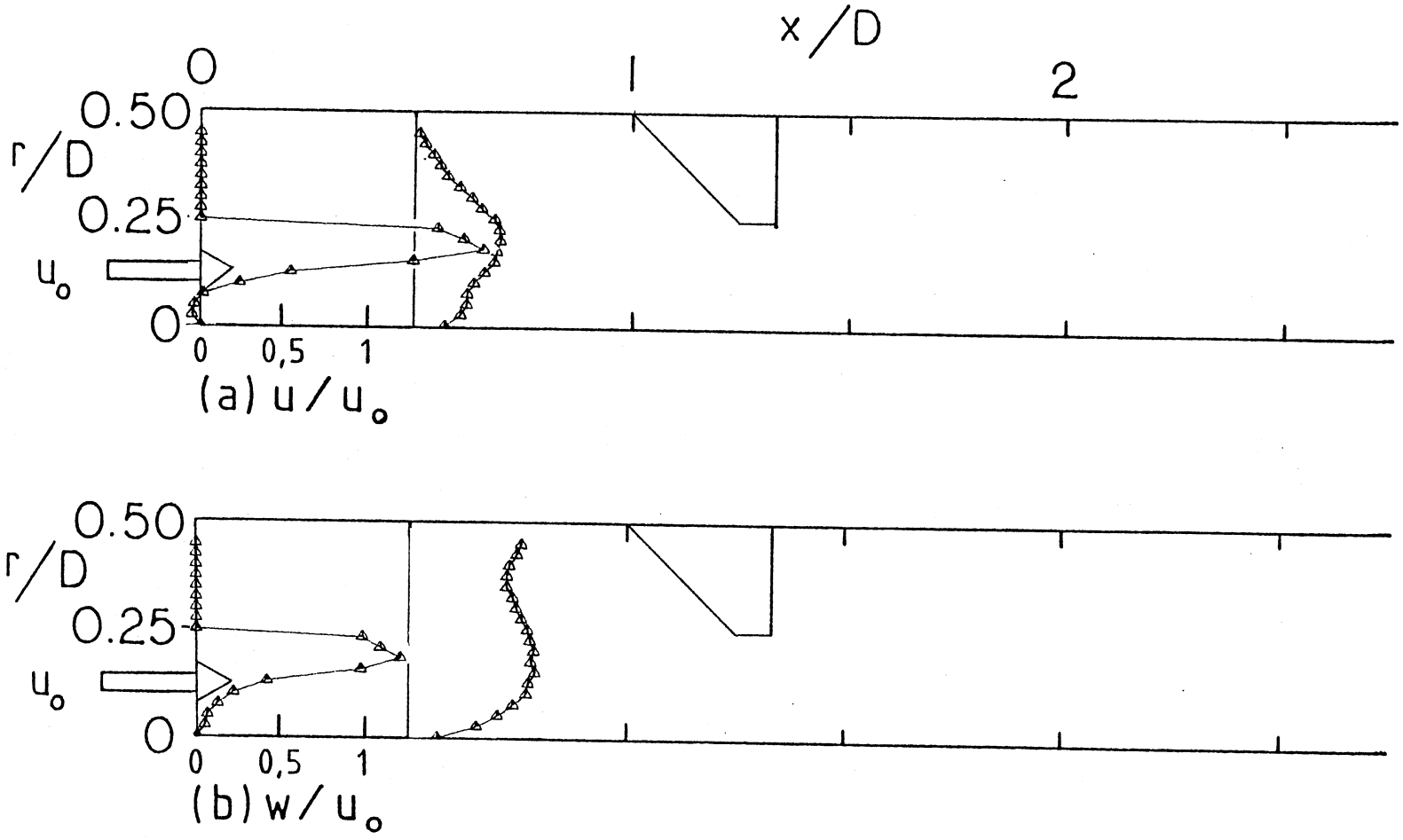

(a) L/D = 1.0

Figure 19. Velocity Profiles for Swirl Vane Angle ϕ = 45° with Strong Contraction Nozzle.

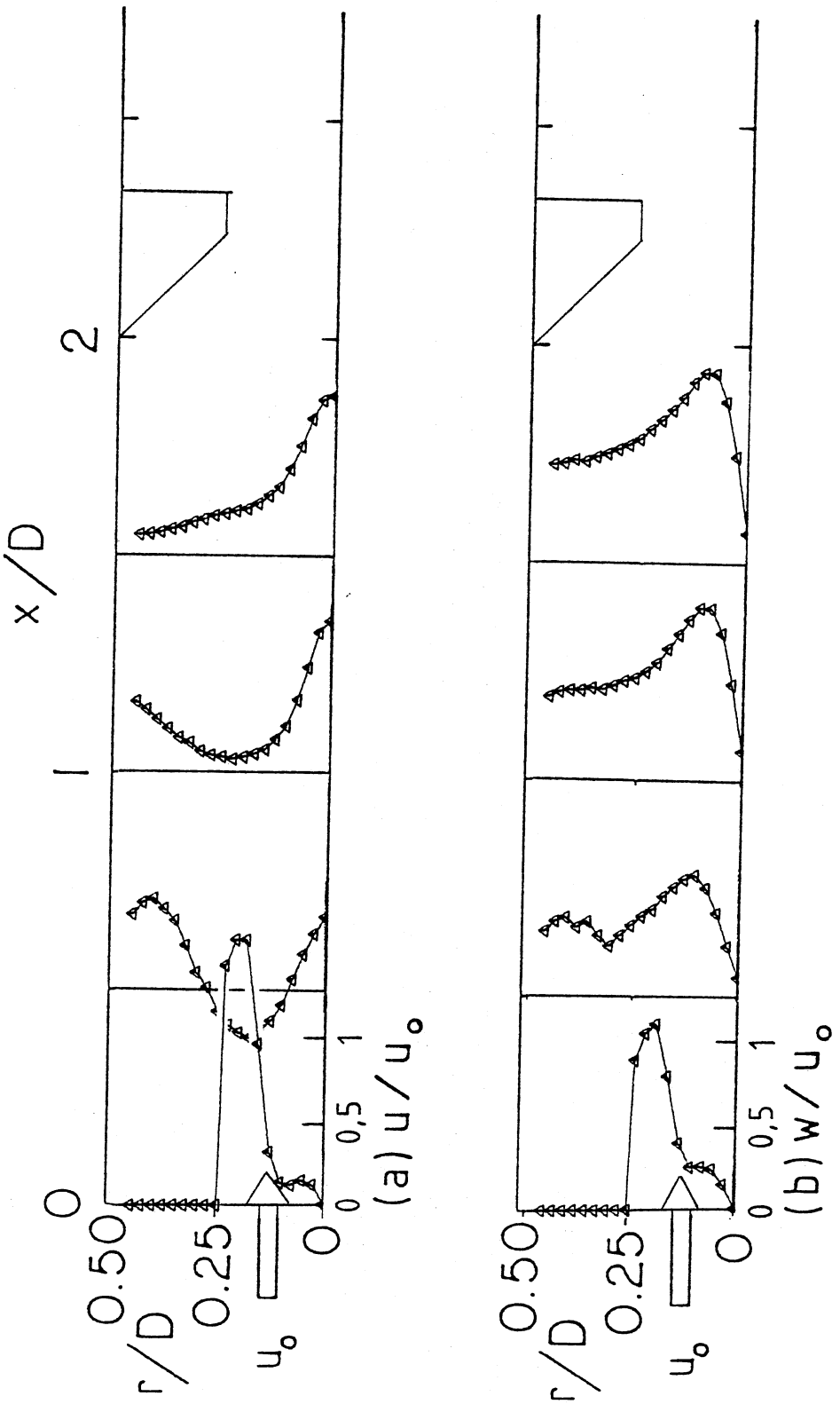

(b) L/D = 2.0

Figure 19 (Continued)

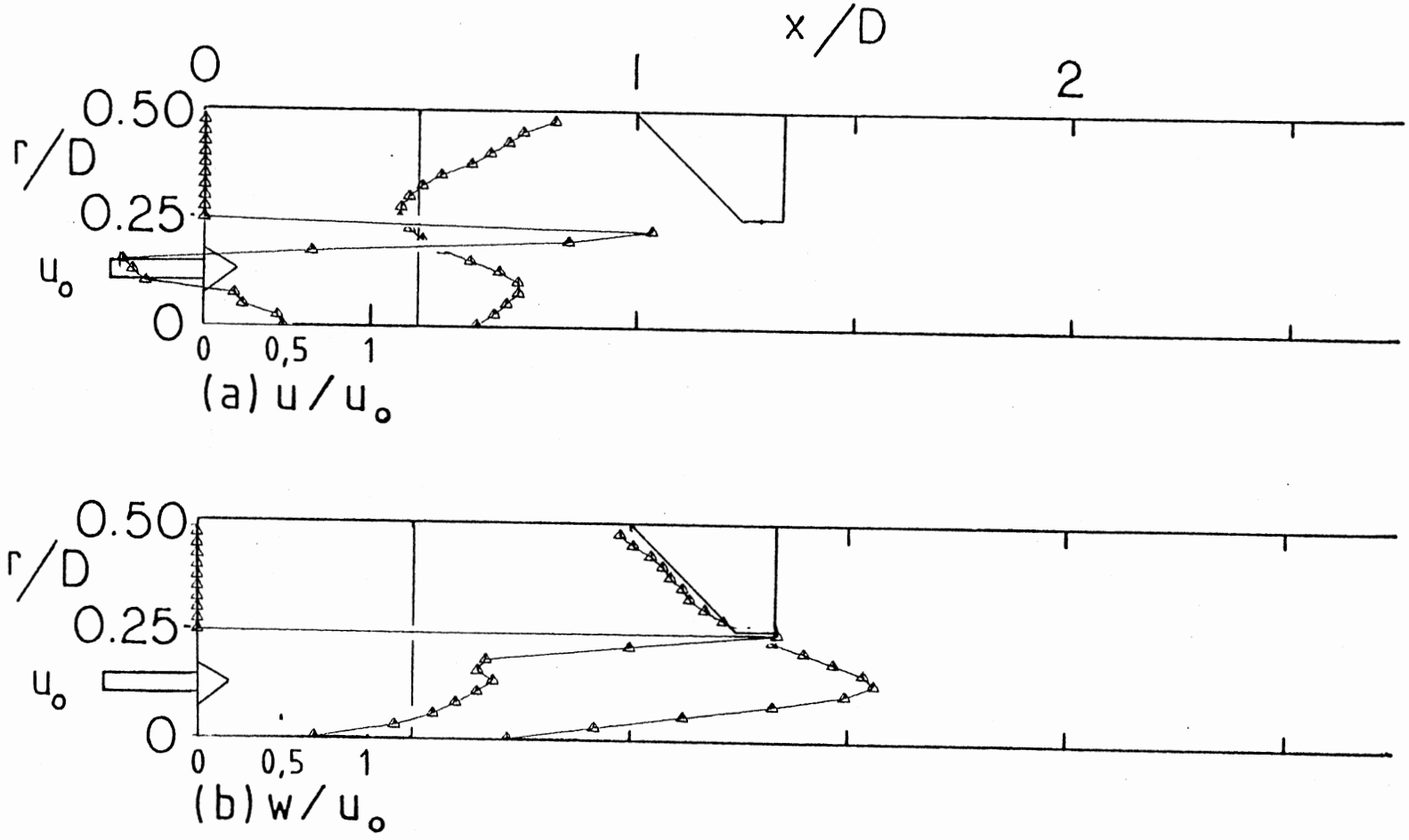

(a) L/D = 1.0

Figure 20. Velocity Profiles for Swirl Vane Angle ϕ = 70° with Strong Contraction Nozzle.

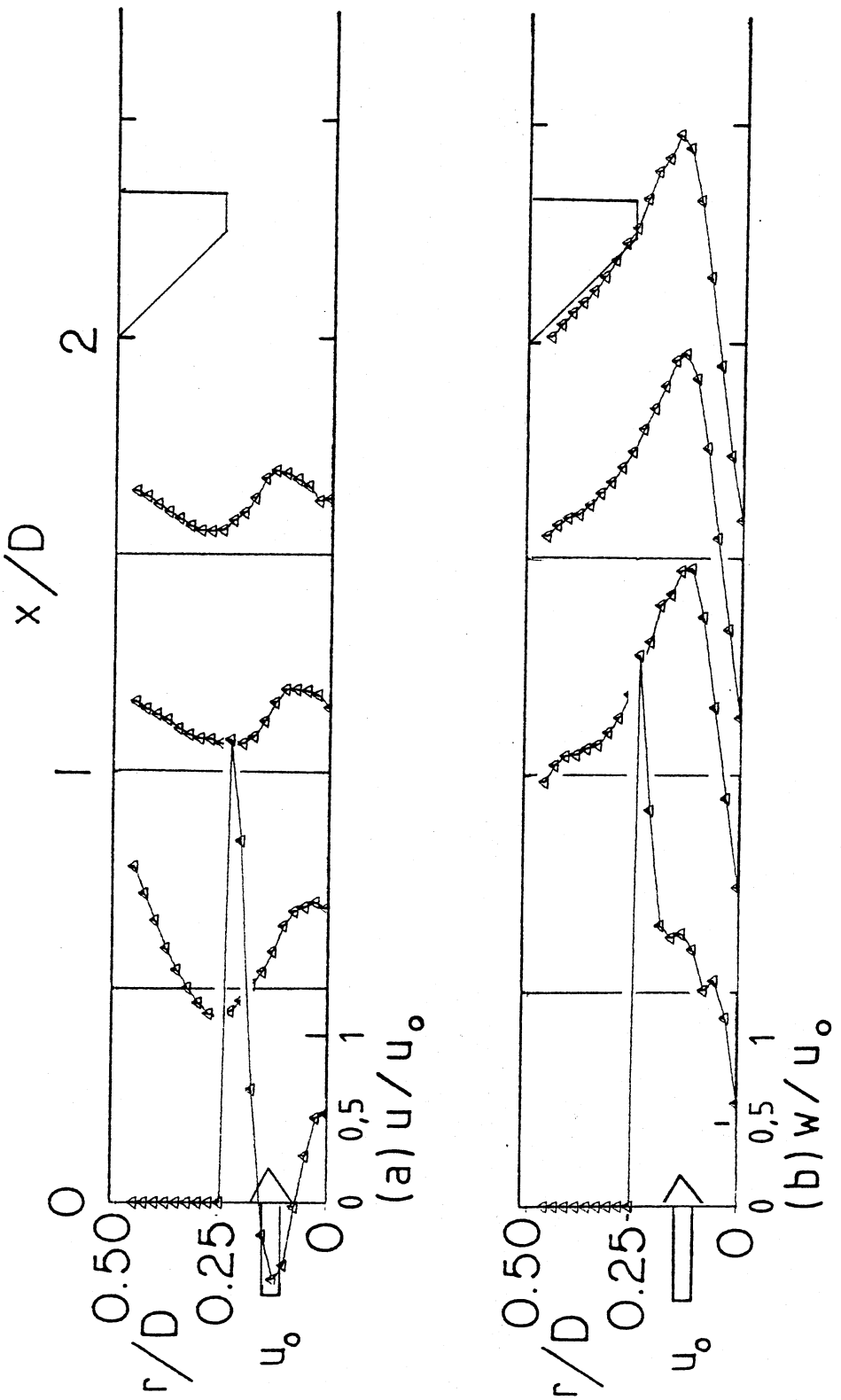

(b) L/D = 2.0

Figure 20 (Continued)

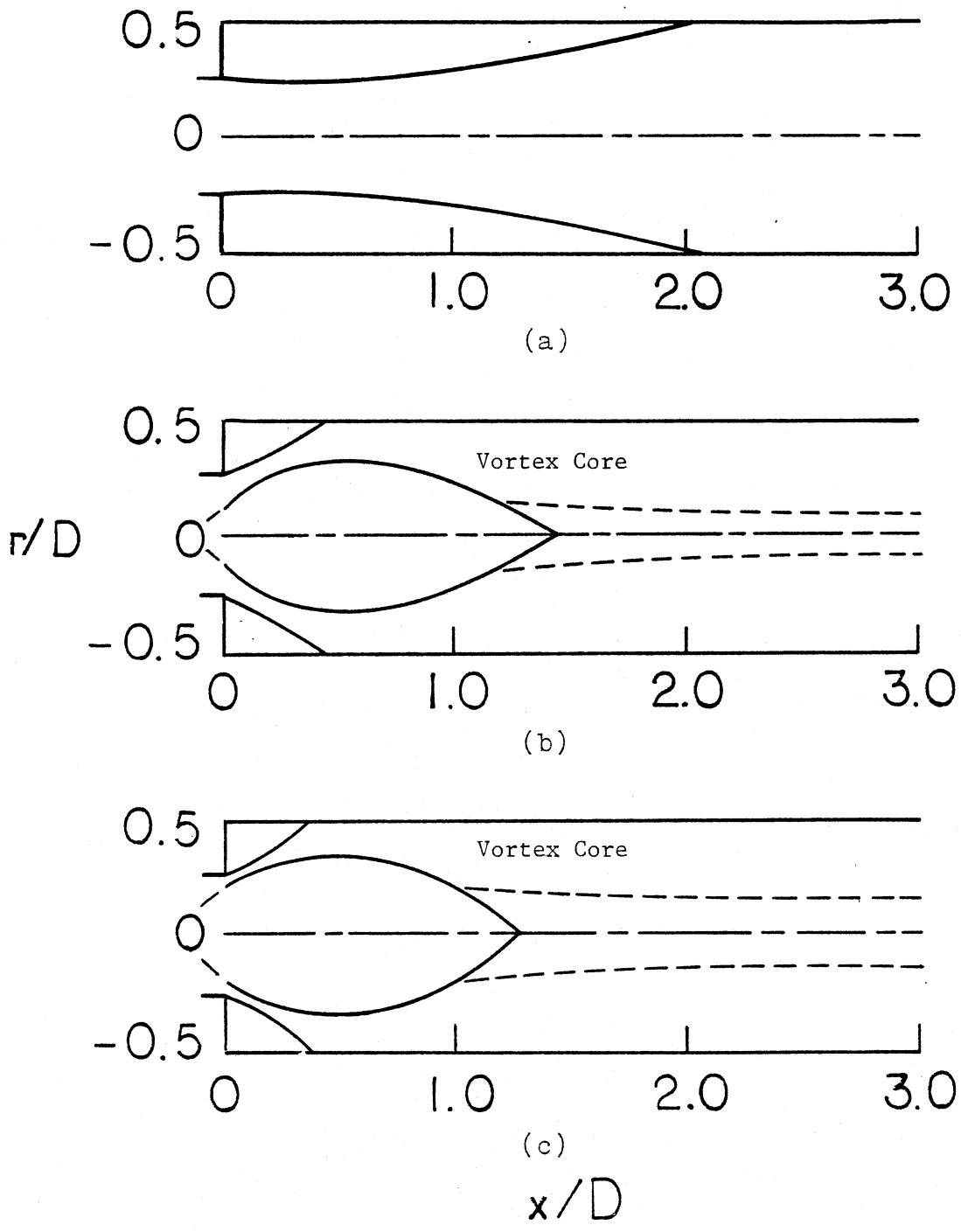

Figure 21. Artistic Impressions of Dividing Streamline without Contraction Block for Side-Wall Expansion Angle $\alpha = 90°$ and Swirl Vane Angle: (a) $\phi = 0°$ (b) $\phi = 45°$ and (c) $\phi = 70°$.

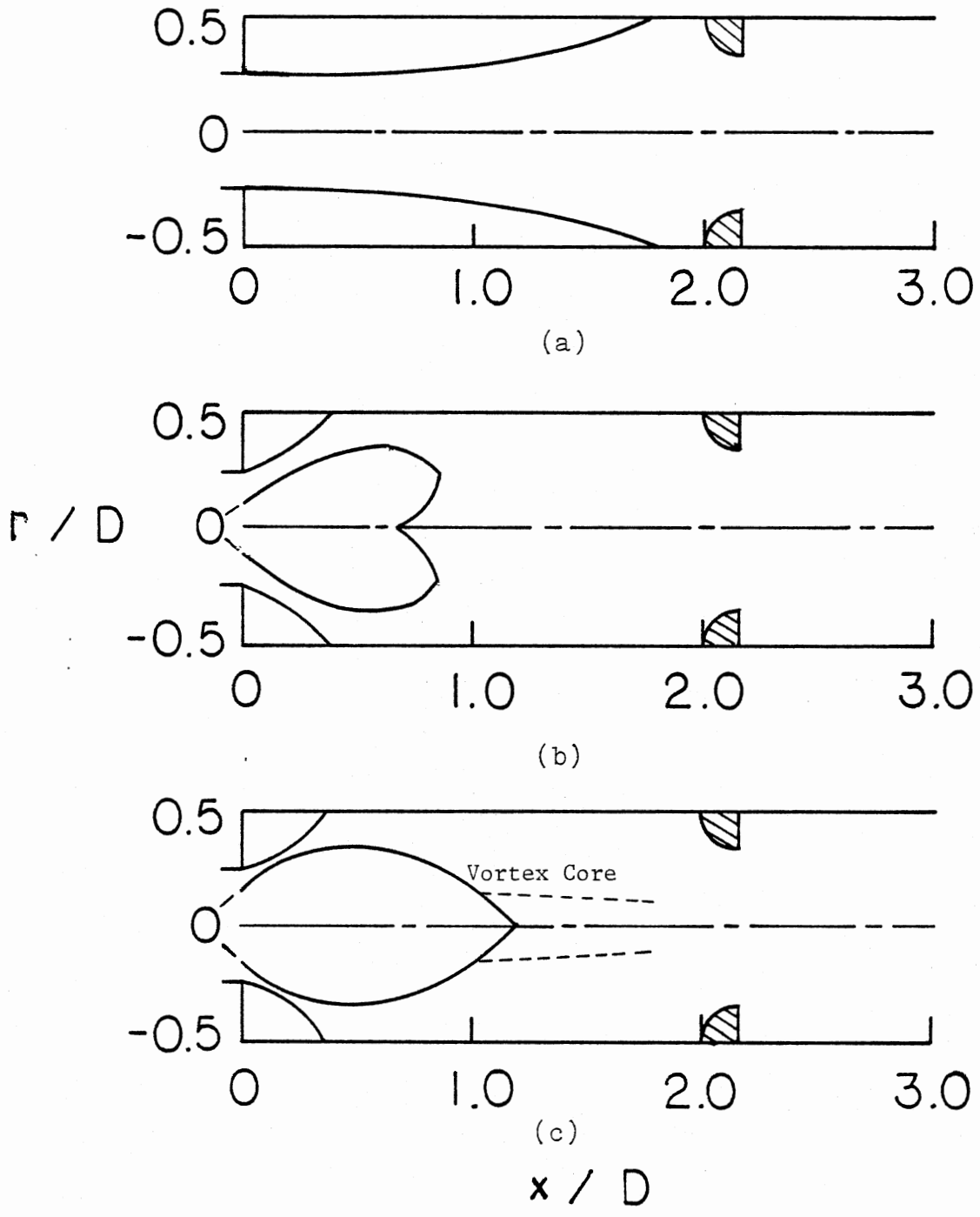

Figure 22. Artistic Impressions of Dividing Streamlines with Contraction Block at L/D = 2.0 for Side-Wall Expansion Angle α = 90° and Swirl Vane Angle: (a) ϕ = 0° (b) ϕ = 45° (c) ϕ = 70°.

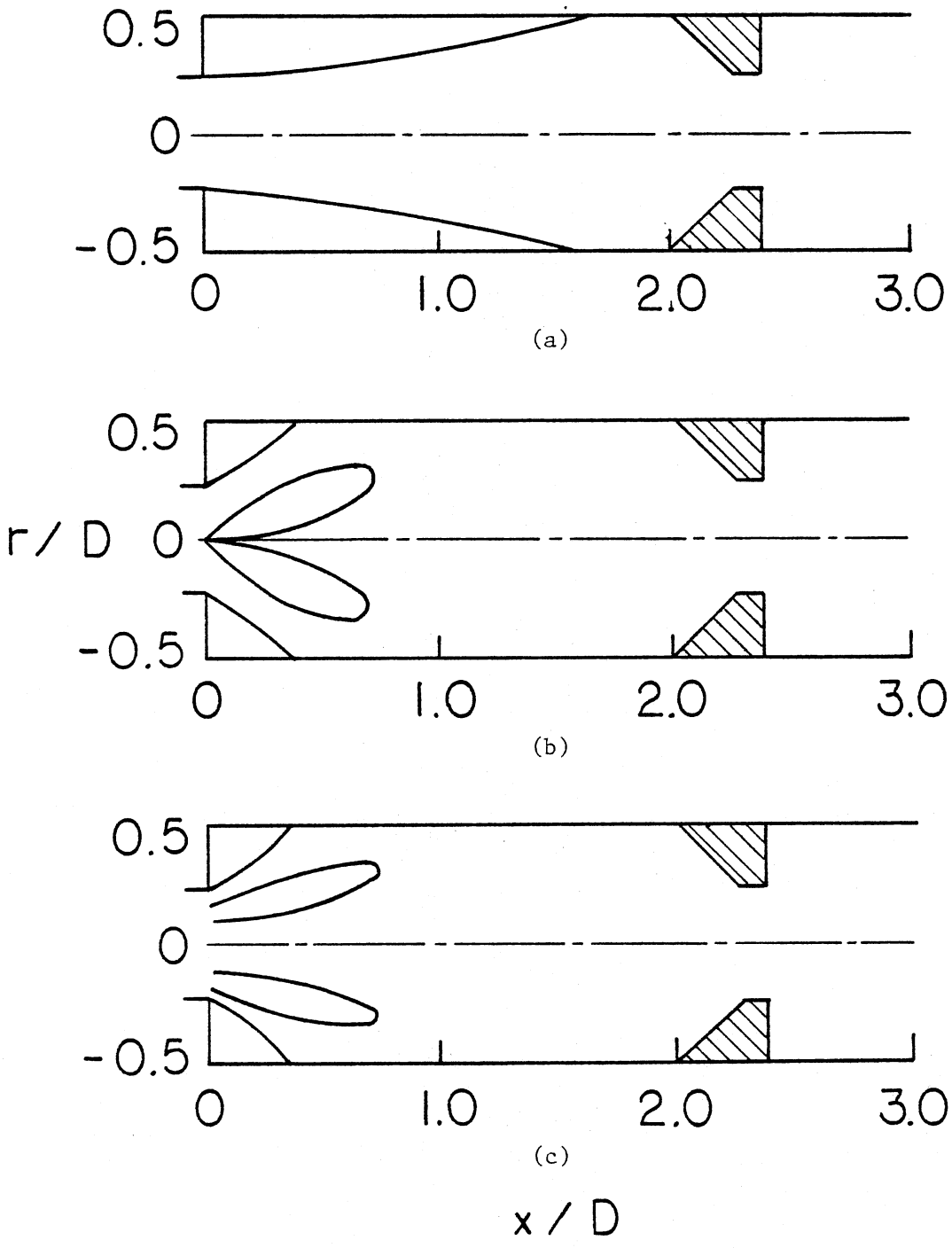

Figure 23. Artistic Impressions of Dividing Streamlines with Contraction Block at L/D = 2.0 for Side-Wall Expansion Angle α = 90° and Swirl Vane Angle: (a) ϕ = 0° (b) ϕ = 45° (c) ϕ = 70°.

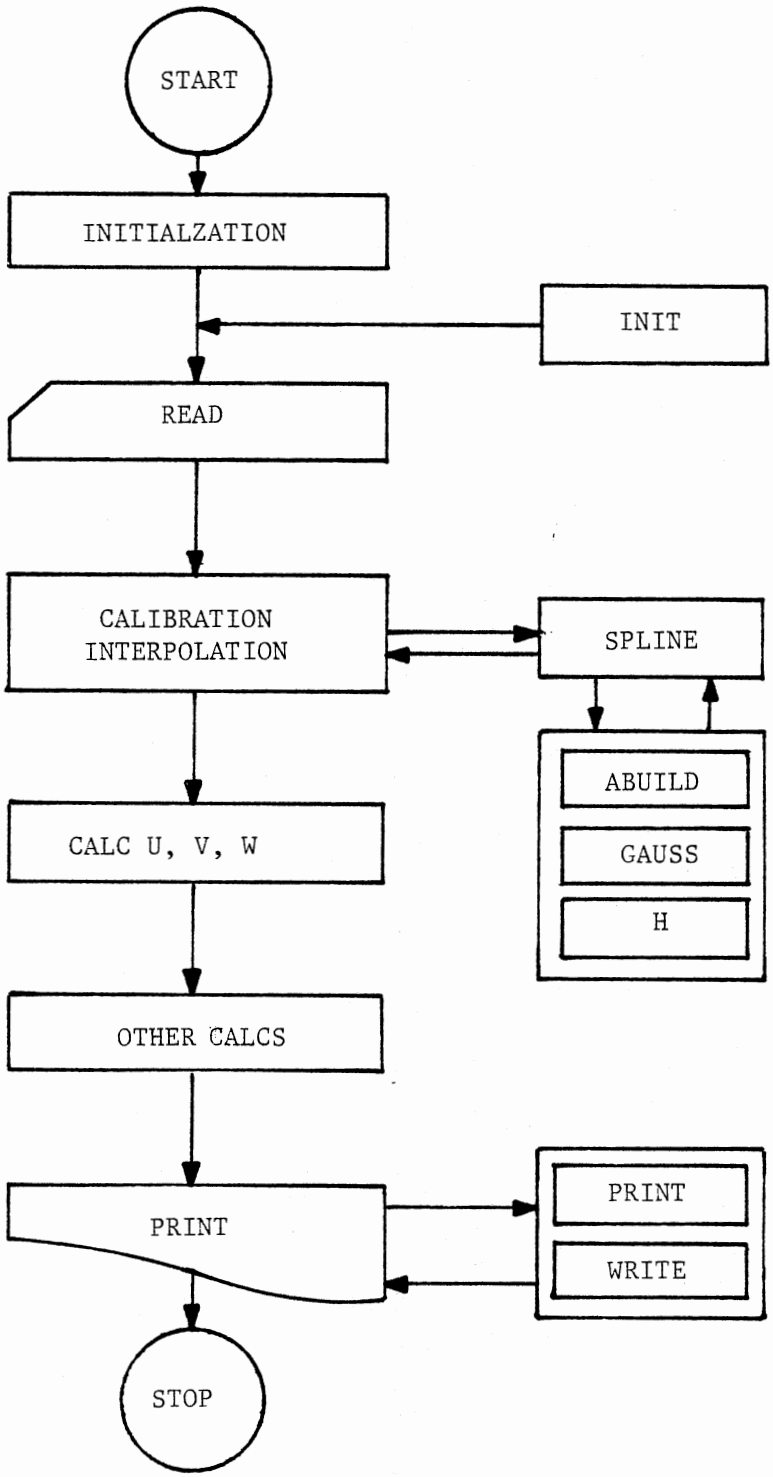

Figure 24. Flow Chart of Data Reduction Computer Program.

APPENDIX C

USER'S GUIDE TO FIVE-HOLE PITOT PROBE DATA REDUCTION COMPUTER PROGRAM

A FORTRAN computer program to reduce five-hole pitot probe measurement data was written by Rhode (5). The data reduction program consists of one main subprogram, two functions and five subroutines. A cubic spline interpolation technique is employed to interpolate calibration data. This user's guide emphasizes the basic mathematical concepts together with analytical and numerical methods employed in this program. For user's convenience, sample input and output are given. The flow chart of this program is shown in Figure 24.

1. MAIN Subprogram

MAIN characterizes the particular conditions being investigated. Entire solution procedure is controlled by MAIN. So, it is the section of the program to which a user will devote most of his attention. It is divided into four chapters, each with a specific task, and a description of the individual chapters of MAIN now follows.

CO Preliminaries

Dimension and common are followed by input logical parameters, which activate, when specified as TRUE, certain special features of program. IWRITE writes solutions onto allocated disk storage and DIAGNS activates diagnostic write statements. Some geometric parameters

are specified as user input values. Input read statement for alpha-numeric headings is given. Initialization of all variables to be zero by calling subroutine INIT is followed by two input read statements, which read calibration and raw measurement data.

C1 Data Reduction

This is a main part to reduce raw measurement data. Data reduction consists of a cubic spline interpolation of calibration data and calculations of u, v and w velocity components. A pitch coefficient is calculated by $(P_N - P_S)/(P_C - P_W)$. With the calculated pitch coefficient, a pitch angle δ is obtained from the corresponding calibration characteristic by calling function SPLINE. The corresponding velocity coefficient C for the resulting pitch angle δ is also obtained by calling function SPLINE once again.

IDID is a parameter to define caliration ranges. If pitch angle δ or velocity coefficient C is out of the calibration range $[-3.759 \leq (P_N - P_S)/(P_C - P_W) \leq 3,399,\ |\delta| \leq 58]$, respectively, the corresponding value is taken to be zero with IDID = 0.

With the above obtained information, three velocity components and magnitude of the total velocity vector are calculated from

$$V = \left[\frac{2}{\rho}(P_c - P_w) \cdot C\right]^{1/2} \tag{A3.1}$$

$$u = V \cos\delta \cos\beta \tag{A3.2}$$

$$v = V \sin\delta \tag{A3.3}$$

$$w = V \cos\delta \sin\beta. \tag{A3.4}$$

C2 Auxiliary Calculations

This part consist of calculations of geometric quantities and nondimensionizations of velocities. A mass flow rate and axial flux of angular momentum are calculated by a finite difference integration method as following:

$$\text{mass flow rate} = \sum_i u_i \Delta A_i \tag{A3.5}$$

and

$$\text{axial flux of angular momentum} = \sum_i \rho u_i w_i r_i^2 \Delta r_i \tag{A3.6}$$

Mean axial velocity is calculated by

$$\text{mean axial velocity} = \Sigma u_i \Delta A_i / A$$

A nozzle inlet axial velocity is obtained from the conversion of the measured dynamic static pressure (inch H_2O) at the nozzle throat into the corresponding velocity (m/sec). All velocities are nondimensionized by the nozzle inlet axial velocity.

C3 Ouput

All reduced data are printed out according to a standard format by calling subroutines WRITE and PRINT.

2. INIT Subroutine

In this subroutine, all variables are initialized to be zero even though some are set to obviously nonzero values. All variables in the subprogram MAIN communicate with those in the subroutine INIT through common statements.

3. SPLINE Function

A cubic spline data fitting technique (25) is employed to interpolate pitch angle δ and velocity coefficient C from the corresponding calibration characteristics. For a certain x value, which lies between the points (X_i, Y_i) and (X_{i+1}, Y_{i+1}), a cubic polynomial equation can be written by

$$Y = a_i (X - X_i)^3 + b_i (X - X_i)^2 + C_i (X - X_i) + d_i \tag{A3.7}$$

with application of the proper end point conditions, it reduces to

$$h_{i-1} S_{i-1} + 2 (h_{i-1} + h_i) S_i + h_i S_{i+1} = b\left(\frac{Y_{i+1} - Y_i}{h_i} - \frac{Y_i - Y_{i-1}}{h_{i-1}} \right) \tag{A3.8}$$

$$h_i = X_{i+1} - X_i \tag{A3.9}$$

During the foregoing procedures, the coefficients are also reduced as

$$a_i = (S_{i+1} - S_i)/[6 h_i] \tag{A3.10}$$

$$b_i = S_i/2 \tag{A3.11}$$

$$C_i = \frac{Y_{i+1} - Y_i}{h_i} - \frac{2h_i S_i + h_i S_{i+1}}{6} \tag{A3.12}$$

$$d_i = Y_i \tag{A3.13}$$

The equation (A3.8) forms (n - 2) equations for n unknowns. Two more equations needed to solve n unknowns are obtained when the conditions

pertaining to the end intervals are specified. Linear extrapolation techniques is employed to obtain the end point conditions. The relations for end conditions of the whole curve are at the left end:

$$S_1 = \frac{(h_1 + h_2)\, S_2 - h_1 S_3}{h_2} \qquad \text{(A3.14)}$$

and the right end:

$$S_n = \frac{(h_{n-2} + h_{n-1})\, S_{n-1} - h_{n-1}\, S_{n-2}}{h_{n-2}} \qquad \text{(A3.15)}$$

Finally, n equations including two conditions are obtained for n unknowns.

With the above mathematic concept in mind, one can follow the calculation steps employed in this program. Two calibration and raw measurement data in MAIN communicate with those in SPLINE through parameters X, FX and X1.A Parameter A is an array for the coefficients of n simultaneous cubic polynomial equations. The (n-2) by (n-2) components of an array A are built by calling the subroutine ABUILD. The end point components A(1,J) and A(N,J) are built in the function SPLINE. The Gauss-Jordan elimination method is employed to solve (n-2) equations for (n-2) unknowns simultaneously. These solutions are translated back to the SPLINE by a parameter A.

With the obtained solutions, the coefficient of a cubic polynomial equation are calculated by equations (A3.10) through (A3.13). Finally, an interpolation is achieved by substituting the known coefficient values into the equation (A3.7). An interpolated value is translated back to the MAIN through a variable SPLINE.

4. H Function

This function calculates the interval ΔX_i between the points (X_i, Y_i) and (X_{i+1}, Y_{i+1}).

5. ABUILD Subroutine

This routine builds an (n-2) by (n-2) array for the coefficients of a cubi polynomial equation. This forms a tridiagonal matrix with a column vector of (n-2) components. The notation employed here is as follows:

$$a_{i,i-1} = h_{i-1}$$

$$a_{i,i} = 2(h_{i-1} + h_i)$$

$$a_{i,i+1} = h_i$$

and

$$a_{i,n+1} = 6\left(\frac{Y_{i+1} - Y_i}{h_i} - \frac{Y_i - Y_{i-1}}{h_{i-1}}\right)$$

6. GAUSS Subroutine

This routine solves (n-2) equations simultaneously with a Gauss-Jordan elimination method. Solutions are stored in the $a_{i,n+1}$.

7. PRINT and WRITE Subroutines

The tasks of subroutines PRINT and WRITE are to pritn out the values of a 2-D array PHI, together with associated heading HEAD, the last parameter of the call list. The only difference between PRINT

and WRITE is that WRITE is used to print out one line and PRINT is used to print out multiple lines at a time. The first two parameters of the call list, ISTART and JSTART, are usually 1 and 1, so that all internal and external values are printed to help diagnostics.

8. Sample Input

Alphanumeric headings, calibration data and raw measurement data are read by input read statements. Sample input data are given for the sample case of side-wall expansion angle α = 90 degrees, swirl vane angle ϕ = 45 degrees and contraction nozzle located L/D = 1.

(a) Alphanumeric headings: These alphanumeric headings are used to accompany the output descriptively. Nineteen lines of such headings are read in via the first read statement. The current alphanumeric headings are given in Table XIV.

(b) Calibration Data: Calibrations are done for pitch angle and velocity coefficient characteristics. Calibration input data consist of pitch coefficient $(P_N - P_S)/(P_C - P_W)$ and velocity coefficient $\rho V^2/[2(P_C - P_W)]$ for 24 different pitch angles δ. Sample calibration input data are tabulated in Table XV. This table consists of pitch coefficient in the first column, corresponding pitch angle in the second and corresponding velocity coefficient in the third.

(c) Measurement Data: Sample raw measurement data are given for two axial stations in Table XVI. Nineteen radial traverse measurement data are taken at each axial station. For each axial station, axial distance (inch), maximum number of radial positions and dynamic pressure (in H_2O) are read as shown in lines 10380 and 10580 of Table XVI. Lines 10390 to 10570 are measurement data for the axial station

x/D = 0.0 and lines 10590 to 10770 are for the axial station x/D = 0.5. The input measurement data consists of four column input data: the first is for radial measurement point (inch), the second for measured flow angle (360.0 - β degree), the third for $P_N - P_S$ (volt) and the fourth for $P_C - P_W$ (volt).

9. Sample Output

Typical output consists of yaw angle, pitch angle and three velocity components. The corresponding output for the sample input data just described is given in Table VI, as described earlier in Section 4.1 In this table, I and J denote the axial and radial station number, respectively. Also X and Y denote the normalized axial and radial station by the test section diameter, respectively. Yaw angle β and pitch angle δ are given in degrees. These velocity components are values normalized by the nozzle inlet axial velocity deduced from the pitot static pressure probe located upstream of the inlet to the test section, as described in Section 2.1.

As auxiliary output, geometric specifications and quantities are printed out in front of the typical output. Geometric specifications include expansion angle (degree). Swirl vane angle (degree), inlet radius (m) and combustor radius (m). On the other hand, flow quantities include mass flow rate (kg/s), nozzle inlet axial velocity (m/s), mean axial velocity (m/s) and axial flux of angular momentum (N.m). In each of these items, data relevant to each axial station are presented - these may be different with different axial stations and depend on the particular run conditions at the time of each tranverse. Output for the sample input data is given in Table XVII.

```
C     SUBROUTINE MAIN
C
CA*****************************************************************
C
C
C     A COMPUTER PROGRAM FOR DATA REDUCTION OF FIVE-HOLE PITOT
C     MEASUREMENTS IN TURBULENT, SWIRLING, RECIRCULATING, FLOW
C     IN COMBUSTOR GEOMETRIES
C
C     VERSION OF JULY,1982
C
C     H K YOON
C     MECHANICAL AND AEROSPACE ENGINEERING
C     OKLAHOMA STATE UNIVERSITY
C     STILLWATER, OK     74078
C
C
CA*****************************************************************
CHAPTER  0  0  0  0  0  0  PRELIMINARIES  0  0  0  0  0  0  0  0
C
      DIMENSION HEDM(9),HEDUMN(9),HEDNMS(9),HEDCMW(9),
     #HEDU(9),HEDV(9),HEDW(9),HEDVT(9),HEDUST(9),
     #HEDVST(9),HEDWST(9),HEDVTS(9),HEDDEL(9),HEDBET(9),
     #HEDMMF(9),HEDMIV(9),HEDMIP(9),HEDMPP(9),HEDAM(9)
C
      COMMON
     #/CALIB/CPITCH(26),CDELTA(26),CVELCF(26)
     #/MEASUR/RBETA(48,24),RPNMPS(48,24),RPCMPW(48,24),NDATA(48)
     #      ,MAXJPT,RDNPRS(48)
     #/GEOM/X(48),R(24),XND(48),RND(24),DYPS(24),DYNP(24),
     #     SNS(24),NSTATN,XINCHS(48),RINCHS(24)
     #/CALC/VTOTAL(48,24),U(48,24),V(48,24),W(48,24),
     #     VTSTAR(48,24),USTAR(48,24),VSTAR(48,24),WSTAR(48,24),
     #     PICHCF(48,24),VELCF(48,24),DELTA(48,24),BETA(48,24),
     #ANGMOM(48), UMEAN(48),MASS(48),MASFLO(48),UIN(48)
      REAL MASS,MASFLO
      LOGICAL IWRITE,DIAGNS
C --------- SET IWRITE=.TRUE. FOR WRITING SOLN. ON DISK STORASE
C --------- SET DIAGNS=.TRUE. TO ACTIVATE DIANOSTIC WRITE STATEMENT
C --------- NSTATN IS NO. OF AXIAL STATIONS FOR WHICH DATA IS
C              SUPPLIED
C --------- MAXJPT IS MAX. NO. OF RADIAL POSITIONS FOR ALL AXIAL
C            STATIONS
C --------- CPITCH IS CALIBRATION PITCH COEFF.
C --------- CDELTA IS CALIBRATION PITCH ANGLE(DEG.)
C --------- CVELCF IS CALIBRATION VELOCITY COEFF.
C --------- NCAL IS NO. OF CALIBRATION POINTS
C --------- XINCHS IS AXIAL POSITION(IN.) OF EACH PARTICULAR RADIAL
C              TRAVERSE
C --------- NDATA IS NO. OF RADIAL LOCATIONS FOR WHICH DATA IS
C              SUPPLIED FOR EACH PARTICULAR RADIAL TRAVERSE
C --------- RDNPRS IS MEASURED DYNAMIC PRESSURE ENTERING THE
C              SWIRLER
C --------- RBETA IS MEASURED FLOW ANGLE(DEG.) WHERE YAW
C              ANGLE BETA = 360.0 - RBETA
C --------- RDNPRS IS MEASURED VOLTS FOR PNORTH - PSOUTH
C              DIFF. PRESSURE
C ---------RPCMPW IS MEASURED VOLTS FOR PCENTER - PWEST
C              DIFF. PRESSURE
C --------- PICHCF IS REDUCED VALUE FOR PITCH COEFF.
C --------- DELTA IS REDUCED VALUE FOR PITCH ANGLE(DEG.)
C --------- VELCF IS REDUCED VALUE FOR VELOCITY COEFF.
C --------- BETA IS REDUCED VALUE FOR PROBE YAW ANGLE(DEG.)
C --------- VTOTAL IS TOTAL VECTOR VELOCITY MAGNITUDE(M/SEC)
C --------- U IS AXIAL VELOCITY (M/SEC)
C --------- V IS RADIAL VELOCITY (M/SEC)
C --------- W IS SWIRL VELOCITY(M/SEC)
C --------- VTSTAR IS DIMENSIONLESS TOTAL VELOCITY
C --------- USTAR IS DIMENSIONLESS AXIAL VELOCITY
C --------- VSTAR IS DIMENSIONLESS RADIAL VELOCITY
C --------- WSTAR IS DIMENSIONLESS SWIRL VELOCITY
```

```
C --------- ALL PRIMARY USER INPUTS ARE LOCATED HERE
      IWRITE=.TRUE.
      DIAGNS=.FALSE.
      ALPHA=90.
      PHI=45.
      VISCOS=1.8E-5
      NSTATN=2
      MAXJPT=19
      PATM=75.1
      TATM=20.
      IT=48
      JT=24
      RLARGE=1.75/(2.0*39.37)
      RSMALL=RLARGE/2.0
      READ(5,205) HEDM,HEDUMN,HEDU,HEDV,HEDW,
     #    HEDVT,HEDUST,HEDVST,HEDWST,HEDVTS,HEDDEL,HEDBET,
     #HEDNMS,HEDCMW,HEDMMF,HEDMIV,HEDMIP,HEDMPP,HEDAM
  205 FORMAT(9A4)
C---------INITIALIZE VARIABLES TO ZERO
      CALL INIT
C---------READ FIVE-HOLE PITOT CALIBRATION DATA
      NCAL=25
      DO 10 I=1,NCAL
      READ(5,210) CPITCH(I),CDELTA(I),CVELCF(I)
   10 CONTINUE
  210 FORMAT(3F10.5)
      IF(DIAGNS) WRITE(6,400) (CPITCH(I),I=1,25)
      IF(DIAGNS) WRITE(6,400) (CDELTA(I),I=1,25)
      IF(DIAGNS) WRITE(6,400) (CVELCF(I),I=1,25)
  400 FORMAT(///,1X,13(F8.4,1X),//,5X,12(F8.4))
C---------READ RAW MEASURED DATA TO BE REDUCED
      DO 30 I=1,NSTATN
      READ(5,230) XINCHS(I),NDATA(I),RDNPRS(I)
      JPTS=NDATA(I)
      DO 20 J=1,JPTS
      READ(5,220) RINCHS(J),RBETA(I,J),RPNMPS(I,J),RPCMPW(I,J)
   20 CONTINUE
   30 CONTINUE
C---------CONVERT X AND R FROM INCHES TO METERS
      DO 35 I=1,NSTATN
      X(I)=XINCHS(I)*0.0254
      JPTS=NDATA(I)
      DO 32 J=1,JPTS
      R(J)=RINCHS(J)*0.0254
   32 CONTINUE
   35 CONTINUE
  220 FORMAT(4F10.5)
  230 FORMAT(1F10.5,1I10,1F10.5)
      IF(DIAGNS) WRITE(6,470) (NDATA(I),I=1,NSTATN)
      IF(DIAGNS) WRITE(6,450) (X(I),I=1,NSTATN)
      IF(DIAGNS) WRITE(6,500) (R(J),J=1,JPTS)
      DO 37 I=1,NSTATN
      IF(DIAGNS) WRITE(6,500) (RBETA(I,J),J=1,JPTS)
      IF(DIAGNS) WRITE(6,500) (RPNMPS(I,J),J=1,JPTS)
      IF(DIAGNS) WRITE(6,500) (RPCMPW(I,J),J=1,JPTS)
   37 CONTINUE
  450 FORMAT(///,40X,1(F8.4,1X))
  500 FORMAT(///,20X,10(F8.4))
C
CHAPTER  1  1  1  1  1  DATA REDUCTION  1  1  1  1  1  1
C
  470 FORMAT(///,40X,1(I8,1X))
C---------CALC PICHCF AND INTERPOLATE FOR DELTA FROM
C---------    PITOT CALIBRATION CURVE
      IDID=0
      DO 50 I=1,NSTATN
      JPTS=NDATA(I)
      DO 40 J=1,JPTS
      IF((RPCMPW(I,J) .EQ. 0.0) .AND. (RPNMPS(I,J) .EQ. 0.0))
     #    GO TO 38
```

```
      PICHCF(I,J)=RPNMPS(I,J)/(RPCMPW(I,J)+1.E-6)
      IF((PICHCF(I,J).GT.3.399) .OR. (PICHCF(I,J).LT.-3.759))
     #   GO TO 38
      IF(IDID .EQ. 0) DELTA(I,J)=SPLINE(CPITCH,
     #    CDELTA,NCAL,PICHCF(I,J))
      IF(IDID .GT. 0) DELTA(I,J)=SP(CPITCH,CDELTA,
     #    NCAL,PICHCF(I,J))
      IDID=1
      GO TO 40
   38 CONTINUE
      DELTA(I,J)=0.0
      WRITE(6,850) I,J
  850 FORMAT(20X,'PICHCF IS OUT OF RANGE OF CALIBRATION AT I=
     #',I3,' AND J=',I3)
   40 CONTINUE
   50 CONTINUE
C---------INTERPOLATE FOR VELCF FROM PITOT CALIBRATION DATA
      IDID=0
      DO 80 I=1,NSTATN
      JPTS=NDATA(I)
      DO 70 J=1,JPTS
      IF((RPCMPW(I,J) .EQ. 0.0) .AND. (RPNMPS(I,J) .EQ. 0.0))
     #   GO TO 65
      IF((ABS(DELTA(I,J))) .GT. 58.0) GO TO 65
      IF(IDID .EQ. 0) VELCF(I,J)=SPLINE(CDELTA,
     #CVELCF,NCAL,DELTA(I,J))
      IF(IDID .GT. 0) VELCF(I,J)=SP(CDELTA,CVELCF,
     #NCAL,DELTA(I,J))
      IDID=1
      GO TO 70
   65 CONTINUE
      VELCF(I,J)=0.0
      WRITE(6,890) I,J
  890 FORMAT(20X,'DELTA IS OUT OF RANGE OF CALIBRATION DATA
     #AT I=',I3,' AND J=',I3)
   70 CONTINUE
   80 CONTINUE
      DO 85 I=1,NSTATN
      IF(DIAGNS) WRITE(6,500) (PICHCF(I,J),J=1,JPTS)
      IF(DIAGNS) WRITE(6,500) (DELTA(I,J),J=1,JPTS)
      IF(DIAGNS) WRITE(6,500) (VELCF(I,J),J=1,JPTS)
   85 CONTINUE
C---------CALC MAGNITUDE OF TOTAL MEAN VELOCITY VECTOR AND
C---------    U, V, & W COMPONENTS
      RHO=PATM*(136.0/0.102)/(287.0*(TATM+273.0))
      PI=3.14159
      DO 100 I=1,NSTATN
      JPTS=NDATA(I)
      DO 90 J=1,JPTS
      BETA(I,J)=360.-RBETA(I,J)
      IF((RPCMPW(I,J).EQ.0.0) .AND. (RPNMPS(I,J).EQ.0.0))
     #   BETA(I,J)=0.0
      VTOTAL(I,J)=SQRT(ABS(2.0/RHO*VELCF(I,J)*RPCMPW(I,J)*133.9))
      U(I,J)=VTOTAL(I,J) * COS(DELTA(I,J)*PI/180.0) *
     #    COS(BETA(I,J)*PI/180.0)
      V(I,J)=VTOTAL(I,J) * SIN(DELTA(I,J)*PI/180.0)
      W(I,J)=VTOTAL(I,J) * COS(DELTA(I,J)*PI/180.0) *
     #    SIN(BETA(I,J)*PI/180.0)
   90 CONTINUE
  100 CONTINUE
      IF(DIAGNS) WRITE(6,500)(VTOTAL(I,J),J=1,JPTS)
      IF(DIAGNS) WRITE(6,500)(U(I,J),J=1,JPTS)
      IF(DIAGNS) WRITE(6,500)(V(I,J),J=1,JPTS)
      IF(DIAGNS) WRITE(6,500)(W(I,J),J=1,JPTS)
CHAPTER  2  2  2  2  2  2  AUXILIARY CALCULATIONS  2  2  2  2  2
C
      DO 130 I=1,NSTATN
C---------CALC GEOMETRIC QUANTITIES
      JPTS=NDATA(I)
```

```
      JPTSM1=JPTS-1
      DYPS(1)=0.0
      DYNP(JPTS)=2.0*(RLARGE-R(JPTS))
      DO 110 J=1,JPTSM1
      DYNP(J)=R(J+1)-R(J)
      DYPS(J+1)=DYNP(J)
  110 CONTINUE
      DO 115 J=1,JPTS
      SNS(J)=0.5*(DYNP(J)+DYPS(J))
  115 CONTINUE
      IF(DIAGNS) WRITE(6,500) (DYNP(J),J=1,JPTS)
      IF(DIAGNS) WRITE(6,500) (SNS(J),J=1,JPTS)
      FLOW=0.0
      WMOM=0.0
      DO 120 J=1,JPTS
      WMOM=WMOM+RHO*R(J)**2*SNS(J)*U(I,J)*W(I,J)
      FLOW=FLOW+2.*PI*R(J)*SNS(J)*U(I,J)
      IF(DIAGNS) WRITE(6,900) J,FLOW,WMOM,RHO
  900 FORMAT(///,I5,4(F12.4,2X))
  120 CONTINUE
      ANGMOM(I)=WMOM
      MASS(I)=RHO*FLOW
      UMEAN(I)=MASS(I)/(RHO*PI*RLARGE**2)
  130 CONTINUE
      IF(DIAGNS) WRITE(6,450) (UMEAN(I),I=1,NSTATN)
      IF(DIAGNS) WRITE(6,450) (MASS(I),I=1,NSTATN)
C----------NONDIMENSIONALIZE VELOCITIES
      DO 150 I=1,NSTATN
      XND(I)=X(I)/(2.0*RLARGE)
      JPTS=NDATA(I)
      UIN(I)=(SQRT(2.0/RHO*RDNPRS(I)*249.08))*(6.312/5.94)**2
      MASFLO(I)=2.0*PI*RHO*UIN(I)*RSMALL**2/2.0
      DO 140 J=1,JPTS
      VTSTAR(I,J)=VTOTAL(I,J)/UIN(I)
      USTAR(I,J)=U(I,J)/UIN(I)
      VSTAR(I,J)=V(I,J)/UIN(I)
      WSTAR(I,J)=W(I,J)/UIN(I)
  140 CONTINUE
  150 CONTINUE
      DO 160 J=1,MAXJPT
      RND(J)=R(J)/(2.0*RLARGE)
  160 CONTINUE
C
CHAPTER  3  3  3  3  3  OUTPUT  3  3  3  3  3  3  3
C
      IF(.NOT. IWRITE) GO TO 165
      WRITE(11) X
      WRITE(11) R
      WRITE(11) U
      WRITE(11) V
      WRITE(11) W
  165 CONTINUE
      WRITE(6,311)
      WRITE(6,325) ALPHA
      WRITE(6,330) PHI
      WRITE(6,335) RSMALL
      WRITE(6,340) RLARGE
      WRITE(6,355) VISCOS
      WRITE(6,360) RHO
C
      CALL WRITE(1,1,NSTATN,1,IT,JT,X,R,MASFLO,HEDMMF)
      CALL WRITE(1,1,NSTATN,1,IT,JT,X,R,MASS,HEDM)
      CALL WRITE(1,1,NSTATN,1,IT,JT,X,R,UIN,HEDMIV)
      CALL WRITE(1,1,NSTATN,1,IT,JT,X,R,UMEAN,HEDUMN)
      CALL WRITE(1,1,NSTATN,1,IT,JT,X,R,ANGMOM,HEDAM)
      CALL PRINT(1,1,NSTATN,MAXJPT,IT,JT,X,R,U,HEDU)
      CALL PRINT(1,1,NSTATN,MAXJPT,IT,JT,X,R,V,HEDV)
      CALL PRINT(1,1,NSTATN,MAXJPT,IT,JT,X,R,W,HEDW)
      CALL PRINT(1,1,NSTATN,MAXJPT,IT,JT,X,R,DELTA,HEDDEL)
      CALL PRINT(1,1,NSTATN,MAXJPT,IT,JT,X,R,BETA,HEDBET)
      CALL PRINT(1,1,NSTATN,MAXJPT,IT,JT,X,R,VTOTAL,HEDVT)
```

```
      CALL PRINT(1,1,NSTATN,MAXJPT,IT,JT,XND,RND,USTAR,HEDUST)
      CALL PRINT(1,1,NSTATN,MAXJPT,IT,JT,XND,RND,VSTAR,HEDVST)
      CALL PRINT(1,1,NSTATN,MAXJPT,IT,JT,XND,RND,WSTAR,HEDWST)
      CALL PRINT(1,1,NSTATN,MAXJPT,IT,JT,XND,RND,VTSTAR,HEDVTS)
      CALL PRINT(1,1,NSTATN,MAXJPT,IT,JT,XINCHS,RINCHS,RPNMPS
     #    ,HEDNMS)
      CALL PRINT(1,1,NSTATN,MAXJPT,IT,JT,XINCHS,RINCHS,RPCMPW
     #    ,HEDCMW)
      CALL WRITE(1,1,NSTATN,1,IT,JT,XINCHS,RINCHS,RDNPRS,HEDMIP)
      CALL PRINT(1,1,NSTATN,MAXJPT,IT,JT,XINCHS,RINCHS,PICHCF
     #    ,HEDMPP)
      STOP
C---------FORMAT STATEMENTS
  311 FORMAT(1H1,T37,'AXISYMMETRIC,ISOTHERMAL, GT COMBUSTOR
     #    FLOWFIELD MEASUREMENTS',//,T53,'USING A FIVE-HOLE
     #    PITOT PROBE')
  325 FORMAT(////,T40,'EXPANSION ANGLE(DEG.) =',T77,1PE13.3)
  330 FORMAT(//,T40,'SWIRL VANE ANGLE(DEG.) =',T77,1PE13.3)
  335 FORMAT (//,T40,'INLET RADIUS(M) =',T77,1PE13.3)
  340 FORMAT(//,T40,'COMBUSTOR RADIUS(M) =',T77,1PE13.3)
  355 FORMAT(//,T40,'LAMINAR VISCOSITY(KG/M/SEC) =',T77,1PE13.3)
  360 FORMAT(//,T40,'DENSITY(KG/CU. M) =',T77,1PE13.3,////)
      END
C
      SUBROUTINE INIT
C*****************************************************************
C
      COMMON
     #/MEASUR/RBETA(48,24),RPNMPS(48,24),RPCMPW(48,24),NDATA(48)
     #    ,MAXJPT,RDNPRS(48)
     #/GEOM/X(48),R(24),XND(48),RND(24),DYPS(24),DYNP(24),
     #    SNS(24),NSTATN,XINCHS(48),RINCHS(24)
     #/CALC/VTOTAL(48,24),U(48,24),V(48,24),W(48,24),
     #    VTSTAR(48,24),USTAR(48,24),VSTAR(48,24),WSTAR(48,24),
     #    PICHCF(48,24),VELCF(48,24),DELTA(48,24),BETA(48,24),
     #     ANGMOM(48),UMEAN(48),MASS(48),MASFLO(48),UIN(48)
      REAL MASS,MASFLO
C
      DO 20 I=1,NSTATN
      MASFLO(I)=0.0
      MASS(I)=0.0
      ANGMOM(I)=0.0
      UMEAN(I)=0.0
      UIN(I)=0.0
      DO 10 J=1,MAXJPT
      VTOTAL(I,J)=0.0
      U(I,J)=0.0
      V(I,J)=0.0
      W(I,J)=0.0
      VTSTAR(I,J)=0.0
      USTAR(I,J)=0.0
      VSTAR(I,J)=0.0
      WSTAR(I,J)=0.0
      RBETA(I,J)=0.0
      BETA(I,J)=0.0
      RPNMPS(I,J)=0.0
      RPCMPW(I,J)=0.0
      PICHCF(I,J)=0.0
      VELCF(I,J)=0.0
      DELTA(I,J)=0.0
   10 CONTINUE
   20 CONTINUE
      RETURN
      END
C
      FUNCTION SPLINE(X, FX, N, X1)
C*****************************************************************
C     CUBIC SPLINE CURVE FITTING IN 2 DIMENSIONAL DATA PLANE
C     INPUT VALUES :
C     X, FX      DATA ARRAYS, ONE DIMENSIONAL, X IN INCREASING ORDER
```

```
C      N          NUMBER OF DATA POINTS IN X, MAX 26
C      X1         POINT OF INTEREST, WHERE F(X1) IS TO BE FOUND
C
C      RETURN VALUE :
C      SPLINE OR SP = F(X1)
C      THIS ROUTINE ACTIVATES ROUTINE ABUILD, H, AND GAUSS.
C      FOR INTERPOLATION OF A LARGE NUMBER OF DATA POINTS, FUNCTION
C      SPLINE MAY BE CALLED ONLY ONCE , AND SUBSEQUENT CALLS MAY US

C      ENTRY POINT SP.
C**********************************************************************
       DIMENSION X(1), FX(1), A(26,27)
C---------CONSTRUCT SPLINE MATRIX
       NP1=N+1
       DO 10  I=1, N
       DO 10  J=1, NP1
10     A(I,J)=0.
       NM1=N-1
       DO 20  I=2, NM1
20     CALL ABUILD(X, FX, A, N, I)
       A(1,1)=H(X,2)
       A(1,2)=-H(X,1)-H(X,2)
       A(1,3)=H(X,1)
       NM2=N-2
       A(N,NM2)=H(X,NM1)
       A(N,NM1)=-H(X,NM2)-H(X,NM1)
       A(N,N)=H(X,NM2)
C---------FIND SECOND DERIVATIVES
       CALL GAUSS(A, N, NP1)
       ENTRY SP(X, FX, N, X1)
C---------FIND F(X1)
       DO 40  I=1, NM1
       IP1=I+1
       IF(X1 .EQ. X(I)) GO TO 50
       IF(X1 .LT. X(I) .AND. X1 .GT. X(IP1)) GO TO 41
       IF(X1 .GT. X(I) .AND. X1 .LT. X(IP1) ) GO TO 41
40     CONTINUE
       IF(X1 .EQ. X(N)) GO TO 60
       WRITE(6, 42) X1
42     FORMAT(' X1=', G14.7, ' OUT OF INTERPOLATION RANGE,
      *   RETURNED VALUE=0')
       SP=0.
       SPLINE=0.
       STOP
41     CONTINUE
       IP1=I+1
       HI=H(X,I)
       HX=X1-X(I)
       AI = (A(IP1,NP1)-A(I,NP1))/(6.*HI)
       BI = A(I,NP1)/2.
       CI = (FX(IP1)-FX(I))/HI-(2.*HI*A(I,NP1)+HI*A(IP1,NP1))/6.
       DI = FX(I)
       SPLINE=AI*HX**3+BI*HX**2+CI*HX+DI
       SP=SPLINE
       RETURN
C
50     CONTINUE
       SPLINE=FX(I)
       SP=SPLINE
       RETURN
C
60     CONTINUE
       SPLINE=FX(N)
       SP=SPLINE
       RETURN
       END
C
       FUNCTION H(X,I)
C**********************************************************************
C      CALCULATE DELTA X WHICH IS USUALLY CALLED AS H.
C**********************************************************************
```

```
      DIMENSION X(1)
      IP1=I+1
      H=X(IP1)-X(I)
      RETURN
      END
C
      SUBROUTINE ABUILD(X, F, A, N, I)
C*****************************************************************
C     CONSTRUCT  SPLINE MATRIX FOR FINDING 2ND DERIVATIVES.
C*****************************************************************
      DIMENSION X(1), F(1), A(26,27)
      IM1=I-1
      IP1=I+1
      NP1=N+1
      HI=H(X,I)
      HIM1=H(X,IM1)
      A(I,IM1)=HIM1
      A(I,I)=2.*(HIM1+HI)
      A(I,IP1)=HI
      A(I,NP1)=( (F(IP1)-F(I))/HI - (F(I)-F(IM1))/HIM1 )*6.
      RETURN
      END
C
      SUBROUTINE GAUSS(A, N, NP1)
C*****************************************************************
C     GAUSS-JORDAN ELIMINATION
C*****************************************************************
      DIMENSION A(26,27)
      NM1 = N-1
      DO 3  L=1, NM1
      LP1=L+1
      DO 3  I=LP1,N
      CONST=A(I,L)/A(L,L)
      DO 3  J=L, NP1
3     A(I,J)=A(I,J)-CONST*A(L,J)
      DO 6 I=1, NM1
      IP1=I+1
      DO 6  L=IP1,N
      CONST=A(I,L)/A(L,L)
      DO 6  J=I, NP1
6     A(I,J)=A(I,J)-CONST*A(L,J)
      DO 10  I=1, N
      A(I,NP1)=A(I,NP1)/A(I,I)
10    A(I,I)=1.
      RETURN
      END
C
      SUBROUTINE PRINT(ISTART,JSTART,NI,NJ,IT,JT,X,Y,PHI,HEAD)
CA****************************************************************
C
      DIMENSION PHI(IT,JT),X(IT),Y(JT),HEAD(9),STORE(48)
      ISKIP=1
      JSKIP=1
      WRITE(6,110)HEAD
      ISTA=ISTART-12
  100 CONTINUE
      ISTA=ISTA+12
      IEND=ISTA+11
      IF(NI.LT.IEND)IEND=NI
      WRITE(6,111)(I,I=ISTA,IEND,ISKIP)
      WRITE(6,114)(X(I),I=ISTA,IEND,ISKIP)
      WRITE(6,112)
      DO 101 JJ=JSTART,NJ,JSKIP
      J=JSTART+NJ-JJ
      DO 120 I=ISTA,IEND
      A=PHI(I,J)
      IF(ABS(A).LT.1.E-20) A=0.0
120   STORE(I)=A
  101 WRITE(6,113)J,Y(J),(STORE(I),I=ISTA,IEND,ISKIP)
      IF(IEND.LT.NI)GO TO 100
      RETURN
```

```
  110 FORMAT(1H0,17(2H*-),7X,9A4,7X,17(2H-*))
  111 FORMAT(1H0,13H      I =     ,I2,11I9)
  112 FORMAT(8H0 J     Y)
  113 FORMAT(I3,0PF8.5,1X,1P12E9.2)
  114 FORMAT(11H       X = ,F8.5,11F9.5)
      END
C
      SUBROUTINE WRITE(ISTART,JSTART,NI,NJ,IT,JT,X,Y,PHI,HEAD)
C ***************************************************************
C
      DIMENSION PHI(IT),X(IT),Y(JT),HEAD(9),STORE(48)
      ISKIP=1
      JSKIP=1
      WRITE(6,110)HEAD
      ISTA=ISTART-12
  100 CONTINUE
      ISTA=ISTA+12
      IEND=ISTA+11
      IF(NI.LT.IEND)IEND=NI
      WRITE(6,111)(I,I=ISTA,IEND,ISKIP)
      WRITE(6,114)(X(I),I=ISTA,IEND,ISKIP)
      DO 101 JJ=JSTART,NJ,JSKIP
      J=JSTART+NJ-JJ
      DO 120 I=ISTA,IEND
      A=PHI(I)
      IF(ABS(A).LT.1.E-20) A=0.0
120   STORE(I)=A
  101 WRITE(6,113) (STORE(I),I=ISTA,IEND,ISKIP)
      IF(IEND.LT.NI)GO TO 100
      RETURN
  110 FORMAT(1H0,17(2H*-),7X,9A4,7X,17(2H-*))
  111 FORMAT(1H0,13H      I =     ,I2,11I9)
  113 FORMAT(12X,1P12E9.2)
  114 FORMAT(11H       X = ,F8.5,11F9.5)
C
      END
```

VITA[2]

Hyung Kee Yoon

Candidate for Degree of

Master of Science

Thesis: FIVE-HOLE PITOT PROBE TIME-MEAN VELOCITY MEASUREMENTS IN CONFINED SWIRLING FLOWS

Biographical:

Personal Data: Born in Ham Pyeong, Korea, March 15, 1954, the son of Mr. and Mrs. In S. Yoon.

Education: Graduated from Sung Nam High School, Seoul, Korea, in March, 1973; received Bachelor of Engineering degree in Mechanical Engineering from Korea University, March, 1980; completed requirements for the Master of Science degree at Oklahoma State University in July, 1982.

Professional Experience: Research assistant, School of Mechanical and Aerospace Engineering, Oklahoma State University, Stillwater, Oklahoma, 1981-present.

Honor Society: Phi Kappa Phi

Professional Society: AIAA